Spring 5-11-2019

Investigating the Time-dependent and the Mechanical Behavior of Wood Plastic Composite Lumber Made from Thermally Modified Wood in the Use of Marine Aquacultural Structures

Murtada A. Alrubaie
University of Maine, murtada.alrubaie1@maine.edu

INVESTIGATING THE TIME-DEPENDENT AND THE MECHANICAL BEHAVIOR OF WOOD PLASTIC COMPOSITE LUMBER MADE FROM THERMALLY MODIFIED WOOD IN THE USE OF MARINE AQUACULTURAL STRUCTURES

By

Murtada Abass A. Alrubaie

B.Sc. University of Basra, 2005

M.Sc. Universiti Putra Malaysia, 2010

A DISSERTATION

Submitted in Partial Fulfillment of the

Requirements for the Degree of

Doctor of Philosophy

(in Civil Engineering)

The Graduate School

The University of Maine

May 2019

Advisory Committee:

Roberto A Lopez-Anido, Professor of Civil Engineering, Co-Advisor

Douglas J. Gardner, Professor of Forest Operations, Bioproducts and Bioenergy, Co-Advisor

William G. Davids, Professor of Civil Engineering

Yousoo Han, Associate Research Professor of Forest Operations, Bioproducts and Bioenergy

Mehdi Tajvidi, Assistant Professor of Renewable Nanomaterials

INVESTIGATING THE TIME-DEPENDENT AND THE MECHANICAL BEHAVIOR OF WOOD PLASTIC COMPOSITE LUMBER MADE FROM THERMALLY MODIFIED WOOD IN THE USE OF MARINE AQUACULTURAL STRUCTURES

By Murtada Abass A Alrubaie

Dissertation Co-Advisors: Dr. Roberto Lopez-Anido, P.E.

Dr.Douglas J. Gardner

An Abstract of the Dissertation Presented
in Partial Fulfillment of the Requirements for the
Degree of Doctor of Philosophy
(in Civil Engineering)
May 2019

Wood Plastic Composite (WPC) lumber based on a patent-pending formulation is being explored for use in the manufacture of an aquaculture fish cage structure (Aquapod net pen cage), as an alternative to the current high density polyethylene (HDPE) lumber. The use of WPC lumber in structural applications in marine environments requires a comprehensive effort to understand the material viscoelastic behavior and the structural performance of the WPC lumber in marine environments where the WPC lumber is exposed to the combined effect of saltwater immersion and temperature (hygrothermal). The evaluation of the viscoelastic behavior of WPC lumber in marine environments was conducted through series of short-term of dynamic mechanical and thermal analysis (DMTA) creep and creep-recovery experiments, where the WPC specimens were preconditioned and tested under the combined effect of temperature and water immersion at different target levels of stress. Long-term creep experiments of WPC and HDPE lumber under the same controlled conditions and stress levels are necessary to evaluate

and compare the viscoelastic behavior of WPC and HDPE lumber. An understanding of the structural behavior of WPC lumber in an aquaculture structure was advanced through testing components (triangular panels) from a spherical shape geodesic frame (Aquapod) structure made from WPC and HDPE lumber, respectively. The hygrothermal viscoelastic response of WPC lumber was characterized and modeled. The experiments included measuring 30 minutes of creep and 30 minutes of creep-recovery on the specimens immersed in saltwater and distilled water at two different levels of flexural stresses (9% and 14% of the ultimate flexural strength, Fb) and three temperature values (25, 35, and 45℃). The creep strain fractional increment (CSFI) of the WPC in this study under all conditions was 86% lower than the CSFI of the WPCs reported in previous studies. The WPC material in this study exhibited linear viscoelastic and nonlinear viscoelastic behavior based on the effect of temperature only, and the combined temperature and water immerstion effect, respectively. The 180-day creep behavior of the WPC and HDPE lumber in flexure was characterized and compared for WPC and HDPE lumber (with 853 mm support span) subjected to three levels of creep stress: 7.5, 15, and 30% of the ultimate flexural strength (Fb). The 180-day creep deformation of HDPE specimens was six times higher than the creep deformation of WPC specimens at the 30% creep stress level. A power law model was used to describe 180-day creep deflection of WPC lumber beams. Modeling results predicted that the strain to failure in the HDPE and WPC lumber would occur in 1.5 years and 150 years at a flexural stress of 30% Fb, respectively. A pair of connected triangular panels of the Aquapod structure with and without wire mesh made from WPC and HDPE lumber were tested in compression to evaluate and compare the buckling capacity of the panels, respectively.

ACKNOWLEDGEMENTS

There are a numerous number of people that I am genuinely very grateful for their; support, efforts, guidance, and knowledge. I would like to first and foremost thank my co-advisor Dr. Douglas J. Gardner for offering me the honor to work on part of his projects, be one of his research team, and for the extraordinary efforts and support throughout the journey of this research. Without him it would have never happened. I also thank my co-advisor Dr.Roberto A. Lopez-Anido for his efforts, advice, knowledge, and guidance. Furthermore, I sincerely thank Dr. Mehdi Tajvidi, Dr. Yousoo Han, and Dr. Bill Davids for their efforts and the time dedicated for this research. I also thank Chris West, Justin Crouse, Rich Fredericks, Ben Herzog, Russell Edgar Steve Ruell, from InnovaSea during his employment, Ray Lawrence, and Duncan Mayes from Stora Enso. I thank every; employee and graduate student at the Advanced Structures and Composites Center at the University of Maine, Orono, Maine, USA, who always show their help during my experimental work. I acknowledge the Higher Committee for Education Development in Iraq (HCED-Iraq) for their financial support throughout my Ph.D. study.

I would like to thank and acknowledge my family in Iraq who some of them passed away (my father and my brother) during the years of this research and my family in Maine for their constant support and encouragement throughout my educational career. My mother, my brothers, my sister, and my wife, Sally. My little ones (starting from the oldest), Masara, Fatima, and Hasan, without your happy faces and the joy you bring to me every day, I wouldn't overcome the study plights, you all made it worthwhile.

The experimental work in this research was conducted at the Advanced Structures and Composites Center at the University of Maine, Orono, Maine (USA). The University of Maine research reinvestment funds (RRF) Seed Grant entitled (Development of structural wood plastic

composite timber for innovative marine application) and the United Stated Department of Agriculture (USDA)-the agricultural research service (ARS) Funding Grant Number (58-0204-6-003) have provided the financial support for this project. The wood plastic composite is based on a patent-pending formulation that has the publication number (WO2018/142314). The thermally modified wood fiber used in this research is supplied by Stora Enso (Finland).

TABLE OF CONTENTS

LIST OF TABLES

LIST OF FIGURES

CHAPTER 1

INTRODUCTION

The mechanical properties of a patent-pending formulation wood plastic composites (WPCs) made from this WPCs to have a potential capability to be used in marine structural application (Gardner & Han 2010). Several researchers (Alvarez-Valencia et al. 2010, Bright & Smith 2007, Haiar 2000, Slaughter 2006, Tamrakar & Lopez-Anido 2011) studied the use of WPCs in structural application, for instance, WPCs in waterfront structures, and in sheet piles. University of Maine researchers have successfully developed a WPC that has approximately 4.3 GPa apparent Modulus of Elasticity (MOE) and "less prone to creep than the current WPCs." InnovaSea Systems, Inc., Morrill, Maine showed a keen interest to use WPCs, instead of the High-Density Polyethylene (HDPE) lumber that is used in the current construction of the AquaPod net pen cages. The latter showed lower apparent MOE, approximately 0.9 GPa and experienced a severe time-dependent deformation (Gardner 2015). Figure *1.1* illustrates the motivation to use WPC lumber in AquaPod net pen cages rather than HDPE lumber based on the high (five times higher) MOE of WPCs, and based on the recorded damage occurred to the Aquapod cage structure (right) made from HDPE lumber.

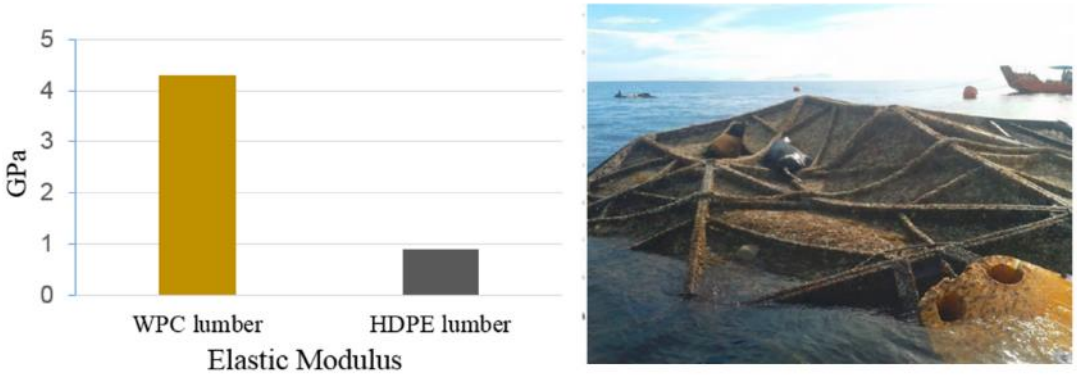

Figure 1.1. (left) the flexural modulus of elasticity of the materials in psi, (right) the time-dependent deformation in the cage attributable to the sustained seals' load on the cage in the presence of high temperature (InnovaSea Systems 2015).

1.1 Motivation of Using WPC Lumber in Aquaculture Cages

InnovaSea Systems, Inc., (InnovaSea Systems 2015), reported damage occurring to an A4800 AquaPod net pen cage that is made of HDPE struts, attributable to the combination of long-term exposure to the tropical heat, the generated waves from a storm that hit the location of the cage in the Gulf of Mexico, and the unexpected live load of the Sea lions that acted on the top of the cage during the cage sun exposure (as a process of cleaning the cage from the biofouling). A pronounced deformation attributable to a sustained point live load of the Sea lions under the effect of temperature is shown in Figure 1.1 (right). Approximate weight of each Sea lion was reported as 500 kg, and two Sea lions were observed (InnovaSea Systems 2015). The following storm created waves that hit the cage repeatedly for more than eight hours and worsened the damage to the cage. Of the 216 triangular panels (648 struts with 2 x 6 cross-

section) required to construct the A4700 AquaPod cage, 78 panels were damaged because of the synergetic forces that were mentioned earlier (InnovaSea Systems 2015).

To investigate the long-term deformation that might occur on the HDPE struts because of the effect of elevated temperature, a series of experimental tests were conducted at the University of Maine, Orono, Maine following the ASTM D6108 (Snape 2015). The compression tests were performed at four different temperatures; 1.2; 21.11℃, 37.78 ℃, 48.89 ℃, and 60℃, respectively. However, the tested specimens from the used struts did not show a decrease in their mechanical properties attributable to the temperature and moisture, compared with unused tested specimens (InnovaSea Systems 2015). The reason for not having a pronounced difference between the used and the unused HDPE specimens is believed to be attributed to the chosen test (i.e., the compression test vertical to the extrusion direction), different results would have been obtained if different tests were used, for instance, tension or flexure test in the direction of the extrusion. InnovaSea systems, Inc., conducts their structural analysis and design, using a finite element analysis software, CADRE PRO 6. The model was run by considering the weight of the two Sea lions, acting on the top face of the cage. The model showed a similar deformation to the actual damage (InnovaSea Systems 2015).

1.2 Time-Dependent Behavior of WPCs

Although WPCs have been explored for use in the different structural applications, the material's long-term behavior is still a subject of concern among the researchers. WPCs, unlike the conventional elastic materials, exhibit viscoelastic behavior. Creep is one of the physical manifestations of the behavior of the viscoelastic materials, when a constant stress is applied to the viscoelastic material, the summation of the elastic strain and the time-dependent strain will represent the total strain (creep strain) of the viscoelastic composite material (Gibson 2016).

Some researchers (Gibson 2016, Haghighi-Yazdi & Lee-Sullivan 2013, Sullivan 1990) consider WPCs to have a linear viscoelastic behavior, whereas other researchers, (Hamel 2011), in their work consider WPCs to have a nonlinear viscoelastic behavior. Linear viscoelastic behavior enables the principle of superposition when long-time deformation can be measured in a shorter duration via accelerated conditions and superimpose the data to construct, so called, the master curve of the creep strain, whereas the nonlinear viscoelastic behavior requires a "mechanics-based" model to predict the long-term behavior (Hamel 2011). The time-dependent strain $\varepsilon(t)$ increases during the period of loading, attributable to the effect of the constant stress, as shown in Equation 1.1.

$$\text{Total Strain} = \varepsilon\_\text{elastic} + \varepsilon(t) \tag{1.1}$$

The time-dependent behavior of WPCs, particularly in this study, the creep, depends on the following; (1) the applied stress, (2) the formulation of the WPCs, (3) both temperature and moisture, (4) physical ageing, and (5) the stress dependency of the parameters of the physical models (Barbero 2013). If the WPC experiences a combination of all these factors acting at the same time, thus the complexity of the time-dependent behavior needs to be addressed and investigated, to have a satisfactory prediction of the service life of the WPC material. Tamrakar and Lopez-Anido reported a significant decrease in the mechanical properties of "water-saturated" specimens compared with dry specimens that are exposed to a range of temperatures (Tamrakar & Lopez-Anido 2011). Cheng reported the effect of immersing a WPC sample in osmotic and sea water for 13 months. Cheng found significant differences in the mechanical properties of the WPC samples (Cheng 2005). The temperature (high or low) and the moisture (water can be humidity, water immersion, or rain) also degrade the constituent of the WPCs and the composite itself. Wood as a WPC constituent exhibits swelling because of water absorption

by the hydrophilic nature of the wood cell wall material. Wood also expands attributable to the change in temperature. The polymer constituent exhibits a viscoelastic behavior and time-dependent change in the mechanical properties because of the thermal effect. Combining both constituents under the hygrothermal effect will worsen the properties of the WPCs further. Microcracks in the interfacial zone between the polymer and the wood flour particles will be created, and adhesion will be degraded. Freeze-thaw degradation can be considered as a type of degradation that is related to the effect of the combination of temperature and moisture (Stark 2008).

To have a better judgment on the most severe environmental impact on the mechanical behavior of WPCs, an understanding of the environmental degradation of WPC constituents, wood flour, and polymer, is necessary. UV has an impact on wood. A combination of (UV) with moisture and air will increase the degradation impact on wood attributable to the hydroxyl groups and the formation of the free radicals (Stark 2008). The second constituent of the WPCs is a polymer, generally including the matrix, the coupling agent, the lubricants, or any other polymer additives also degrades with the exposure to (UV). However, a combination of (UV) and oxygen (air) will have a pronounced impact on the durability of the polymer, so-called, photodegradation. The degradation of the polymer will also result in; forming a free radical, possible chain scission, and crosslinking. As a wood plastic composites (WPCs), the combination of (UV) with other environmental factors will degrade the surface of the WPCs and decrease the mechanical properties of WPCs (Matuana et al. 2011). However, this study will not consider the effect of UV and air on the mechanical properties of WPCs, because the cages will be submerged in its application.

1.3 Aquaculture Cage Structures

To understand the structural behavior of WPC members (struts) in aquaculture cages (AquaPod net pen cages) that are operated in marine environment and exposed to wave and current forces, and to qualify that WPC members can show an acceptable structural behavior in such environment during the service life of the structure, a review of the structural analysis and design that were conducted by other researchers on aquaculture structures is required. There are different types of aquaculture cages that are used for fish- stocks farms in open ocean environment, as shown in Figure 1.2. However, the objective of this study will focus on reviewing the work was conducted on the AquaPod net pen cages. Ocean Farm Technology (OFT)-InnovaSea systems, Inc. manufacture AquaPod cages worldwide and in different capacities. The largest manufactured Aquapod cage has a capacity of 4700 m^3, geodesic spherical shape approximately 20 m diameter (Vandenbroucke & Metzlaff 2013).

Figure 1.2. Types of aquaculture cages. Clockwise from top left: prototype gravity system, AquaPod net pen, Ocean Cage Aquaculture Technology (OCAT) cage, gravity-type flexible cage, tension-leg system, and rigid-frame fish cage (Vandenbroucke & Metzlaff 2013).

The AquaPod net pen cage, among other types of cages, is considered a distinctive containment system for marine aquaculture, not only its rigid spherical shape, but for other remarkable features; utilizing the coded triangular panels that are interchangeable and can be tracked to form cages (six faces assemblies method) in different desired sizes and to track each panel to do the required maintenance to it, respectively, reducing maintenance cost by replacing the damaged panels only, any joint (hub) in the structure can be operated as a mooring point, and it can be rotated

attributable to its rigid spherical geometry. Its spherical shape is constructed from individual triangular net panels that are fastened together using so-called, Gusset blocks. These net panels are simply structural members (struts) and netting, as shown in Figure 1.3. These struts are made of recycled HDPE material (lumber), and plastic-coated welded wire mesh, for the net fabric. A hub connects six panels. Figure 1.4 shows the details of connecting struts to each other in the panel, and panels to the hub. In addition to the function of the triangular net panels to construct the spherical shape of the cage, other panels are utilized as access, feeding window, supporting the floating devices that provide orientation to the cage, and mooring (Vandenbroucke & Metzlaff 2013).

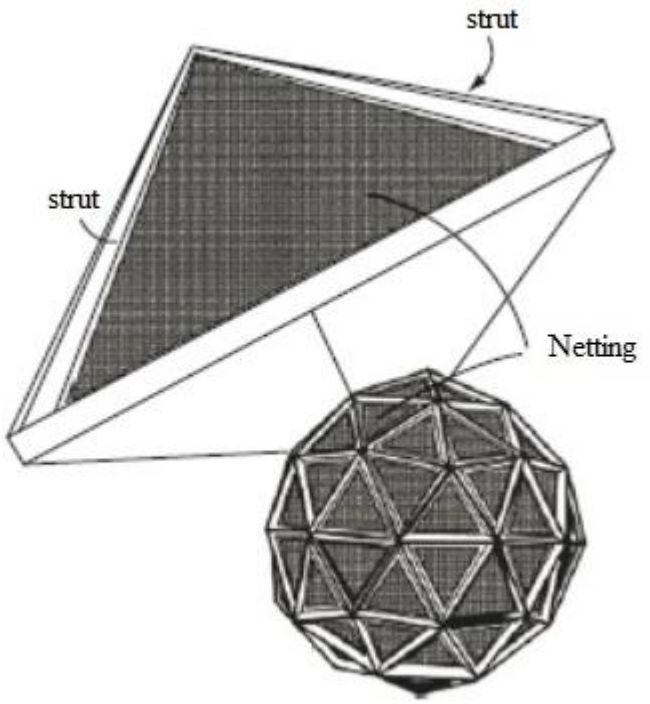

Figure 1.3. Details of the structural component-the triangular net panel (building unit) of AquaPod net pen cage (Vandenbroucke, K. and M. Metzlaff, 2013).

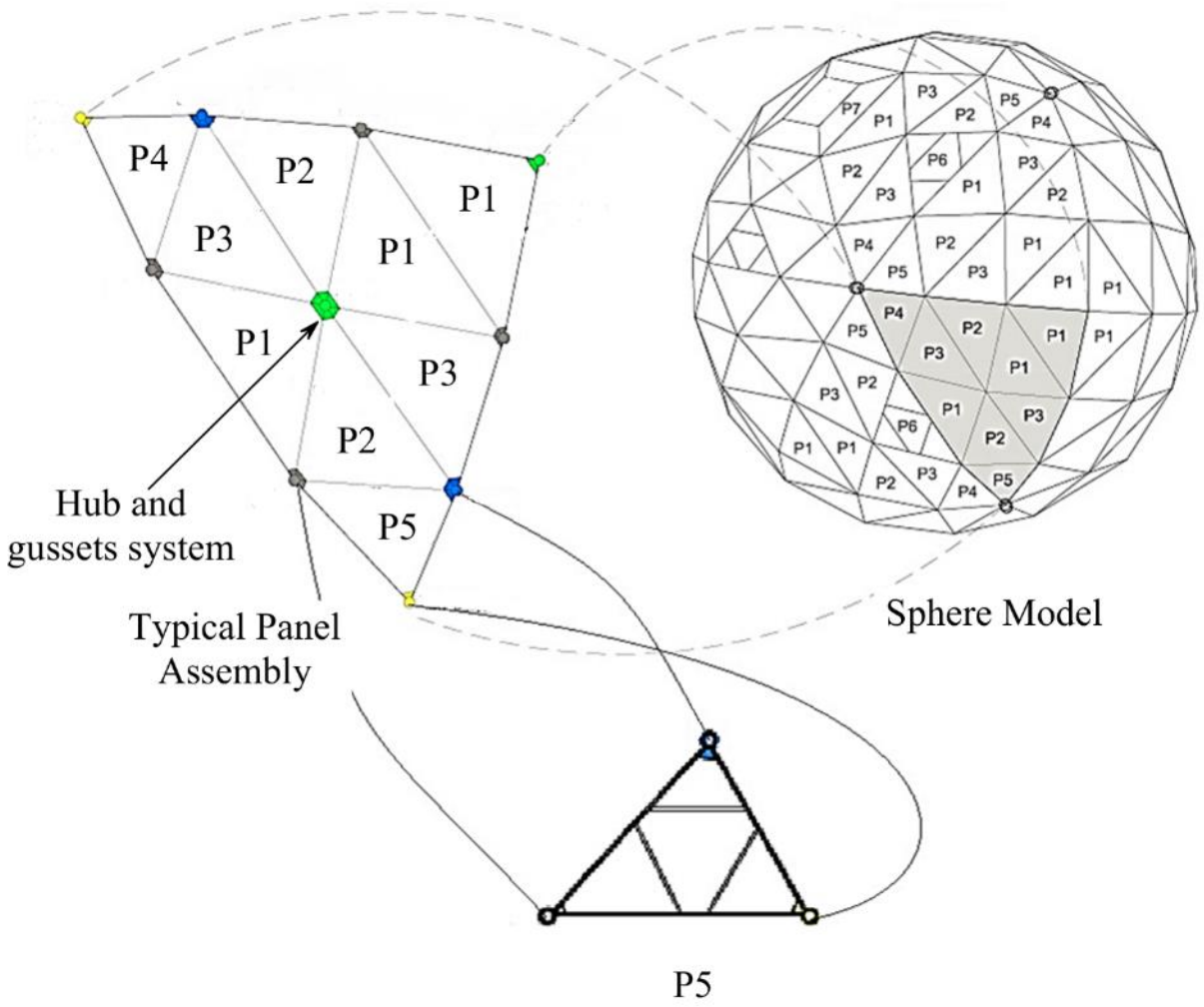

Figure 1.4. Details of; connected struts in the panels and the connected panels to form the cage faces, types of hubs, and the types of the panels (InnovaSea Systems 2017).

An advantageous use of the AquaPod net pen cages in addition to their rigid geometry is the ability to be operated in the marine environment in a depth of water, below the region of destructive energy of the surface waves and currents (Vandenbroucke & Metzlaff 2013), as shown in Figure 1.5 (a).

Different configurations of the grid mooring system are used for either individual or grouped AquaPod net pen cages. However, this study reviews the most common grid mooring configuration that InnovaSea Systems Inc. use, i.e., the fully submerged four-points grid mooring system of a single cage as shown in Figure 1.5 (c).

The geometry of the Aquapod net pen structure is supposed to enable it to maintain its shape and volume under the effect of strong current or towing. However, the struts of the AquaPod cage (A4700) and the plastic-coated welded wire mesh net of the panels, didn't withstand the synergetic forces, for instance, the damage that took place on A4700, when sea lions resting on the cage and the following weather severe storm, as shown in Figure 1.1 (right).

The objectives of this research are: (1) to provide a time-dependent evaluation (short- and long-term) that qualifies the structural use of WPC lumber for struts in the AquaPod structures during their service life in the marine environment, (2) and to describe the effect of temperature and immersion on the structural behavior of WPC struts.

The scope of this study encompasses; short-term creep and creep recovery experiments on WPC specimmens (30-minute creep and 30-minute creep recovery)creep testing, long-term creep (180-day creep experiments) on WPC and HDPE lumber, and mechanical buckling evaluation of two connected (fastened) strucutral componentes of the Aquapod cage structure (triangular panels) . These panels are taken from the 1:4 prototype structure of the AquaPod A4700 cage.

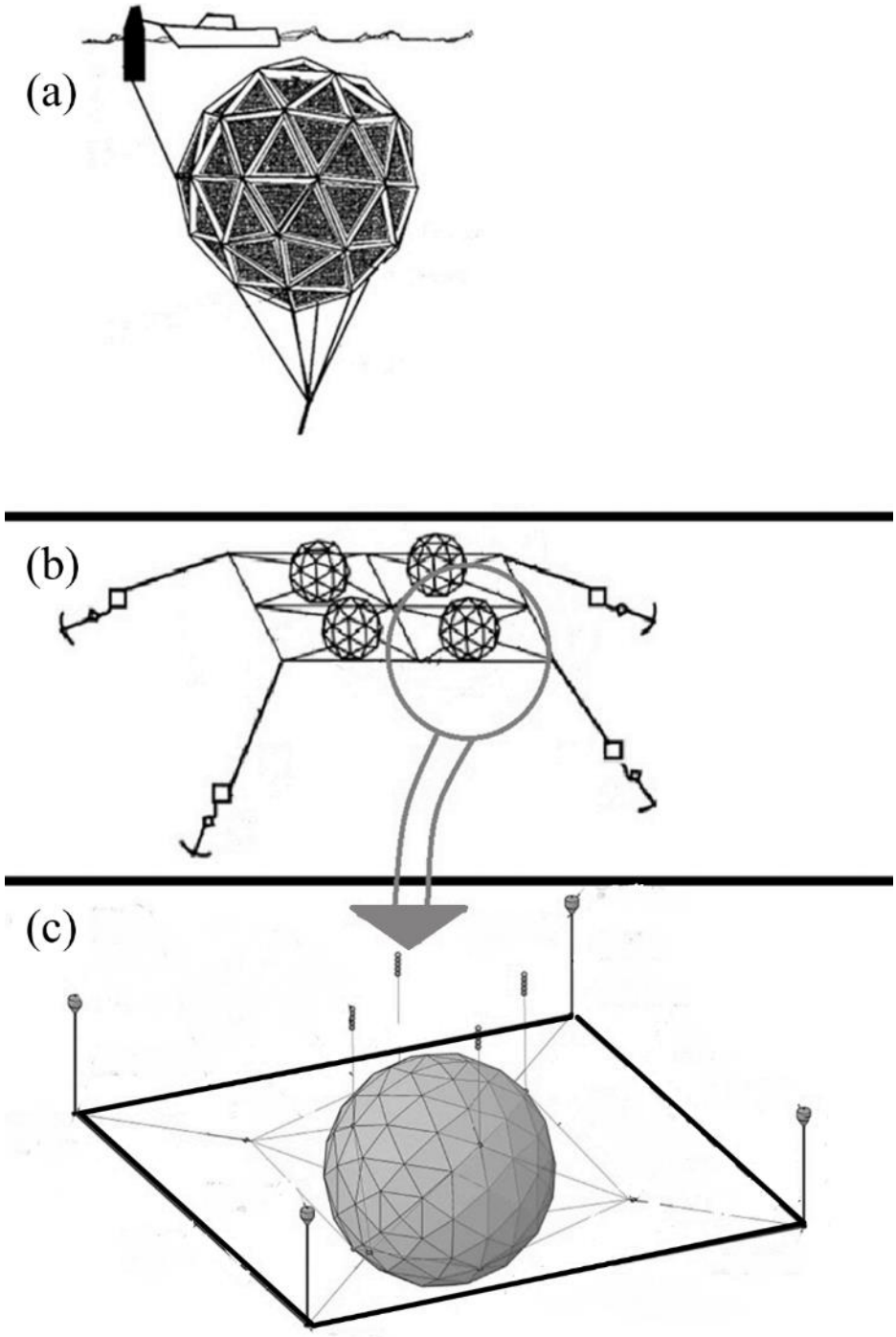

Figure 1.5. (a) fully submerged cage, (b) a configuration of grid mooring system of 4 AquaPod net pen cages, (c) bridle system in grid mooring cell (Vandenbroucke, K. and M. Metzlaff, 2013).

1.4 Research Objectives

The objectives of the current research are to:

- Provide an understanding of the viscoelastic and structural behavior of WPC lumber in marine structural applications
- Investigate the short-term viscoelastic creep and creep-recovery behavior of WPC lumber under the combined effect of water immersion and temperature.
- Describe the creep viscoelastic behavior by modeling it, and implement the model to predict the WPC lumber viscoelastic behavior for durations longer than the experimental test duration.
- Compare the long-term viscoelastic creep behavior of WPC lumber with viscoelastic behavior of HDPE lumber.
- Compare the structural performance of the structural components of Aquapod net pen cage made from WPC lumber with the structural performance of the structural components made from HDPE lumber.

1.5 Organization of the Dissertation Chapters

This dissertation is arranged as a series of six chapters. The focus of chapter two is to investigate the hygrothermal effect on the short-term creep behavior of extruded thermally modified wood fiber high strength styrenic copolymer plastic composites (WPCs) on specimens preconditioned for one month under water immersion (distilled and saltwater). These specimens were then tested in the same conditions for short-term creep and creep-recovery response using a submersible clamp. The short-term creep tests of WPC specimens (that are immersed in water as a function of different temperatures) has not yet been reported in previous studies. The experiments included measuring 30 minutes of creep and 30 minutes of creep-recovery on the

specimens immersed in saltwater and distilled water at two different levels of flexural stresses (9% and 14% of the flexural strength) and three temperature values (25, 35, and 45℃). Chapter two has been published as a journal article in a peer-reviewed journal.

Chapter three presents the modeling to the hygrothermal short-term creep behavior of the WPC specimens. Multiple 3-point bending creep/recovery tests were carried out using a dynamic mechanical thermal analyzer (DMTA) equipped with a submersible clamp. WPC specimens with 15 mm span were subjected to two initial applied stresses; 9 and 14% of the flexural strength in 30 minutes of creep and 30 minutes of creep recovery under the combined effects of temperature (25, 35, 45℃) and water immersion (saltwater and distilled water). A dry condition WPC control was used to compare the hygrothermal effects with respect to the control conditions. A power law model is considered a useful model to describe the creep behavior of WPC specimens with a 15mm span in the control and the saltwater conditions and at 45℃. Chapter three has been published as a journal article in a peer-reviewed journal.

Chapter four presents a characterization and comparison study to the creep behavior of the WPC and high density polyethylene (HDPE) lumber in flexure. Three sample groupings of WPC and HDPE lumber were subjected to three levels of creep stress; 7.5, 15, and 30% of the ultimate flexural strength for a duration of 180 days. Because of the relatively low initial creep compliance of the WPC specimens (five times less) compared with the initial creep compliance of HDPE specimens, the creep deformation of HDPE specimens was six times higher than the creep deformation of WPC specimens at the 30% creep stress level. Modeling results predicted that the strain to failure in the HDPE lumber would occur in 1.5 years at 30% Fb flexural stress while the predicted failure for the WPC would occur in 150 years. Chapter four has been submitted to a peer-reviewed journal and is still under review.

The focus of chapter five is on an experimental study to the structural performance of the connected structural components of the Aquapod cage structure (triangular panels) in buckling. These panels were made from WPC lumber and HDPE lumber and their buckling evaluation was discussed and compared, accordingly.

Finally, chapter six provides conclusions of the research that was conducted for this dissertation. Potential areas of future research are also addressed.

CHAPTER 2

EXPERIMENTAL INVESTIGATION OF THE HYGROTHERMAL CREEP STRAIN OF WOOD PLASTIC COMPOSITE LUMBER MADE FROM THERMALLY MODIFIED WOOD

2.1 Abstract

The hygrothermal effect on the short-term creep behavior of extruded thermally modified wood fiber high strength styrenic copolymer plastic composites (WPCs) was investigated on specimens preconditioned for one month under water immersion (distilled and saltwater). These specimens were then tested in the same conditions for short-term creep and creep-recovery response using a submersible clamp. The short-term creep tests of WPC specimens (that are immersed in water as a function of different temperatures) has not yet been reported in previous studies. The objective of this study was to determine if the hygrothermal creep response of WPC material evaluated through water immersion differs from the creep response published in the literature for other environmental exposure conditions. The experiments included measuring 30 minutes of creep and 30 minutes of creep-recovery on the specimens immersed in saltwater and distilled water at two different levels of flexural stresses (9% and 14% of the flexural strength) and three temperature values (25, 35, and 45℃). The average creep strain recovery (%) of the specimens was higher for the specimens immersed in saltwater during testing than the control specimens. The WPC material is considered to have a potential use in structural applications in environments where the temperature is below 45℃ because of the following factors: the low deformation under the short-term sustained loading; the decrease in the deformation rate with respect to the increase in load duration; maintaining the modulus of elasticity over a range of

temperatures from 25℃ to 45℃ under sustained load; and the ability to recover more than 69% of the average creep strain under water immersion when the loading source is removed. The creep strain fractional increment (CSFI) of the WPC in this study under all conditions was 13% which is 86% lower than the CSFI of the WPCs reported in previous studies.

2.2 Introduction

The time-dependent behavior of WPCs, particularly creep, has been studied by many researchers under the effect of temperature (Chang et al. 2014, Pooler & Smith 2004, Tamrakar et al. 2011). To widen the structural application of WPCs to include, water immersion applications (Alvarez-Valencia et al. 2010), the time-dependent behavior of WPCs under hygrothermal exposure conditions should be investigated. Temperature (low or high) and moisture (humidity or water immersion) can degrade or reduce the mechanical properties of the constituents of the WPC composite, leading to changes in the composite itself. Wood swells because of water uptake caused by the hydrophilic nature of the wood cell wall material. The plastic constituent exhibits viscoelastic behavior and time-dependent changes in mechanical properties produced by thermal effects. Both wood and plastic constituents under hygrothermal effects will impact the mechanical properties of the WPCs. Microcracks in the interfacial zone between the polymer and the wood flour particles can be created, and the adhesion between the wood flour and the plastic will be negatively impacted (Klyosov 2007, Stark 2008).

Tamrakar and Lopez-Anido reported a significant decrease in the mechanical properties of "water-saturated" specimens compared with dry specimens that were exposed to a range of temperatures (Tamrakar & Lopez-Anido 2011). Cheng (Cheng 2005) reported the effect of immersing a WPC sample in osmotic and sea water for 13 months, and found significant decreases in the mechanical properties of the immersed WPC samples (Cheng 2005). Most

researchers have studied the time-dependent behavior of WPCs under the effect of temperature. Kazemi et al. (Kazemi et al. 2008) studied the effect of water content on creep behavior of WPCs. Specimens were conditioned in water for 7 and 30 days, respectively, and then tested for creep and creep-recovery (Kazemi et al. 2008). Their study showed when the specimens were conditioned under immersion for a longer duration, the resulting creep strain increased. However, the moisture content of the specimens was not controlled during the tests, especially when the creep and creep-recovery experiments were conducted at elevated temperatures. Recent studies have investigated the combined effect of temperature and the moisture uptake on the mechanical properties of wood flour-high density polyethylene (HDPE) composites (Fortini & Mazzanti 2018). In an attempt to widen the structural applications of WPC to include structures where temperature and moisture are both acting on the WPC, Fortini and Mazzanti (Fortini & Mazzanti 2018) investigated the combined effect of temperature and the moisture uptake on reducing the mechanical properties of the WPC. Their study included investigating the reduction in the mechanical properties related to the combined effect of temperature and moisture via a Charpy impact test with a load duration less than five seconds. Fortini and Mazzanti did not investigate the combined effect of temperature and moisture on longer duration tests under sustained loads.

Dynamic mechanical thermal analysis (DMTA) instruments and techniques have helped researchers conduct a variety of short-term experiments to predict or evaluate the time-dependent behavior of WPC specimens in a short period of time. This is done to provide a better understanding of the time-dependent behavior of the material over a longer period.

Bases on researcher interests towards the enhancement of the mechanical properties of wood particles for WPC manufacture (Chang et al. 2009, Esteves & Pereira 2008), different

modification methods have been studied. Wood heat-thermal treatment was determined to be one of the treating processes that improves the mechanical properties of the wood particles related to the elimination of the hemicellulose, which is the main component for reducing the mechanical properties of wood particles (Esteves & Pereira 2008). Thermal modification also enhances the compatibility between the wood particles and the polymer matrix and increases interfacial bonding (Hosseinaei et al. 2012). The objective of the research presented here was to experimentally investigate the hygrothermal average (avg.) creep strain and recovery of an extruded WPC material made from thermally modified wood evaluated under water immersion and compare it with the creep response published in the literature for other exposure conditions.

2.3 Experimental Program

In this study, a DMTA instrument with a 3-point bending submersible clamp was used to conduct short-term creep and creep-recovery experiments under the synergistic effects of water immersion and temperature. These results were compared with those of the dry reference state of the specimens. WPC materials exhibit distinctive time-dependent behavior related to their different formulations (i.e., different type of plastic and different types and quantity of the wood flour). The WPC material used in this study is being considered for application in aquaculture cages that are submerged marine structures (Gardner 2015), and hence, an understanding and investigation of the time-dependent avg. creep strain of this material under the effect of water immersion and temperature is essential.

2.4 Material Preparation

2.4.1 Extruded WPC Material

The WPC specimens with dimensions (L, w, h), 15.0 mm, 7.2 mm ± 0.2mm, 2.7 mm ± 0.2mm (uncertainty in the measurement of the dimensions was reported by computing the

standard deviation of 190 specimens) were cut and machined from extruded wood plastic composite lumber with a cross section shown in Figure 2.1, to conduct the DMTA analysis (creep and creep-recovery experimentation). A 3-point bending submersible clamp was used in these experiments (Figure 2.2). This clamp has the ability to conduct bending tests on a specimen submerged in a fluid environment for temperatures between 20°C and 80°C. The WPC lumber cross section (Figure 2.1) was produced using a twin-screw Davis-Standard Woodtruder™ in the Advanced Structures and Composites Center at the University of Maine's Orono campus (Davis-Standard Woodtruder 2018). The WPC examined here is based on a patent-pending formulation that combines a thermally modified wood flour that was produced at a sawmill in Uimaharju, Finland and a high strength styrenic copolymer system in an equivalent weight ratio to each of the two constituents.

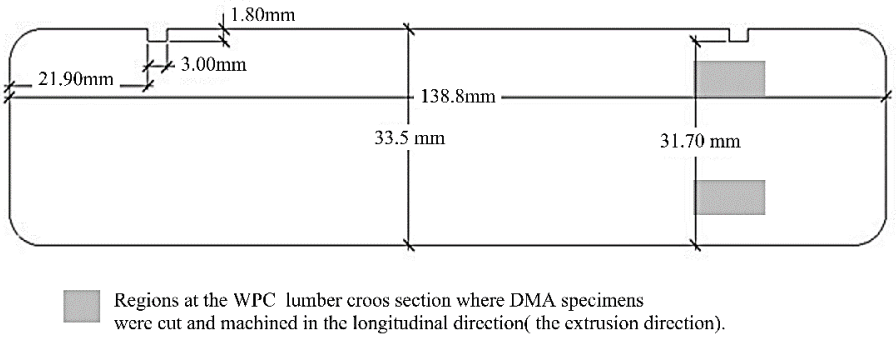

Figure 2.1. WPC cross-section with the highlighted regions where DMTA samples were cut and machined in the longitudinal direction.

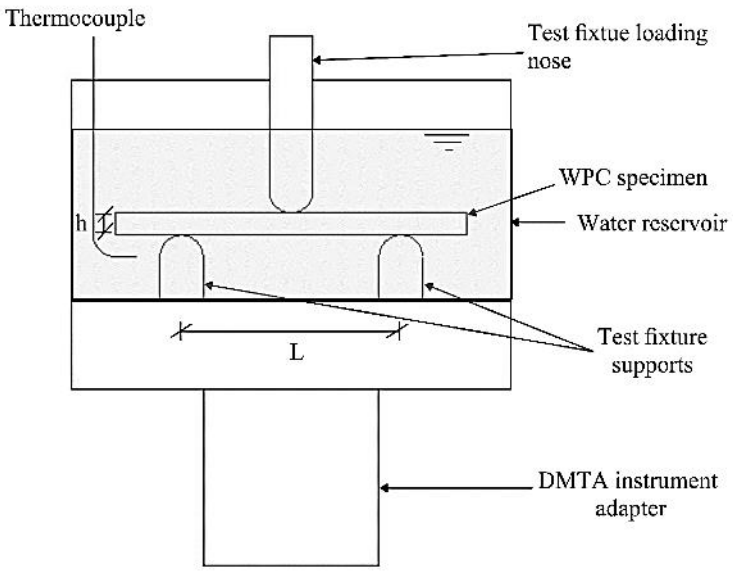

Figure 2.2. Schematic of the DMTA submersible 3-point bending clamp used in the DMTA experiments of WPC specimens with a total specimen span between the supports (L) of 15mm and a thickness (h) of 2.7mm.

2.5 Elastic Modulus and Material Density

The mean modulus of elasticity (three specimens) of the cut and machined WPC specimens was computed for the specimens tested in 3-point bending using two different instruments (non-destructive and destructive): the initial compliance of the creep test that was conducted on the WPC specimens using the DMTA instrument; the other WPC specimens were tested using an Instron dual column tabletop electromechanical (10 kN load cell and in strain control testing). This was done in accordance with ASTM D790 (ASTM) by a linear regression to the linear region (from 10% to 40%) of the flexural load versus the midspan deflection. A density evaluation along the thickness was performed using a QMS density profiler model QDP-01X for ten WPC specimens with the dimensions (length, width, thickness) 51.6 mm, 50.4 mm,

and 33.5 mm to determine the density variation between the surface layer of the WPC lumber and the region in Figure 2.1 where the WPC specimens were cut and machined to be used in DMTA experiments. The mean of the modulus of elasticity (E) from the 3-point bending tests in accordance with ASTM D790, and the WPC density are reported in Table 2.1.

Table 2.1. Mean true modulus of elasticity of WPC specimens obtained from 3-point bending tests and the mean of the density of the WPC lumber.

E (GPa)	4±0.45
Density of the WPC lumber (kg/m^3)	719±9

2.6 The Relationship Between the Modulus of Elasticity (Apparent) and the Length of The WPC Specimen

To investigate the effect of span length on the variation in the modulus of elasticity, a typical flexural load-midspan deflection relationship was obtained for three WPC specimens with different span lengths, and an analysis of variance was performed for the computed modulus of elasticity and the span length, as shown in Figure 2.3. The flexural load-midspan deflection tests were performed to failure for the specimens with a span of 61.9 mm. For the specimens with spans of 50.0 mm and 15.0 mm, the maximum flexural load of the DMTA instrument did not exceed the linear region of the tested WPC specimens.

2.7 Specimen Conditioning

One goal of the study was to compare the hygrothermal avg. creep strain of the WPC material in saltwater and distilled water. Instant Ocean® (Ocean®) mix was added to distilled water to make the saltwater for the conditioning and the testing of WPC specimens. 0.14 kg of

the Instant Ocean® powder was added and mixed with a 3.79 L of distilled water to make the saltwater.

According to the procedure recommended by ASTM D570 (ASTM), the mean of the water uptake (with standard deviation for five specimens at each time the water uptake was measured) was computed and reported as shown in Figure 2.4. Prior to the water absorption process to be conducted, the WPC specimens were dried in an oven at 50℃ for 24 hours. Thereafter, the specimens were immersed in both distilled water and saltwater for one month and the measurement was conducted at each condition (distilled water and saltwater) at one day, one week, two weeks, three weeks, and four weeks, respectively. The specimens were then removed from the water vertically to drain the water from the specimen wiped off using a piece of cotton fabric, and each were weighed. During the preconditioning time (30 days), the WPC did not appear to produce any leachate in the absorption container.

The surface layer of the extruded WPC lumber encapsulates the wood particles with polymer that hinders water uptake by creating a skin layer of polymer at the contact perimeter of the WPC lumber during the extrusion process (6). In this study, however, WPC specimens were produced without a skin layer by machining (using a milling machine with a special blade for cutting plastic-based materials affixed to the head of the milling machine with 150 rpm a rotating speed of the blade) samples far from the surface of the boards. This exposed more wood particles to water during the DMTA tests. In addition, the development of the microcracks on the machined surface of the WPC specimen could also contribute to an increase in water uptake.

2.8 Calculations of the Maximum Flexural Stress Levels

The 3-point bending tests were performed according to ASTM D790 using the Instron electromechanical testing machine. The displacement control method of testing was used with an average strain rate (1.6 mm/min ± 0.2 mm/min) (ASTM) was applied during the flexural test of the five tested WPC specimens. Prior to the testing, the five specimens with dimensions (L = 59.7 mm ± 0.4 mm, w = 7.3 mm± 0.3 mm, h = 3.7 mm ± 0.4 mm) were oven-dried at 50± 3°C for 24 hours (ASTM).

2.9 Dynamic Mechanical Thermal Analysis (DMTA)

Two methods, storage modulus and heat deflection temperature, were used to determine the glassy region of the material behavior by locating the onset of the glassy region by locating the glass transition temperature (T_g) at the onset of the change in the storage modulus curve (E'), as shown in Figure 2.5 (a). A similar approach was used to determine the heat deflection temperature (HDT) by locating the onset of the change in the load-midspan deflection relationship of the specimen in the flexural test, as shown in Figure 2.5 (b). DMTA was carried out using a TA Instruments DMTA Q800 and the 3-point bending submersible clamp to determine the storage modulus (E') and tan δ of the WPC at three conditions: dry; submerged in distilled water; and submerged in saltwater (ASTM, Herzog et al. 2005). Two lines (TA, TB) were constructed by performing a linear regression of the curve at the regions, before and after the change in the curve of storage modulus and the midspan deflection, respectively. The calculation of T_g and HDT was based on the intersection of TA and TB. Specimens with dimensions 15.0 mm ± 0.0 mm, 7.2 mm ± 0.2 mm, 2.7 mm ± 0.2 mm (the uncertainty in measurement of the WPC specimen dimensions was reported based on the computation of standard deviation of 190 WPC specimens) were tested in 3-point bending at 1 Hz frequency and

with 0.01% constant strain amplitude. Tests were conducted over a range of temperature from 25℃ to 80℃, and at a scanning rate of 3℃/min.

The specimens were tested in a fluid environment with a 6:1 span to depth ratio (L/h) (TA instruments) and the maximum flexural creep stress and the maximum avg. flexural creep strain were computed and reported accordingly.

2.10 Strain and Strain Recovery

Creep and creep-recovery experiments were performed using the DMTA instrument model Q800 and using the 3-point bending submersible clamp. A thermocouple extension on the clamp measured the water temperature at 1mm distance from the WPC specimen (Figure 2.2). Two different stress levels and three temperatures were used during the experiments and five replicates for each test were considered. To avoid exceeding 50% of the maximum capacity of the applied load (18 N) of the DMTA instrument and to keep the maximum applied flexural stress in the linear region, the stress levels were 9.2 %, and 13.8% of the maximum flexural strength. Ten minutes of soaking time, prior to the creep and creep-recovery experiment, were followed by 30-minutes creep and 30-minutes recovery.

2.11 Discussion of Results

2.11.1 Hygrothermal Effect on Glass Transition Temperature and Modulus Of Elasticity of WPC.

The moisture content of each specimen was determined with respect to the oven dry weight of the specimens (dry weight). Figure 2.4 shows the water uptake of the WPC specimens during the month of conditioning. T_g and HDT of the three conditions (dry, saltwater, and distilled water) were determined as shown and reported in Figures 2.6 (a and b) and Table 2, and

their values are (44, 38, 41°C) and (44, 45, and 40°C), respectively. The determination of T_g and HDT for the dry and the distilled water immersed samples showed similar values for all the three conditions (ca. 40 and 44°C, respectively), except for the saltwater condition where HDT was 17% higher than T_g. This difference can be related to the effect of the cross-linking (Chakraverty et al. 2015) of the polymer and its effect on the segmental relaxation, which reduces the free volume and increases the HDT, and is believed to occur during the extrusion process of the WPC (11, 24). Since two regions (Figure 2.1) in the cross section of WPC lumber were selected to produce specimens for DMTA, this difference in regions for the specimens can lead into a difference in their storage modulus (modulus of elasticity) produced by the change in the density across the thickness of WPC lumber (Figure 2.6) (23). This is the reason of having the initial values of storage modulus of the specimens tested in water immersion (distilled and saltwater) to be relatively higher than the value of storage modulus in dry conditions (varied from 1.59 to 0.81 GPa). In conclusion, the determination of both T_g and HDT has enabled locating a region for the range of temperatures between 25 and 45°C where the WPC material has the ability to carry loads.

The T_g and E' of the WPC material decreased because of hygrothermal effects. The glassy region for temperatures below T_g represents the region where the WPC material has rigidity and can be effectively used in structural applications (Mark 2007). The hygrothermal effect tends to decrease the glassy region extent by decreasing the value of the T_g. Furthermore, E' experiences a decrease in its value in this region. This reduction is explained by the motion in the molecules of plastics accompanied with the onset of transition from a glassy to the rubbery region. Furthermore, this reduction in T_g and E' can be related to weakening the interfacial bond between the wood particles and the plastics of the WPC, when that molecular transition takes

place . This study showed that the water uptake of the WPC immersed in saltwater is faster than the water uptake of the WPC immersed in distilled water, and according to Chakraverty (Chakraverty et al. 2015), this fast rate can be related to the ionic interaction that might occur between the dissolved salt and the available hydroxyl groups on the thermally modified wood. However, this rate of water uptake decreased during the immersion time from (56% to 6% to 2%) for the periods 1, 7, and 14 days, respectively, until reaching a constant rate at 21 days, as shown in Figure 2.4. It is known that wood particles are the source of the water uptake in WPC (Lenth & Kamke 2007), but in this study, the thermally modified wood of the WPC is less water absorbent because of the reduction in hydroxyl groups resulting from heat treatment . The finding in this study conflicts with what other researchers have reported that more tap water is absorbed in WPC than saltwater, Nonetheless, Kazemi-Najafi (Kazemi & Kordkheili 2011) in his study, showed that the type of water has a significant effect on the degree of uptake of WPC (i.e. WPCs absorb more moisture in saltwater than in distilled water). Kazemi-Najafi correlated the increase in the water uptake produced by the increase in the density of the saltwater compared with the distilled water, and to the existence of the metallic ions in the saltwater (sea water) and their ability to sediment on the wood flour and hence, increase the water uptake of the WPC. Thus, the glassy region of the WPC material immersed in saltwater is narrower than the glassy region of the dry WPC material and WPC material immersed in distilled water, as shown in Figure 2.5, respectively. However, the amorphous polymer used in the WPC of this study, showed a significant plateau that indicates the material maintains the storage modulus (E') as shown in the region A of Figure 2.5 (a and b). This response is dependent on the cross-link density, or on the well-developed interfacial bonding between the modified wood particles and the polymer matrix in the region below the T_g . However, this feature contradicts with the

behavior of the conventional WPCs in the previous studies using semi-crystalline polymers. Therefore, this study suggests that the WPC can be used in structural applications over a range of temperatures below the T_g.

Table 2.2. Glass transition temperature and heat deflection temperature of WPC under three different testing conditions: dry, saltwater and distilled water.

Condition of tested specimens	**T_g from storage modulus-temperature relationship (℃)**	**HDT from mid-span deflection- temperature relationship(℃)**
Dry (D)	44 ± 1	44 ± 2
Saltwater (SW)	38± 2	45 ± 2
Distilled water (DW)	41± 1	40 ± 1

The mean modulus of elasticity (E) was normalized with respect to the modulus of elasticity of the WPC specimens (with span of 15 mm) at 25°C. This modulus of elasticity was computed from the initial compliance (reciprocal of the initial compliance) of the creep experiments in dry (D) condition at 25°C temperature to be 1.4 GPa which is 35% of the true modulus of elasticity (4 GPa) obtained from the WPC specimens with a span of 59.7 mm in accordance with ASTM D790. This reduction in the modulus of elasticity can be related to either the variation in density between the cut and machined specimens and their location from the top surface of the WPC lumber (i.e. the closer the WPC specimen to the surface layer, the higher the E value), or to the effect of the span to depth ratio (L/h) and the development of shear deformation. A density evaluation across the thickness of the WPC lumber was performed using

a QMS density profiler model QDP-01X, to indicate the reduction in the modulus of elasticity as a function in the reduction in the density, along the thickness of the WPC lumber. Pavel, et.al (Pavel et al. 2015) correlated the relationship between the modulus of elasticity and the density of the material via the specific modulus. The higher the specific density, the higher modulus of elasticity is indicated. Nonetheless, a 2.6% reduction in the density of the WPC lumber between the density of the surface layer and the core layer of the WPC lumber as shown in Figure 2.6 was not considered the primary cause for the reduction in the modulus of elasticity in this study. Mehndiratta et al. (Mehndiratta et al. 2018) reported an approximately 42% reduction in the flexural modulus of bi-directional glass fiber reinforced polymer laminate when the span increased from 32 mm to 65 mm for specimens tested in 3-point bending. Garoushi et al. (Garoushi et al. 2012) conducted 3-point bending tests on short fiber reinforced composite resin specimens at six different span lengths: 20 mm; 15 mm; 10 mm; 7 mm; 6 mm; and 5 mm. Danawade et al. (Danawade et al. 2014) conducted a study to investigate the effect of span to depth ratio on the obtained value of modulus of elasticity of wood-filled steel tubes. Four different values of L/h were investigated; 7.09, 14.17, 13.98, and 27.95. The modulus of elasticity was computed in these four different values of L/h for the; wood beams, the hollow section rectangular steel tube beams, and the wood filled steel tube beams. Danawade et al. (Danawade et al., 2014) found that the value of the modulus of elasticity was high when the L/h values were 27.95 and 13.98 for all the three tested beams. Danawade et al. (Danawade et al., 2014) findings agreed with the recommended L/h by ASTM. Thus, the modulus of elasticity can be obtained from the specimens that meet the recommended L/h by ASTM even if the shear deformation is ignored.

The true modulus of elasticity (E_{true}) (shear free modulus of elasticity) is a material independent property and it should not be considered as a function of the total beam span between the supports (L), or the L/h ratio (Berube, Lopez-Anido, & Goupee, 2016, Davids et al., 2017). However, in accordance with ASTM D790, ASTM D2915, ASTM D6109 the shear deformation can be ignored in the computation of the modulus of elasticity and the resulting modulus of elasticity can represent the material independent property for the specimens with large span to depth ratio ($L/h \geq 16$)(Danawade et al. 2014, Gibson 2016). Equation 2.1 can be used to compute the apparent modulus of elasticity when the shear deformation is ignored and can be used for specimens with L/h greater than or equal to 16. Nevertheless, Equation 2.1 does not consider the shear deformation in the computation of the modulus of elasticity. To include the shear deformation (Δ_s) and the flexural deformation (Δ_f) in the computation of the modulus of elasticity, Equation 2.2 (ASTM), Instruments 2018, Timoshenko & Goodier 1951) can be used, but the values of (E/G) are difficult to obtain (Ferdous et al. 2016). According to Carlsson and Pipes (Carlsson et al. 2002), the true modulus (E) of elasticity in the value of E/G is not known, hence, it can be replaced by the tensile modulus and used in the value of E/G. Carlsson and Pipes (Carlsson et al., 2002) reported in their study the computed modulus of elasticity (computed using Equation 2.2) had different values with respect to the values of L/h (from L/h=20 to L/h=120). In DMTA experiments, it is recommended to account for the shear deformation when the L/h is smaller than 10 (Instruments, 2018). However, with the assumption of the WPC as an isotropic and linearly elastic material, the E/G value can be replaced by an expression that contains Poisson's ratio (ν) (Dura 2005, Hamel et al. 2014, TA Instruments, Storage et al. 2013).

Since this study did not conduct experiments to compute the true modulus (shear free modulus) or the shear modulus (G), the "standardized value"(ASTM) [the value of the modulus of elasticity obtained using Eq.1 for the long span in this study (59.7mm)] of the modulus of elasticity was computed using Equation 2.1, to be 4 GPa.

$$E = \frac{mL^3}{4wh^3} \tag{2.1}$$

Where m is the slope of the tangent to the initial straight-line portion of the load-deflection (P-Δ) curve, L, w, h are the dimensions of the specimen.

$$E_{true} = \frac{mL^3}{4wh^3}\left(1 + \frac{6h^2}{5L^2}\left(\frac{E}{G}\right)\right) \tag{2.2}$$

The authors recognize that three replicates is not sufficient to characterize the WPC material (i.e., ASTM D790 suggests more than five specimens). In some studies (Balma 1999, Chang 2011, Decew 2011, Fredriksson et al. 2007), three replicates have been used. For instance, Decew (Decew 2011) conducted a test in accordance with ASTM D638 using three replicates. For the purpose of illustrating that the reduction in modulus of elasticity in this study is a function of the span length, three replicates of the relationship between the modulus of elasticity and the span length were reported, as shown in Figure 2.3.

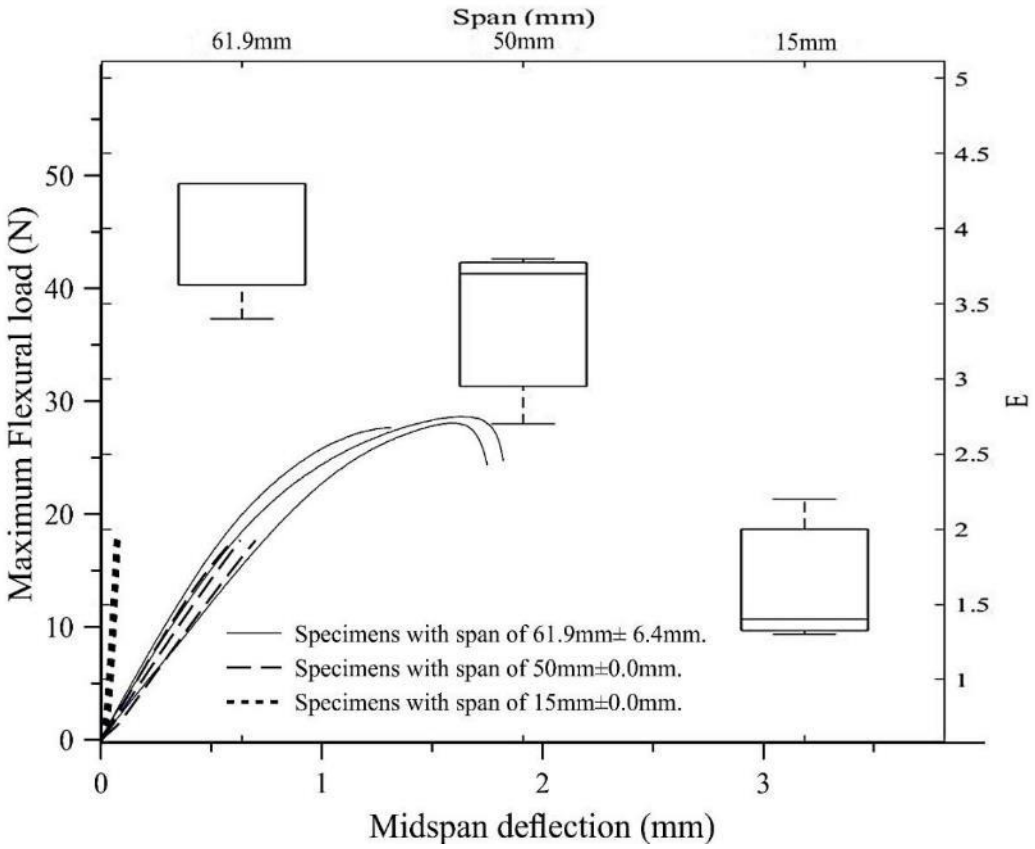

Figure 2.3. Typical flexural load versus midspan deflection for WPC specimens at three different span lengths (15, 50, and 61.9 mm) and the ANOVA analysis of the obtained modulus of elasticity E using Equation 2.1.

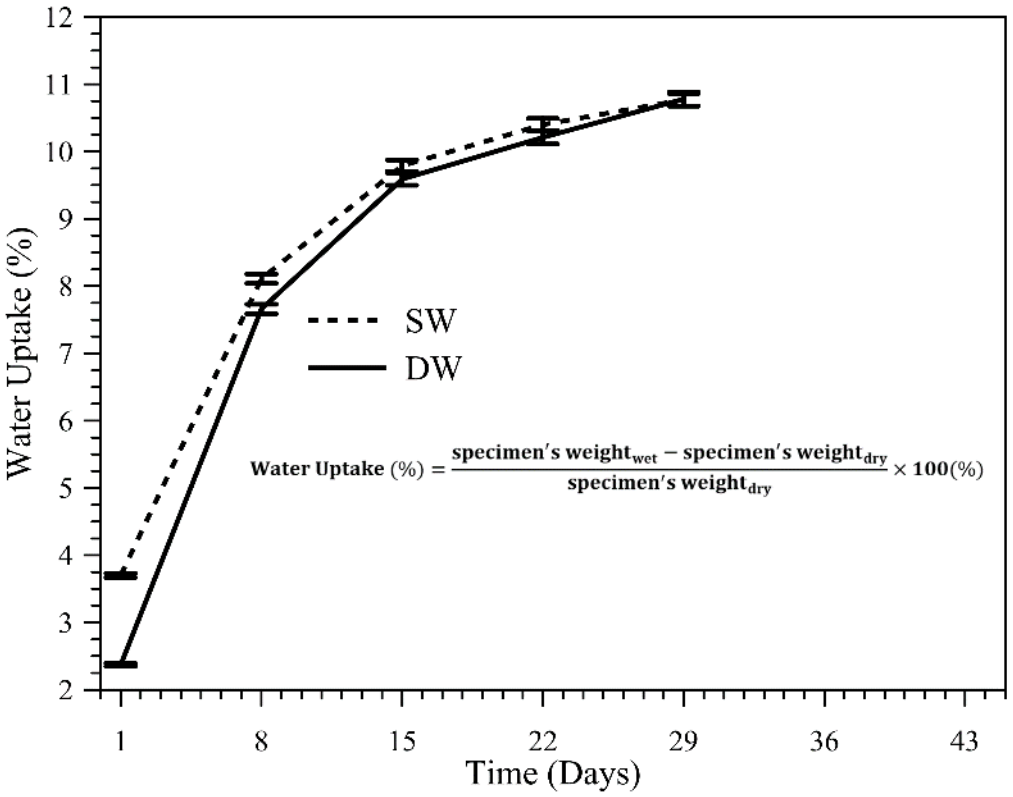

Figure 2.4. Mean of the water uptake of WPC in distilled water and saltwater.

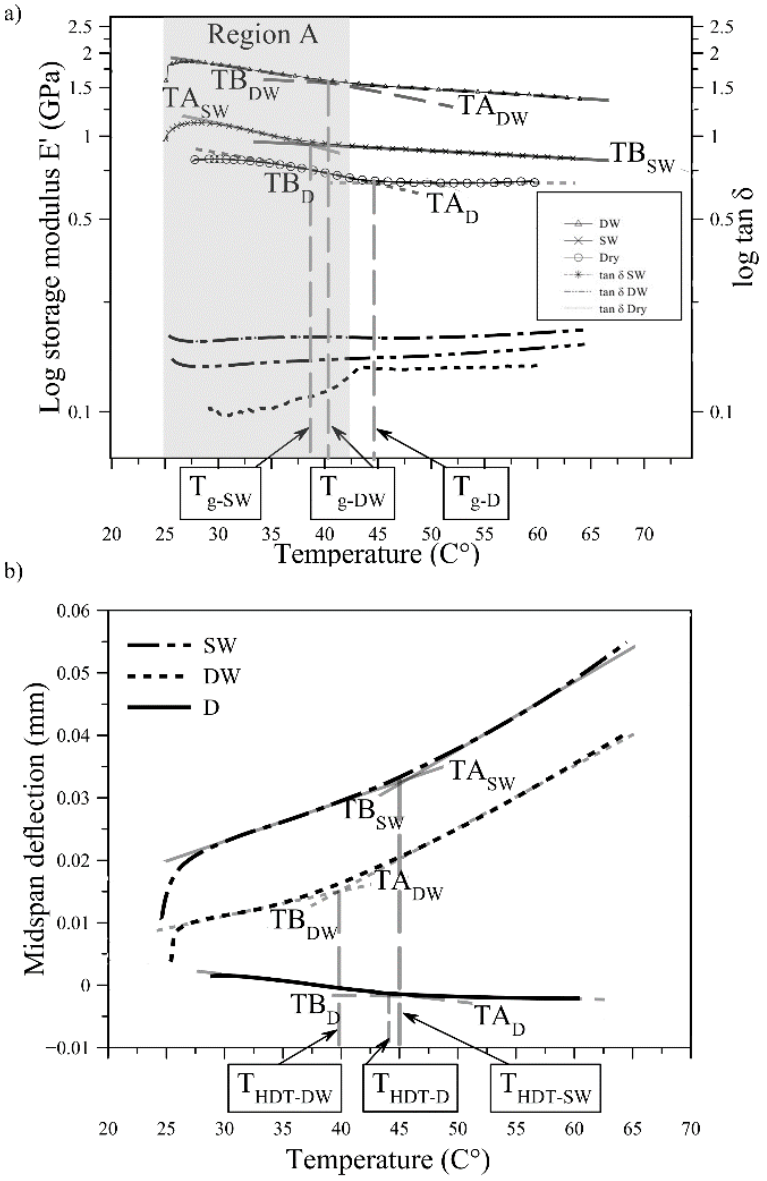

Figure 2.5. a) Storage modulus and tan δ versus temperature of WPC under three different testing conditions; dry (D), saltwater (SW), and distilled water (DW), b) Mid-span deflection versus temperature of WPC under three different testing conditions; dry (D), saltwater (SW), and distilled water (DW).

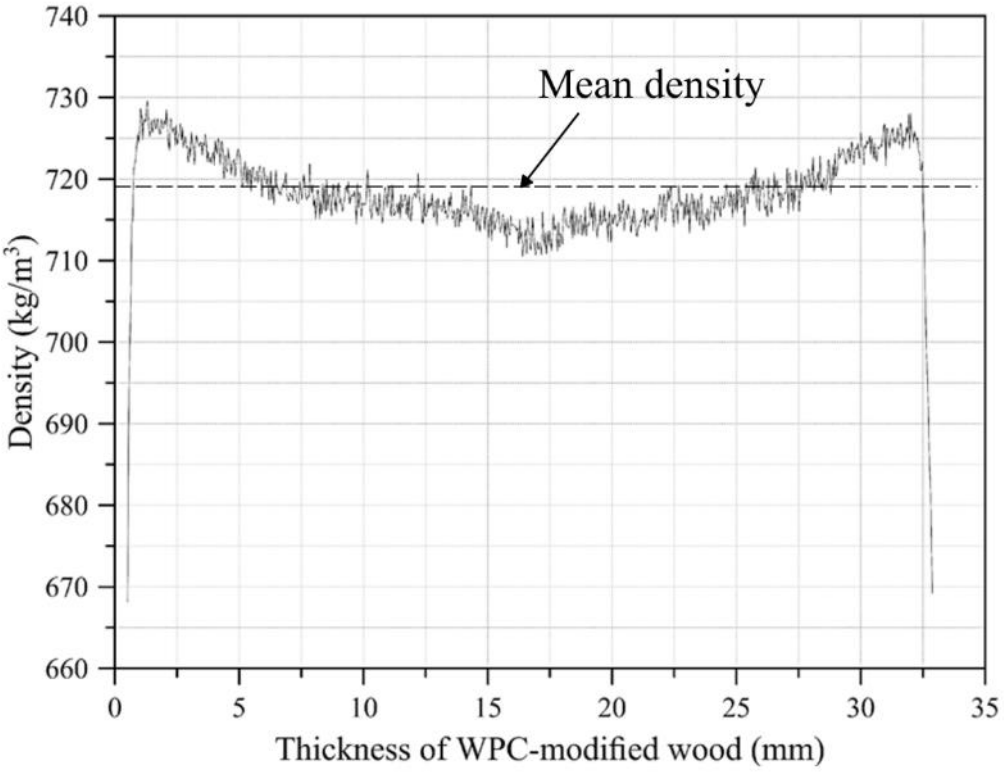

Figure 2.6. Density profile of the WPC lumber.

Unlike polyolefin-based WPCs that have been reported in previous studies, the WPC material in dry condition maintained the normalized value of the modulus of elasticity over the range of temperatures examined (25, 35, and 45 °C) as shown in Figure 2.7. The rate of decrease in normalized (E) for the specimens conditioned and tested in saltwater and distilled did not exhibit a linear relationship and the rate of decrease for temperatures higher than 35°C was smaller than the rate of decrease for the temperature below 35 °C as shown in Figure 2.7. This low rate of decrease is related to the properties of the styrenic polymer comprising the WPC and

its ability to maintain modulus of elasticity (E) at elevated temperatures below the T_g. The hygrothermal effect is attributed to the higher water uptake of the specimens tested in saltwater compared with the specimens tested in distilled water, and the degradation-decrease in the normalized (E) of the specimens in saltwater was higher than the degradation in the specimens tested in distilled water. However, this degradation-reduction produced by saltwater immersion was higher for the range of temperatures below 35℃, and the reduction was smaller than the specimens tested in distilled water. This finding can be beneficial for the use of WPC in aquaculture cages (totally submerged structures) in warmer ocean water (temperature below 45 °C).

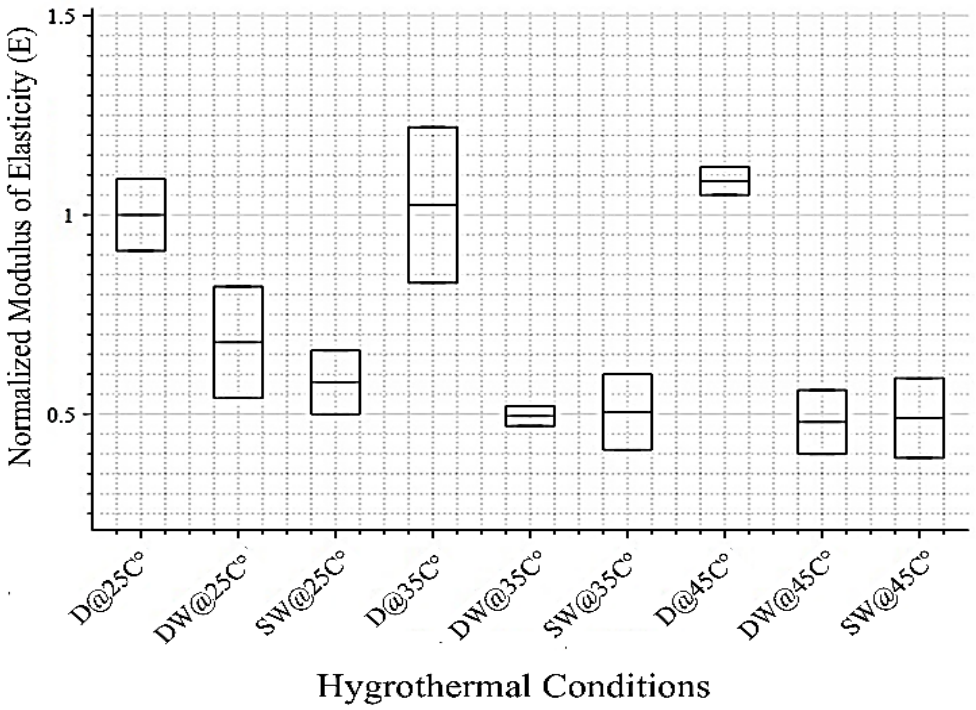

Figure 2.7. Normalized (E) versus temperature at three different testing conditions; dry (D), saltwater (SW), and distilled water (DW).

2.12 Average Creep Strain and Creep Strain-Recovery of WPC

Strain recovery is governed by the elastic behavior of the viscoelastic material, where the unrecoverable strain is governed by the viscous behavior. For all the strain recovery data shown in Table 2.3 and Figure 2.8, the tested WPC specimens under immersion conditions (distilled water and saltwater) have shown higher strain recovery percentages when compared with the WPC specimens tested in the dry condition. The immersion in distilled and saltwater increases the recoverability of the viscous response to be greater than 2% for all the creep experiments under the different hygrothermal environmental conditions and this is attributed to the water uptake (i.e. the higher the water uptake, the higher the strain recovery), and this finding agreed with the findings of Najafi when WPC with 70% wood flour was immersed in water for 30 days

showed higher creep displacement recovery than the WPC immersed in water for seven days. Figure 2.9 illustrates the WPC 30 minutes creep and 30 minutes recovery under 3.75MPa of the maximum applied flexural stress at three different values of temperature 25-45°C at three different exposure conditions: dry (D); saltwater (SW); and distilled water (DW).

Since the WPC material maintains stiffness over the evaluated temperature range and unlike the behavior of polyolefin-based WPCs that show a reduction in the modulus of elasticity as the temperature increases. Further illustration of the maintained behavior of the creep compliance of the WPC, instead of experiencing high deflection, the specimens exhibit less deformation when the duration of the sustained load increases under an increase in the temperature, as shown in the constructed "isochronous curves" in Figure 2.9. Isochronous curves were constructed using the applied maximum flexural stress-strain relationship for the strains (average creep strain) at times 5, 15, and 30 minutes and for two cases of conditioning and testing (dry and saltwater) as shown in Figure 2.9 (a and b) (Gibson, 2016). However, for the case of saltwater conditioning and testing, the stress strain relationship tends to be nonlinear (unlike the linear relationship for the dry condition) at 35 and 45 °C. The WPC was studied using 30 minutes creep and 30 minutes creep recovery under two different levels of stresses and under different hygrothermal conditions (three levels of temperatures and two types of water immersion). For the 2.5 MPa level of stress (at 25, 35, and 45℃), the values of the 30-minute creep strain for the WPC specimens conditioned and tested in saltwater were 12, 25, and 7% higher than the avg. creep strain values of the WPC specimens conditioned and tested in distilled water, whereas at the 3.75 MPa level of stress, the 30-minute creep strain value of the WPC tested in saltwater was 8% higher than the avg. creep strain of the avg. creep strain of the specimens in distilled water at 25 °C, and the avg. creep strain values of the specimens tested in

saltwater were 21 and 17% lower than the creep strain of the specimens tested in distilled water at 35 and 45℃, respectively. The reason of having lower avg. creep strain for the WPC specimens tested in saltwater at 3.75 MPa level of stress and at 35 and 45℃ than the specimens tested in distilled water can be attributed to maintaining the modulus of elasticity of the WPC at elevated temperatures under this level of stress.

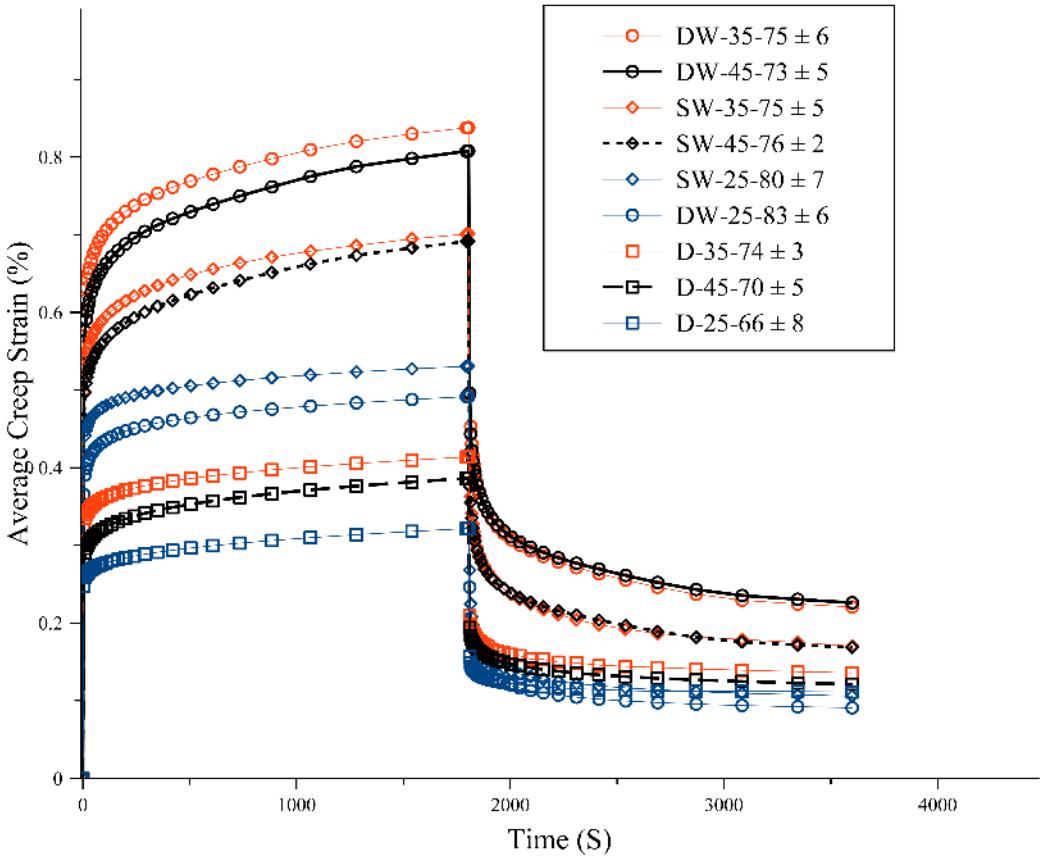

Figure 2.8. Avg. creep strain and strain-recovery of the WPC specimens subjected to a maximum flexural stress of 3.75 MPa at three different temperatures 25, 35, and 45℃ and under three testing conditions (D, SW, and DW).

Table 2.3. Maximum avg. flexural creep strain and strain recovery of WPC in the three different; conditions, values of temperature, and two levels of maximum flexural stress.

Condition **D=Dry** **SW=Saltwater** **DW=Distilled Water**	**Applied Maximum Flexural Stress (MPa)**	**Temperature (°C)**	**Maximum avg. Creep Strain (%)**	**Strain Recovery± standard deviation (%)**
D	2.5	25	0.20	72±4
SW			0.48	84±5
DW			0.43	78±3
D	2.5	35	0.27	67±3
SW			0.66	72±6
DW			0.53	76±5
D	2.5	45	0.24	65±5
SW			0.75	70±5
DW			0.70	77±3
D	3.75	25	0.32	66±8
SW			0.53	80±7
DW			0.49	83±6
D	3.75	35	0.41	74±3
SW			0.62	75±5
DW			0.75	75±6
D	3.75	45	0.39	70±5
SW			0.69	76±2

DW	0.81	73±5

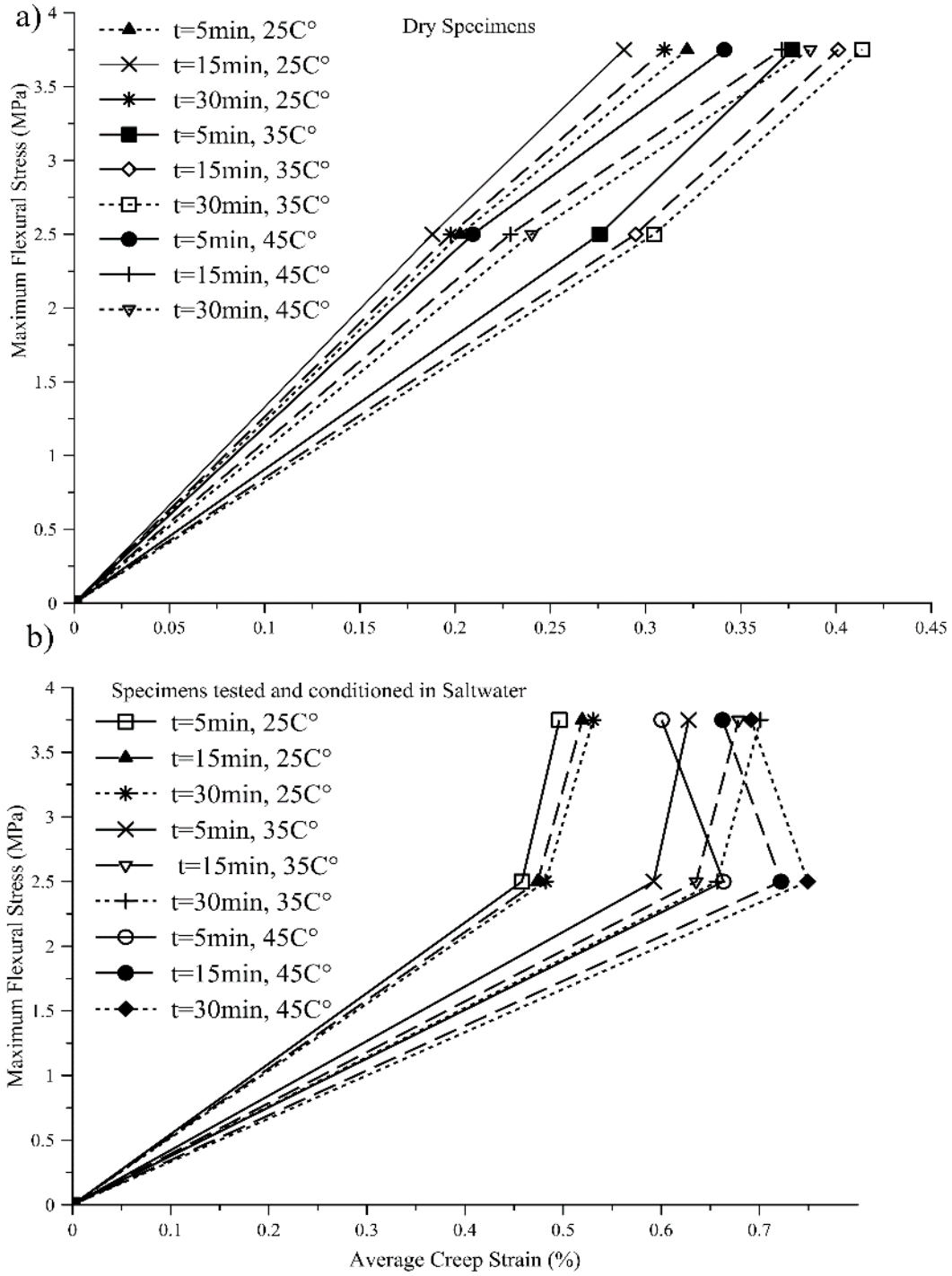

Figure 2.9.Isochronous stress-strain curves: a) WPC specimens in the dry condition, b) WPC specimens conditioned and tested in saltwater.

2.13 Comparison of the WPC Time-Dependent Behavior (Creep Strain) with Previous Studies

The WPC materials in the literature were made with different formulations, for instance, untreated pine wood flour particles, and polypropylene as a plastic, or pine wood flour with HDPE plastic. To quantify the performance of the thermally modified WPC in avg. creep strain with other formulations in terms of creep behavior, creep strain fractional increment (CSFI) values were computed for the purpose of comparison as shown in Equation 2.3. For further illustration and comparison purposes, a 250-minute creep experiment was conducted at the three conditions under 2.5 MPa of the maximum flexural stress and at 45℃ temperature.

$$\text{CSFI} = \frac{\text{maximum avg. creep strain - instantaneous strain}}{\text{instantaneous strain}} \times 100\% \qquad (2.3)$$

It can be concluded from the comparison results reported in Table 4 that the WPC in this study has a lower increase in avg. creep strain for all the conditions; dry, saltwater, distilled water. Even though previous studies did not test the WPC in an immersed environment over a range of temperatures, this study showed lower CSFI for specimens conditioned and tested in distilled water compared with the finding by. Dry specimens showed very low time-dependent deformation for specimens tested for 250 minutes. The reason of this enhancement in the low time-dependent deformation of the WPC can be related to the thermal treatment of the wood flour and its contribution to increasing the modulus of elasticity of the wood wall cells, and to the enhanced interfacial bonding between the wood particles and the polymer. This enhanced time-dependent behavior enables the material to be used in structural applications especially when low levels of stress are applied.

Furthermore, the material has potential to be used in marine applications where the material is immersed in warm tropical waters for instance; the Gulf of California, Mexico, the Pacific Islands, South Padre Island TX (Buoy 42003), San Juan P.R. (Atlantic Site), Virginia Key, FL, Key West FL, and Hawaiian Island Coast (Commerce 2018).

Table 2.4. Comparison of WPC creep behavior with previous studies.

Source	**Loading stress**	**Duration (s)**	**Applied stress (MPa)**	**Condition of testing or specimen conditioning**	**CSFI**
This paper	Flexural	1800	3.75	D@ 25℃	29%
				DW@ 25℃	34%
				SW@ 25℃	27%
				D@ 45℃	40%
				DW@ 45℃	51%
				SW@ 45℃	48%
		15000	2.5 MPa	Dry@ 45℃	37%
				DW@ 45℃	10%
				SW@ 45℃	80%
Kazemi et al.	Flexural	1800	ca 4.2	7 days immersion	58%
				30 days immersion	58%
Chang	Flexural	600	5	D @ 45℃	95%

2.14 Conclusions

1. The creep strain fractional increment (CSFI) of the WPC specimens conditioned at the highest level of temperature and under water immersion was 13% which is 86% lower than the CSFI of the preconditioned and dry specimens reported in previous studies. The WPC material in this study maintained (E) at elevated temperatures and exhibited relatively low time-dependent deformation compared with polyolefinic WPC materials from the literature, most-likely attributed to its strong interfacial bond between the wood and polymer.

2. Since water immersion has an ability to mitigate the effect of temperature on the viscous behavior of the viscoelastic WPC, the ability to recover the deformation after the loading source was removed was high for the specimens under the synergistic effect of temperature and immersion, compared with the deformation recovery of the same material under just the temperature effect. That indicates in addition to the deformation recovery attributed to the elastic behavior, a recovery to the viscous part of the viscoelastic WPC occurred.

3. According to the low variation in density along the thickness of the WPC lumber, it is believed that this material has a unique formulation, hence it has enhanced modulus of elasticity by maintaining E at higher temperatures over the range of temperatures below T_g, related to the developed interfacial bonding between the wood particles and the polymer matrix. Furthermore, the low variation in density suggests good dispersion of the wood flour throughout the thickness of the WPC lumber and uniform structure of the composite.

CHAPTER 3

MODELING THE HYGROTHERMAL CREEP BEHAVIOR OF WOOD PLASTIC COMPOSITE (WPC) LUMBER MADE FROM THERMALLY MODIFIED WOOD

3.1 Abstract

The viscoelastic behavior of an extruded wood plastic composite (WPC) made from thermally modified wood under hygrothermal treatment was studied and modeled. Multiple 3-point bending creep/recovery tests were carried out using a dynamic mechanical thermal analyzer (DMTA) equipped with a submersible clamp. WPC specimens with 15 mm span were subjected to two initial applied stresses; 9 and 14% of the flexural strength in 30 minutes of creep and 30 minutes of creep recovery under the combined effects of temperature (25, 35, 45℃) and water immersion (saltwater and distilled water). A dry condition WPC control was used to compare the hygrothermal effects with respect to the control conditions. The WPC material in this paper exhibited a linear viscoelastic behavior under the effect of temperature, whereas, a nonlinear viscoelastic behavior was observed under immersion conditions. A power law model is considered a useful model to describe the creep behavior of WPC specimens with a 15mm span in the control and the saltwater conditions and at 45℃. A power law model was used to describe 180-day creep deflection of WPC lumber beams with a 853 mm span subjected to 12 MPa of the flexural strength in 4-point bending at 50% RH and at 21℃. The power law model predicts that the WPC lumber will reach a flexural strain in outer fiber of 1% in approximately 150 years.

3.2 Introduction

Wood plastic composites, unlike elastic materials, exhibit viscoelastic behavior. Gibson (Gibson, 2016) reported that thermoplastic composites in general, exhibit a linear viscoelastic

behavior, and that can be represented as a physical model; for instance, spring-dashpot in a series arrangement. The spring represents the elastic behavior (i.e., following Hooke's law) of thermoplastic composites, whereas the dashpot represents the "Newtonian fluid" viscosity. However, other researchers (Pooler & Smith 2016) reported that WPC materials exhibit nonlinear viscoelastic behavior that can be related to the effect of the filler (i.e., the wood flour). Barbero (Barbero 2013) distinguished between the linear and the nonlinear viscoelasticity behavior of viscoelastic materials via the stress dependency of the models' parameters.

To better understand the viscoelastic behavior of WPCs, different models have been proposed in the literature; Maxwell, power law, generalized Burger's, standard linear solid, standard nonlinear solid, Maxwell-Kelvin, linear solid Zener, and improved Zener (a.k.a. Prony Series) models. The time-dependent viscoelastic behavior of the material based on these models is governed either by an empirical (mathematical) equation similar to the power law model, or by the number of the spring and dashpot elements in the model (physical model), and on the arrangement of these elements (parallel or in series) (Barbero 2013; Gibson 2016; Nuñez et al. 2004; Tajvidi & Simon 2015). Certain models can describe the short-term time-dependent behavior of the viscoelastic material, whereas, other models can describe the long-term time dependent behavior of viscoelastic materials.

Dynamic mechanical thermal analysis (DMTA) instruments and techniques have helped researchers to conduct a variety of short-term experiments, to predict or evaluate the time-dependent behavior of wood plastic composite (WPC) specimens in a short period of time, and hence, to provide a better understanding of the time-dependent behavior of the material over a longer period of time. Tamrakar et al.(Tamrakar et al. 2011) applied a generalized Burger's model to describe the strain of WPC and polyvinyl chloride (PVC) specimens under a short-term

(100 min.) tensile creep test. Pooler (Pooler 2001) used a power law and Prony Series models to describe the 10 min. and 600 min. creep behavior of WPCs. Xu et al (Xu et al. 2001) implemented a three parameter power law model to investigate the creep behavior of wood filled polystyrene/high-density polyethylene. Slaughter used a three parameter power law model to describe the creep behavior of wood polypropylene plastic composites(Slaughter 2006). Hamel (Hamel et al. 2011) implemented a two parameter power law model on WPC for seven different formulations in axial creep experiments.

WPC flexural creep experiments have not been implemented solely for short-term (below 24 hours) behavior using small specimens (DMTA specimens that has the span $\leq$ 50 mm), but also long-term (> 24 hrs.) creep implemented on large-scale specimens (WPC specimens have spans >100 times the size of DMTA specimens) (Alvarez-Valencia et al. 2010). For instance, Brandt and Fridley (Brandt & Fridley 2003) conducted 90-day creep experiments on specimens with span length of 1830 mm in flexure. Likewise, Hamel (Hamel et al. 2011) conducted creep experiments for three years in compression, tension on specimens with gage lengths of 12.7 and 57.1 mm, respectively. Hamel (Hamel et al. 2011), further predicted the creep behavior of WPC in flexure for 90 days for WPC specimens with a span of 2130 mm.

The objective of the research presented here was to characterize the hygrothermal creep response of a WPC material evaluated under water immersion and compare it with the creep responses (displacements) published in the literature for other exposure conditions.

In this study, a DMTA instrument with a 3-point bending submersible clamp was used to conduct short-term creep and creep-recovery experiments under the combined effects of water immersion and temperature on preconditioned WPC specimens with a 15 mm span, and to

compare that with the control (reference) dry state of the specimens. The WPC materials exhibit different time-dependent behavior, attributable to their different formulations (i.e. different type of plastics and different types and quantity of wood flour). A further description on the creep behavior of the WPCs was conducted by using 250-minute and 180-day creep experiments using power law models. The WPC material used in this study has potential for application in submerged marine structures (Gardner & Han 2010), and hence, an understanding and investigation of the time-dependent behavior of this material under the effect of water immersion and temperature is necessary.

3.3 Experimental

3.3.1 Materials and Equipment

3.3.1.1 30-Minute and 250-Minute Creep Experiments

WPC specimens with dimensions (L, w, h), 15.00 mm, 7.24 mm ± 0.18 mm, 2.69 mm ± 0.24 mm were cut and machined from extruded wood plastic composite lumber with width and thickness equal to 139 and 34 mm, respectively. A dynamic mechanical thermal analyzer (DMTA) (TA Q800) instrument was used to conduct the creep and creep recovery experiments. A 3-point bending submersible clamp was used in these experiments as shown in Figure 3.1 a. This clamp has the ability to conduct a 3-point bending test on a specimen submerged in a fluid environment over a range of temperatures from room temperature (ca.20℃) to 80℃. To ensure the temperature measurement in the liquid environment is the specimen's temperature, an extended thermocouple in the liquid environment of the clamp was located at 1mm distance from the tested specimen The WPC lumber was produced using a counter rotating twin screw Davis-Standard Woodtruder™ in the Advanced Structures and Composites Center at the University of Maine, Orono, Maine (USA) ("Davis-Standard Woodtruder" 2018).

3.3.1.2 180-day Creep Experiments

Five WPC lumber specimens with a span length of 853 mm, were loaded in a 180-day creep experiment in 4-point bending, as shown in the schematic of Figure 3.1 b. The 180-day experiment was conducted in the creep room at the Advanced Structures and Composites Center at the University of Maine, Orono, Maine. The relative humidity (RH) and temperature were controlled during the 180 days to be 50% ± 5%, and 21℃ ± 2℃. The WPC examined here is based on a patent-pending formulation that combines thermally modified wood flour that was produced at Uimaharju sawmill in Finland with a high strength styrenic copolymer system in an equivalent weight ratio to each of the two constituents. WPC specimens were preconditioned for one month in both saltwater and distilled water.

3.3.2 Mechanical Testing

3.3.2.1 DMTA Creep Experiments

To obtain the flexural strength WPC used in the DMTA creep experiments (the cut and machined specimens), 3-point bending tests were performed according to ASTM D790 using an Instron dual column tabletop electromechanical testing machine. A 10 kN load cell was used in displacement control method of testing with an average crosshead speed motion of 1.59 mm/min ± 0.17 mm/min (ASTM) was applied during the flexural tests of the five WPC specimens, (ASTM). Prior to the testing, the five WPC specimens with dimensions (L, w, h) (59.68 mm ± 0.39 mm, 7.25 mm± 0.25 mm, 3.73 mm ± 0.39 mm), were oven-dried at 50± 3℃ for 24 hrs. (ASTM).

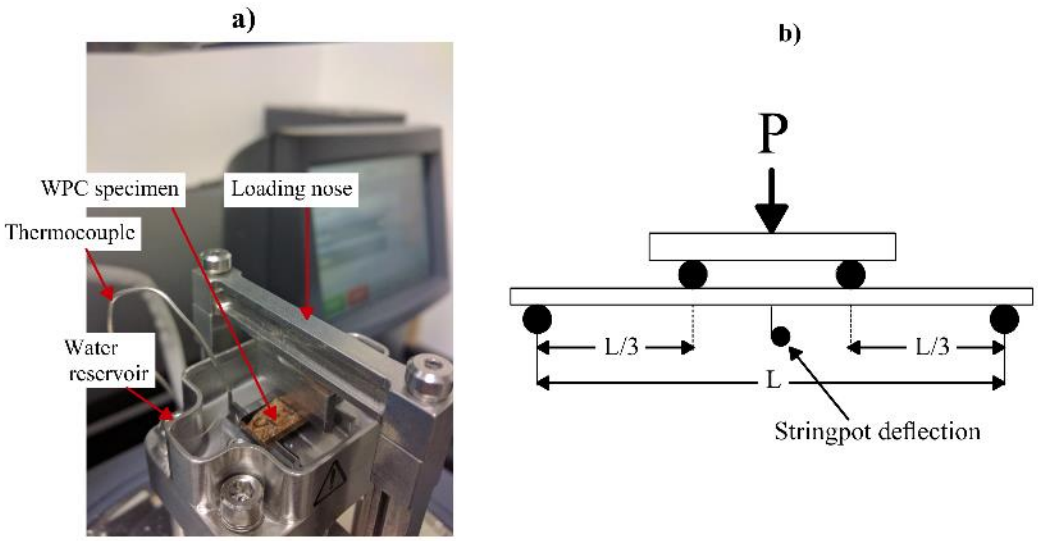

Figure 3.1.a) 3-point bending DMTA submersible clamp, b) a schematic of the 180-day creep experiment in 4-point bending.

The applied initial flexural stress levels of the WPC specimens in the DMTA experiments were selected to be 9.20 %, and 13.8% of the ultimate flexural strength. This selection of the stress levels was made based on the recommendation from previous studies; for instance, Hamel (Hamel et al. 2011) recommended studying stress levels that are below 20% of the ultimate stress. Thus, the stress levels in this study were selected to be below 15%. The average ultimate flexural strength was 27.22 MPa ± 3.88 MPa with a coefficient of variation (COV) of 13% and hence, the applied initial flexural stresses in the DMTA experiments were 2.5, and 3.75 MPa, respectively. Three different temperatures (25, 35, and 45℃) were evaluated and five replicates to each stress level were studied on the reference (dry) condition and the preconditioned WPC specimens (one month immersion) in both distilled water and saltwater immersion, respectively. Ten minutes of soaking time was applied prior to the DMTA flexural creep and creep-recovery experiments.

3.3.2.2 180-day Creep Experiments

The 180-day creep experiments of the WPC lumber (with 853mm length) was conducted in accordance with ASTM D6112, (ASTM). The applied initial flexural load [(P) as shown in Figure 3.1 b] in the 180-day creep experiment was 2243.2 N± 15.2 N (12 MPa flexural stress). In accordance with the loading rate mentioned in ASTM D6109, the maximum applied flexural load was applied to the WPC specimen during the instantaneous loading phase (four minutes) with a crosshead rate motion of 39.4 mm/min. This crosshead rate motion was computed using the equation stated in the ASTM D6109 by considering a strain of 1% at the outer fiber. This loading rate was similar to the quasi-static rate so that the instantaneous duration is maintained within the short-time stated in the ASTM D6109 (not less than 10 sec. and not more than 10 min.).

3.4 Results and Discussion

3.4.1 Power Law Model

The relationship between the creep compliance of a material and the stress is shown in Equation 1. Furthermore; in accordance with the ASTM D6109, the creep displacement of the WPC lumber in 4-point bending test was computed using Equation 2.

$$S(t) = \frac{\epsilon(t)}{\sigma_0} \tag{3.2}$$

$$d(t) = \frac{0.21\varepsilon(t)l^2}{D} \tag{3.3}$$

where S(t) is the creep compliance, $\epsilon(t)$ is the creep strain, σ_0 is the applied stress, d(t) is the midspan creep deflection (vertical displacement), $\varepsilon(t)$ is the creep strain (mm/mm), l is the span length, D is the depth (thickness) of the WPC lumber.

An empirical power law model was used to describe the creep compliance of the WPC in dry, distilled water, and saltwater conditions. Prior to and during the creep test, both the distilled water and saltwater immersion WPC specimens were subjected to flexural stresses and range of temperatures in the immersed environment. The power law, as shown in Equation 3 (Barbero 2013), is suggested for these experiments based on the assumption of the linear viscoelastic behavior of the WPC specimens in this study (Gibson 2016). The initial value of the compliance represents the reciprocal of the modulus of elasticity (E). The power law model was implemented on the creep compliance vectors obtained from the 30-minute and 250-minute creep experiments on WPC specimens tested in the DMTA submersible clamp. Parameters of the model and the initial experimental compliance values are reported in Table 3.1-3.3.

$$S(t) = S_0 + S_1 t^n \tag{4.3}$$

where S(t) is the total creep compliance of the model, S_0, S_1, n represent the model's parameters that can be found from the experimental data fitting using a written code in Matlab ("MATLAB" 1994-2018), and t is the time of the creep experiment. Parameters of the model for each condition (stress, temperature, and environmental condition) are reported in Table 3.1-3.3. In addition to reporting the coefficient of determination (R^2) that shows the degree of agreement between the model and the experimental data, and to quantify the degree of the agreement between the model and the experimental data to each condition, the summation of the square error (SSE) vector was also reported in Table 3.1-3.3. Figure 3.2 illustrates the viscoelastic linearity and nonlinearity of the WPC specimens used in this study, whereas, Figure 3.3 and 3.4 illustrate the combined effect of the high value of temperature in this study (45°C) and the water immersion (saltwater and distilled water) on the creep compliance values of the 30-minute of

WPC specimens under the 2.5 and 3.75 MPa of the applied initial flexural stresses in logarithmic scale. Table 3.1-3.3 show that the WPC specimens for the both selected initial flexural stress levels exhibit a reduction in creep compliance at a temperature of 35°C, compared with creep compliance of the WPC specimens at 25 and 45°C. This reduction in the creep compliance at temperatures below the glass transition temperature (T_g) can be related to the developed interfacial bonding between the amorphous polymer and the thermally modified wood particles of the WPC of this study. A similar trend was noticed on the neat and sisal fibers reinforced polystyrene composites that was studied by Manikandan et al. (Nair et al. 2001), when they investigated the variation in the storage modulus with respect to temperature to polystyrene reinforced with different percentages of sisal fibers. According to a study reported elsewhere (Alrubaie et al. 2019) and according to the constituents of the WPCs used in this study, this reduction in the creep compliance at 35° is related to the properties of the amorphous polymer of the WPC and its ability to maintain modulus of elasticity (E) at elevated temperatures below the T_g and that was observed in storage modulus versus temperature relationship.

3.4.2 The 30-Minute Creep of WPC

To investigate the viscoelastic behavior of the WPC, isochronous curves were constructed at 5, 15, and 30 minutes to the two applied creep flexural stresses for the purpose of evaluating whether the WPC exhibits a linear or nonlinear viscoelastic behavior and these constructed isochronous curves were reported elsewhere (Alrubaie et al.2019) and as shown in Figure 3.2. Three conditions were selected for the purpose of illustration and comparison, the dry (control) and the saltwater (SW) and the distilled water (DW) immersion conditions at 25°C. The WPC specimens show a linear viscoelastic behavior under the dry condition and nonlinear viscoelastic at the other immersion conditions. Isochronous curves at different immersion

conditions and at different values of temperature were reported elsewhere (Murtada Abass A. Alrubaie et al., 2019).

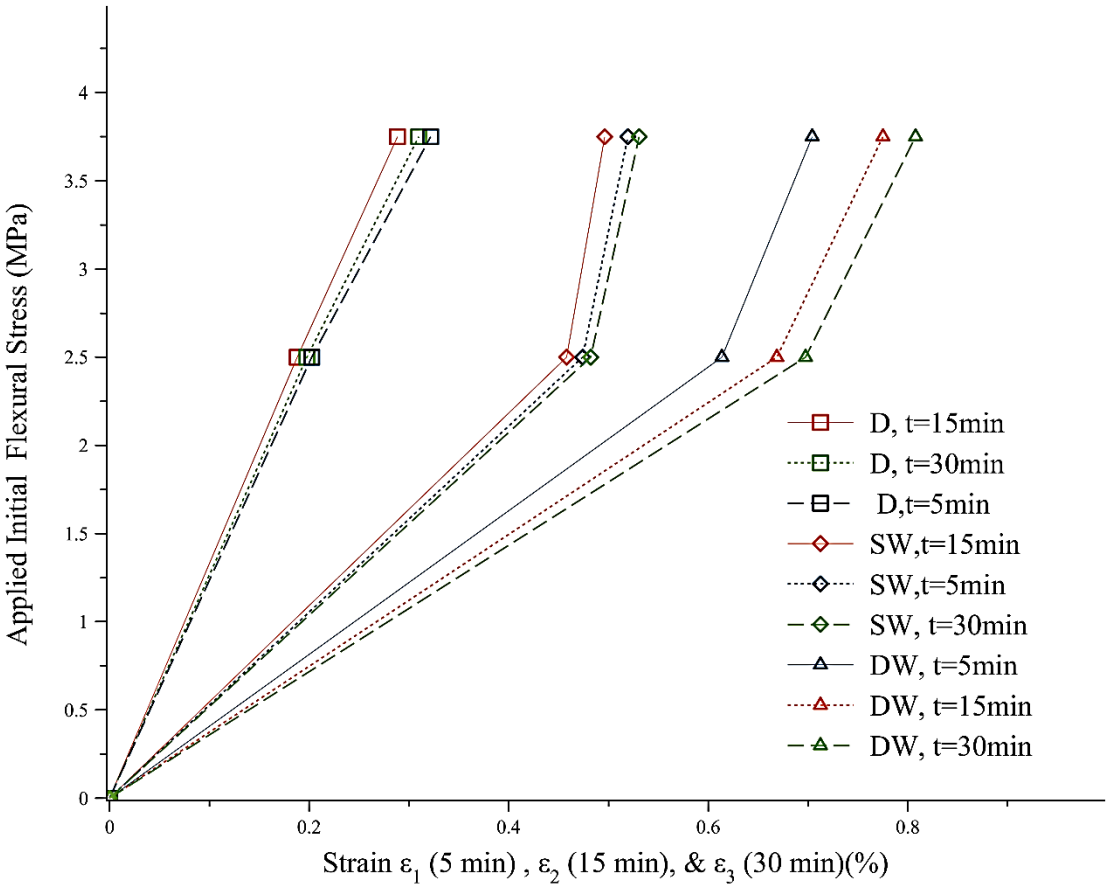

Figure 3.2. Isochronous curves of the WPC specimens at the creep time; 5, 15, and 30 minutes at the three different conditions; D, SW, and DW at 25°C.

A preliminary study was conducted to apply different models to describe the behavior of WPC, and the power law model exhibited the lowest SSE among the other models examined. For all the cases of the applied flexural stress and hygrothermal conditioning, two distinctive regions

in the creep compliance curve can be observed; a high creep compliance rate region at the time below 5 minutes, and a steady-state rate response for a time greater than 5 minutes. These two distinctive regions are attributable to the behavior of the WPC material by maintaining its creep compliance and hence, decreasing the deformation under the sustained applied flexural stress (Alrubaie et al. 2019). This can be observed in dry conditions where the moisture degradation is not considered. Once the hygrothermal effect is considered, the creep compliance rate in the steady state region started to increase and it was higher in saltwater, compared with the distilled water, because it was found the degradation of the saltwater is higher than the degradation of the distilled water.

Table 3.1. Power law model parameters of the creep compliance curves of WPC specimens tested in the dry (D) condition.

Condition(Flexural stress (MPa)-Temperature (°C)	**Initial Compliance (GPa^{-1})**	**Power Law Model-Parameters (S_0, S_1, n)**	**SSE (%)**	**R^2**
2.5-25	0.65	0.3485, 0.2813, 0.0649	0.03	0.99
2.5-35	0.90	0.1252, 0.7294, 0.0527	0. 08	0.99
2.5-45	0.68	0.0950, 0.5232, 0.0638	0.20	0.99
3.75-25	0.66	2.72e-04, 1.0798, 0.0360	0. 13	0.98
3.75-35	0.85	5.082e-04, 0.8014, 0.0409	0.10	0.99
3.75-45	0.73	0.1512, 0.5250, 0.0666	0.11	0.99

Table 3.2. Power law model parameters of the creep compliance curves of WPC specimens conditioned and tested in saltwater (SW) condition.

Condition (Flexural stress (MPa)-Temperature (°C))	**Initial Compliance (GPa^{-1})**	**Power Law Model-Parameters (S_0, S_1, n)**	**SSE (%)**	**R^2**
2.5-25	1.58	0.1111, 1.4370, 0.0316	0.29	0.98
2.5-35	1.89	0.0947, 1.6918, 0.0529	0.43	0.99
2.5-45	2.10	1.3114, 0.6977, 0.1162	0.63	0.99
3.75-25	1.11	0.0280, 0.5871, 0.0432	0. 16	0.98
3.75-35	1.33	7.239e-04, 1.2307, 0.0550	0. 17	0.99
3.75-45	1.24	0.8332, 0.3509, 0.1398	0. 28	0.99

Table 3.3. Power law model parameters of the creep compliance curves of WPC specimens conditioned and tested in distilled water (DW) condition.

Condition (Flexural stress (MPa)-Temperature (°C))	**Initial Compliance (GPa^{-1})**	**Power Law Model-Parameters (S_0, S_1, n)**	**SSE (%)**	**R^2**
2.5-25	1.42	0.1308, 1.2577, 0.0297	0.14	0.98
2.5-35	1.58	0.1178, 1.3859, 0.0481	0.24	0.99
2.5-45	1.90	0.0193, 1.7394, 0.0605	0.82	0.99
3.75-25	0.97	9.192e-04, 0.9389, 0.0446	0. 17	0.98
3.75-35	1.52	1.102e-04, 1.4215, 0.0597	0. 39	0.99
3.75-45	1.42	0.6509, 0.69, 0.1027	0.42	0.99

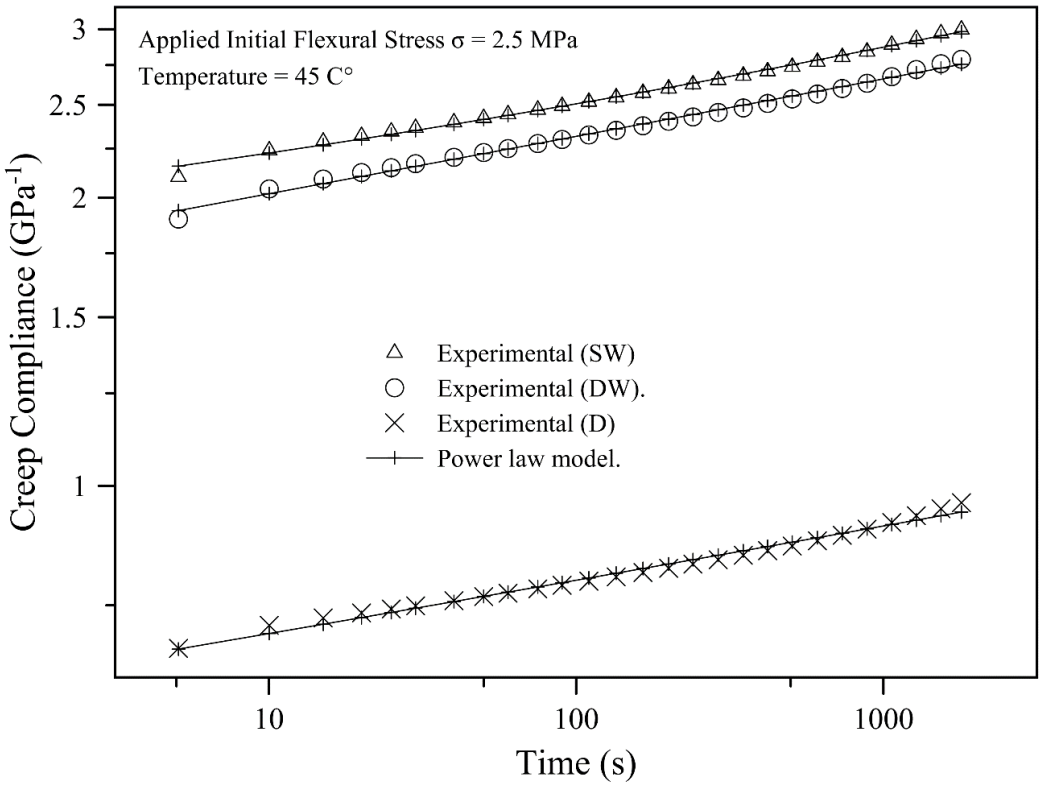

Figure 3.3. 30-minute creep compliance of WPC specimens (with 15 mm length) subjected to a maximum flexural stress of 2.5 MPa at 45°C in three different testing conditions; dry (D), saltwater (SW), and distilled water (DW) conditions.

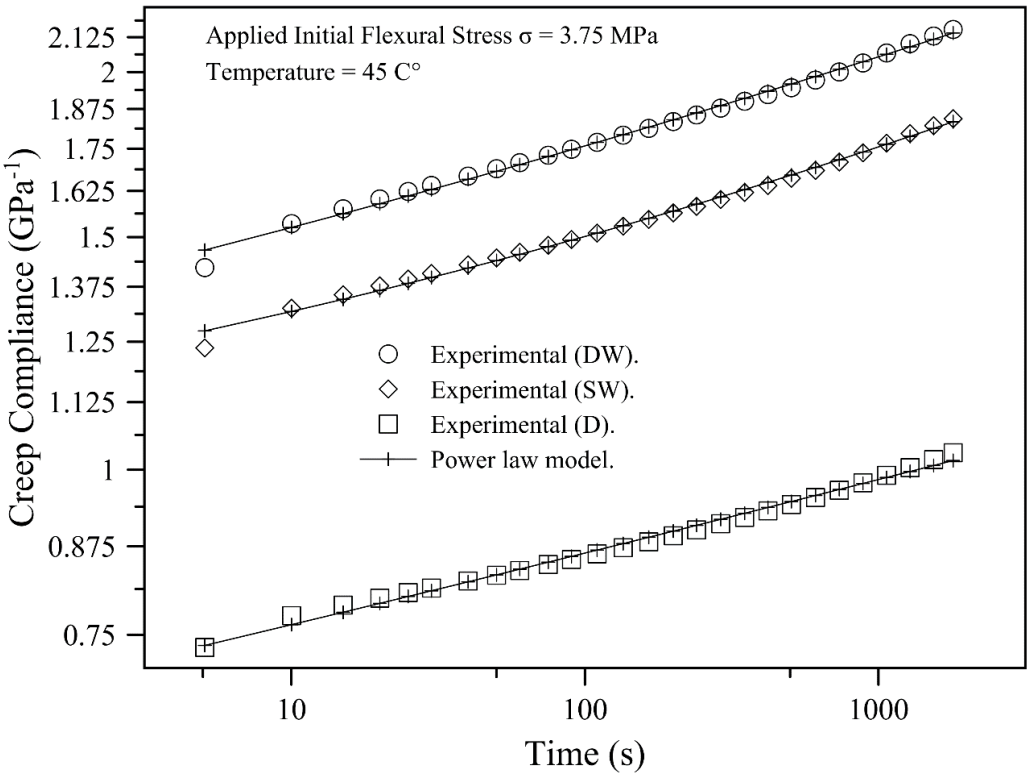

Figure 3.4. 30-minute creep compliance of WPC specimens (with 15mm length) subjected to a maximum flexural stress of 3.75 MPa at 45°C at three different testing conditions; D, DW, and SW conditions.

3.5 Application of the Power Law Model: 250-Minutes Creep of WPC Specimen

To verify the power law model used in this study to describe the 30-minute creep compliance of WPC specimens, a 250-minute creep experiment (stress = 2.5 MPa, and temperature = 45℃) was conducted in dry and immersion environments (distilled water and saltwater) using the DMTA submersible clamp. The power law model shows good agreement with the experimental data at all three testing conditions; dry, distilled water, and saltwater, as shown in Figure 3.5.

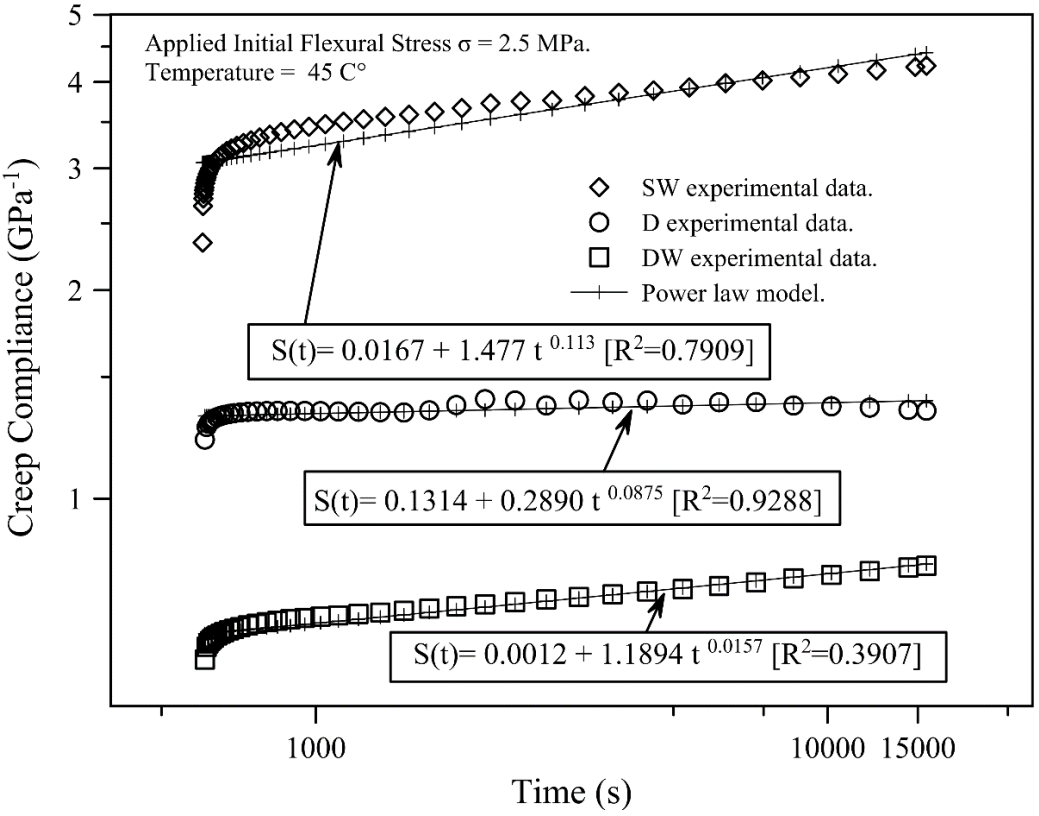

Figure 3.5. 250-minute creep compliance values and models' data fitting of WPC specimens under σ = 2.5MPa tested at 45℃ in D, DW, and SW conditions.

3.6 Application of the Power Law Model: 180-Day Creep Of WPC Lumber

For the purpose of evaluating the extension of the application of the power law model from the short-term to include the long-term creep experiments, the power law model was used to describe the 180-day creep behavior of WPC lumber with a span length 853mm, tested in creep under a flexural load. The power law model showed good agreement with experimental creep displacement data, as shown in Figure 3.6. According to ASTM D6109 (ASTM) and to the Equation 2, the flexural yield strength is computed for the stress corresponding to 1% of the

flexural strain. Thus, in this study, a prediction of the creep displacement of the WPC lumber is presented using the power law model. Based on the assumption that the WPC should fail at a flexural strain in outer fiber of 1%, (similar to the failure strain value mentioned in ASTM D6109), the computed midspan creep deflection will be 44.9 mm. The WPC lumber in this study will reach this creep mid-span deflection under a sustained flexural stress (11.8 MPa ± 0.08 MPa) after approximately 150 years, as shown in Figure 3.7.

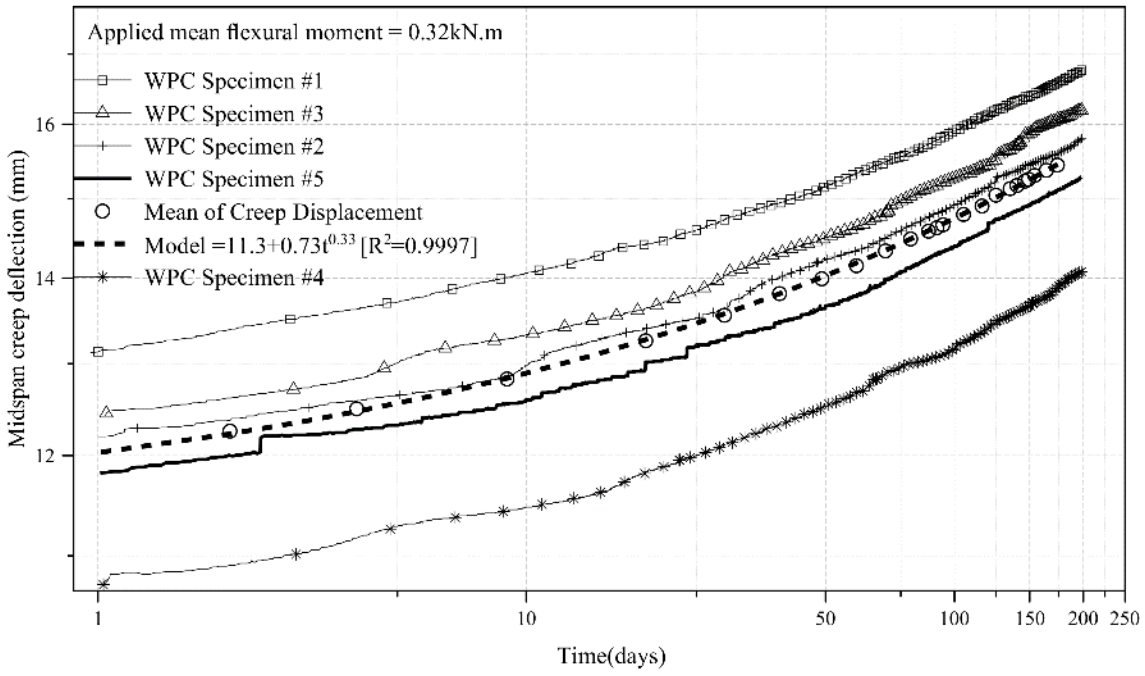

Figure 3.6. 180-day creep displacement of WPC specimens under 2243 N± 15.20 N of applied flexural load in a four-point bending test configuration.

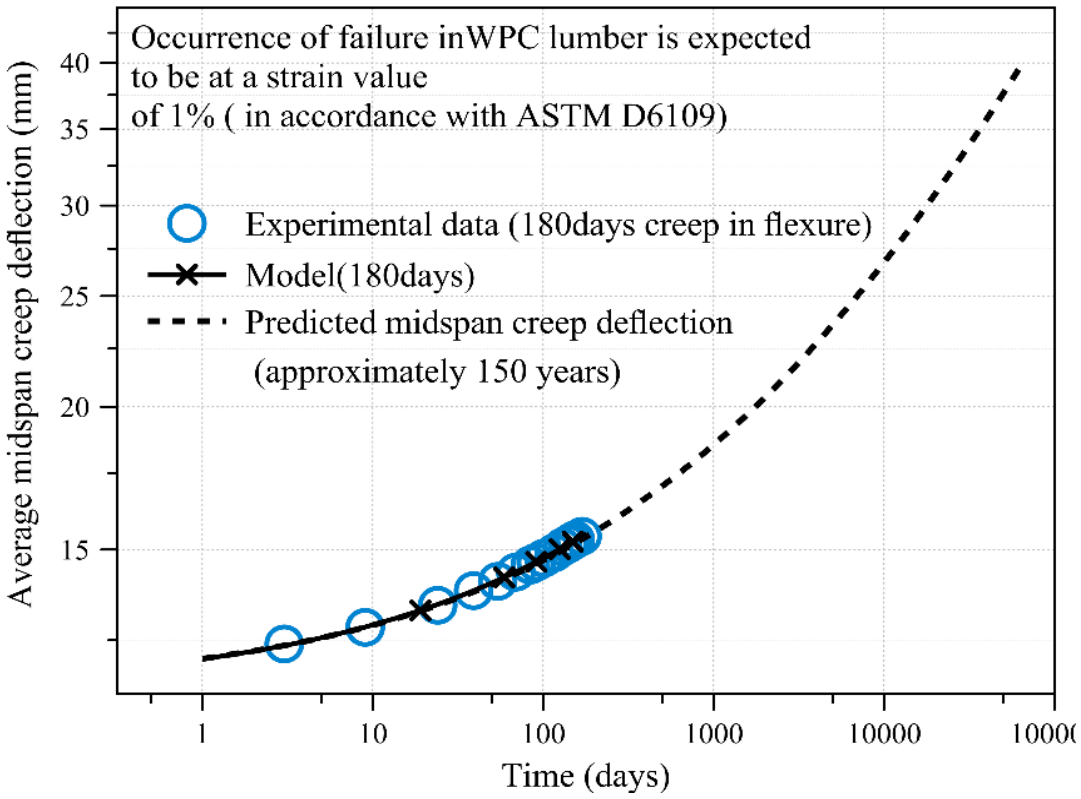

Figure 3.7. Implementation of the power law model that was used in the description of creep behavior of 30-minute creep, 250 minutes, and 180-day creep to predict the time-dependent displacement of WPC lumber in flexure.

3.7 Comparison of WPC Creep Response and the Predicted Creep Lifetime of Previous Studies

To evaluate the time-dependent behavior of the WPC used in this study, a comparison to the predicted creep displacement of the WPC studied in this paper and the WPCs studied by other researchers is reported in Table 3.4. The short-term viscoelastic extrapolated creep techniques, for instance, the time-temperature or time-temperature-stress superposition (Chang et al. 2013, Hadid et al. 2004, Pedrazzoli & Pegoretti 2014, Tajvidi et al.2005, Tamrakar et al. 2011) are used to have an understanding of the long-

term behavior of the viscoelastic material (WPC) by applying the principle of superposition and superimpose the short-term relationships to construct the master curve that describes the viscoelastic behavior of the WPC at longer duration of testing. However, these extrapolated experiments encompassed exposing the WPC specimens to high temperature (above the glassy region of the material) and the WPC specimens used in the experiments are small (below 50mm) compared with the size of the WPC members in service. Thus, the prediction of the long-term viscoelastic behavior of these specimens are not representative of the viscoelastic behavior of the WPC members in service, especially when the exposure temperature of the member in service is usually below the glass transition temperature of the material. Besides, the difference in size of the specimens used in the extrapolated experiments and the size of the member in service and the accompanied change in the mechanical properties resulting from these differences (Chang et al. 2013; Garoushi et al. 2012; Mehndiratta et al. 2018; Nuñez et al. 2004; Pedrazzoli & Pegoretti 2014, Pooler & Smith 2016, Stark 2008, Struik 1989, Tajvidi et al. 2005, Tamrakar et al. 2011). Furthermore, these techniques are implemented on the assumption of the linear viscoelasticity and hence the principle of superposition on the short creep curves can be applied, whereas, the WPCs in this study showed a nonlinear viscoelastic behavior under the combined effect of temperature and water immersion. Thus, the extrapolated techniques cannot be used to predict the hygrothermal behavior of the WPC specimens in this study.

The viscoelastic models are another tool (approach) in addition to the extrapolated techniques are utilized to describe the viscoelastic behavior of the WPC for longer durations than the experiments' durations. However, both the extrapolated

techniques and the viscoelastic models do not describe the viscoelastic behavior in the tertiary region. Likewise, the model of this study has not considered the prediction of the creep behavior in the tertiary region, even though it predicted the creep behavior for 150 years. The creep lifetime prediction can be used to evaluate the WPC in the primary and the secondary regions. Barbero (Barbero 2013) emphasizes the importance of studying the time dependence of the viscoelastic behavior of the material in structural applications in the primary and the secondary regions. The power law model in this study and unlike the previous studies, was applied for different; time-durations, specimens lengths, and testing conditions (temperature only or hygrothermal). The model showed good agreement with the different hygrothermal conditions in addition to the different test durations and at different specimen lengths, compared with previous studies, as shown in Table 3.4. In accordance with ASTM D6815 (ASTM), the WPC in this study can attain the acceptable fractional creep limit in approximately 10 years whereas the deflection limit L/20 (Shao et al. 2006, Slaughter 2006) of the WPC of this study can be reached in approximately more than 150 years. Furthermore, and according to Shao (Shao et al. 2006) when a 70% increase to the initial creep deflection is expected to occur during the service life of the pultruded FRP sheet pile, the expected 70% increase to the initial deflection of the WPC in this study is predicted to be in four years.

For most of the experimental conditions, the parameter (n) in the power law model of this study was dependent on hygrothermal effects (i.e. the value of n increases with the increase of temperature). However, power law models used in previous studies had an independent parameter (n), as was found in the models used by Hamel et

al.(Hamel et al. 2011; King & Hamel 2013). However, a similar temperature dependency to the power law model parameter (n) was observed in Pooler's study (Pooler 2001).

The WPC material in this study shows a potential to be used in applications in dry environments where the values of the temperature are below the maximum temperature used in this experiment (45℃) and subjected to low levels of applied stresses. Whereas, the time-dependent performance of the WPC materials used in the studies reported by Tamrakar (Tamrakar et al. 2011) and Alvarez-Valencia (Alvarez-Valencia et al. 2010) have shown a potential of the WPC used in their study to be used in structural applications, but with the belief of having shorter lifetime of the WPC material used in this study as shown in Table 3.4, attributable to the predicted creep tensile displacement and the experimental creep mid-span deflection, respectively.

In accordance with; ASTM D790, ASTM D2915 (ASTM), and ASTM D6109 (ASTM), the shear deformation can be ignored in the computation of the total midspan deflection when the used span to depth ratio (L/h) is greater than or equal to 16. However; the L/h ratio used in this study for the DMTA experiments was six. Thus, an investigation was required for the accountability or the ignorance of the shear deformation of the short span (L/h <16. The inclusion of the shear deformation is considered in the computation of the modulus of elasticity (E). In the DMTA experiments, the modulus of elasticity is computed by the multiplication of the stiffness (applied flexural force divided by the measured vertical displacement) of the tested WPC specimen by the geometry factor (GF), as shown in Equation 4. To account for the shear deformation, the GF has been modified to make the measured vertical midspan displacement to include the shear deformation component in addition to the bending

deformation component, as shown in Equation 5 (TA Instruments 2018, Storage et al. 2013). Thus, by substituting the GF obtained from Equation 5 in Equation 4, the computed modulus of elasticity is computed by accounting the shear deformation, and this Equation is analogous to Timoshenko's theory of beam deflection (Timoshenko & Goodier 1951) where the shear deformation component is included in the computation of the total midspan deflection.

$$\text{modulus of elasticity} = \text{stiffness} \times \text{Geometry factor (GF)} \tag{3.5}$$

Where the value GF in case of ignoring the shear deformation equals to $L^3/4wh^3$.

$$GF = \frac{L^3}{4wh^3}\left(1 + \frac{12}{5}\frac{h^2}{L^2}(1+\nu)\right) \tag{3.6}$$

Where ν is Poisson's ratio. However, Poisson's ratio was not computed in this study. Thus, a value of ν was adopted from the previous studies conducted by Hamel et al.(Hamel et al. 2014) and Dura (Dura et al. 2005) to be 0.33. These computations were conducted with the assumption that the WPC behaved as linearly elastic and an isotropic. The computed values of the elastic moduli for the WPC specimens with L/h=16 and L/h=6 with the inclusion of the shear deformation were 3% and 12.5% higher than the computed moduli with the ignorance of the shear deformation.

Table 3.4. Comparison of the experimental and predictied creep lifetime of WPCs .

Source	**This Paper**	**Alvarez (Alvarez-Valencia 2010)**	**Tamrakar (Tamrakar et al. 2011)**
Loading configuration	4-point bending	4-point bending	Tensile
Value of the applied stress (MPa) or load (N)	12(MPa), 2243(N)	11,700(N)	5.45(MPa)
Length of the WPC specimen (mm)	853	4700	246
Condition of testing and/or the specimen conditioning	21℃@50%RH	~20℃@~3-50%	Dry@ 21℃
Predicted failure occurrence (years)	154	-	~1.5
Maximum experimental, and predicted creep displacement value (mm), respectively.	14.60, 44.9	Ca 86, -	4.77, -

Conclusions

1. The WPCs in this study have the potential to be used in marine applications (warm water regions) because of the high level of creep recovery after the low sustained load is removed resulting from maintaining the creep compliance at temperatures between 25-45℃, and the reduced water uptake attributed to the thermally treated wood fibers used in the WPCs.

2. The WPC in this study has a potential to be used in long-term application where low sustained flexural stresses (below 15% of the flexural strength) are applied.

3. The viscoelastic behavior of the studied WPC material (whether linear viscoelastic or nonlinear viscoelastic) was characterized in this study as a function of hygrothermal effects.

4. Limiting the increase in creep compliance in the range of temperatures between 25 and 45℃ (at 35℃)in dry condition to be lower than 39% at the both flexural stress levels (related to formulation of the WPC in this study) is useful for the considering this material in environments over a range temperatures below 45℃.

CHAPTER 4

FLEXURAL CREEP BEHAVIOR OF HDPE LUMBER AND WPC LUMBER MADE FROM THERMALLY MODIFIED WOOD

4.1 Abstract

The application of wood plastic composite lumber as structural members in a marine application is challenging based on the tendency of WPCs to creep and absorb water. A novel patent pending WPC formulation that combines a thermally modified wood flour and a high strength styrenic copolymer has been developed with advantageous viscoelastic properties compared with the conventional WPCs (low initial creep compliance and creep rate). In this study, the creep behavior of the WPC and high density polyethylene (HDPE) lumber in flexure was characterized and compared. Three sample groupings of WPC and HDPE lumber were subjected to three levels of creep stress; 7.5, 15, and 30% of the ultimate flexural strength (Fb) for a duration of 180 days. Because of the relatively low initial creep compliance of the WPC specimens (five times less) compared with the initial creep compliance of HDPE specimens, the creep deformation of HDPE specimens was six times higher than the creep deformation of WPC specimens at the 30% creep stress level. Power law model results predicted that the strain (3%) to failure in the HDPE lumber would occur in 1.5 years at 30% Fb flexural stress while the predicted strain (1%) failure for the WPC would occur in 150 years.

4.2 Introduction

Wood plastic composites (WPCs) are commonly used for deck boards and railings attributable to their low maintenance and durability compared with conventional pressure-treated lumber (Klyosov 2007). However, extensive efforts have been made to expand the use of WPCs to include the structural applications (Alvarez-Valencia 2010, Dura 2005, Gardner & Han 2010, Haiar 2000, Hamel et al. 2011, Kahl 2006, Slaughter 2006) because of their mechanical

properties, longer lifetime, and their competing commercial prices with the conventional types of lumber (Alvarez-Valencia 2010, Bright & Smith 2007, Haiar 2000, Slaughter 2006, Tamrakar & Lopez-Anido 2011). Furthermore, WPCs made from thermally modified wood have shown potential to be used in structural applications, since they have been shown to exhibit relatively low time-dependent deformation under sustained flexural loads (Alrubaie et al. 2019, Alrubaie et al. 2019). Likewise, plastic lumber is also used in low-cost structural applications. One type of plastic lumber, high density polyethylene (HDPE) lumber, is used in the construction of aquaculture-offshore fish cages (a.k.a. Aquapod Net Pen cages) (InnovaSea Systems, Vandenbroucke & Metzlaff 2013). However, HDPE lumber has experienced damage during its service life attributable to exposure to severe ocean conditions (wave action and high temperatures during the summer, ca. 48°C in the Gulf of Mexico(Vandenbroucke & Metzlaff 2013)) and when these cages are partially surfaced and not submerged (Vandenbroucke & Metzlaff 2013), predators; for instance, the lounging sea lions caused damage to the exposed struts of the structure of the cage (in the partially surfaced cages) (Commerce, Gardner 2015, InnovaSea Systems), as shown in Figure 4.1.

Figure 4.1. Buckled Aquapod cage made from HDPE lumber and netting (covered with biofouling) with two lounging sea lions on the exposed struts (InnovaSea Systems 2015).

The need to have a material that has a reasonable cost for the construction of aquaculture cages that also exhibits satisfactory structural performance during the service life of these cages suggests that WPC lumber can be considered a potential alternative to HDPE lumber (Alrubaie et al. 2019, Alrubaie et al. 2019). Although WPCs have been explored for use in structural applications, the material's long-term behavior is still a subject of concern among researchers especially in wet applications. WPC lumber exhibits viscoelastic behavior. When a constant stress is applied to the viscoelastic material, the summation of the elastic strain (instantaneous strain) and the time-dependent strain will represent the total strain (creep strain) of the

viscoelastic composite material (Barbero 2013, Gibson 2016). One dimensional (1D) viscoelastic models (power law, Maxwell, Kelvin, Prony series, and four element viscoelastic model) have been used in previous studies to describe both the short, and long-term creep-behavior of viscoelastic materials (Alvarez-Valencia et al. 2010, Pooler 2001, Slaughter 2006, Tamrakar et al. 2011) . Alrubaie (Alrubaie et al. 2019) implemented a 1D power law viscoelastic model to describe the 180-day creep behavior of WPC lumber made from thermally modified wood with a span of 853 mm in 4-point bending (flatwise). Alvarez-Valencia (Alvarez-Valencia et al. 2010) conducted a full-scale 90-day creep rupture in 4-point bending of a Z-shape WPC sheet piling with 4.70m in length, to evaluate the time-dependent structural behavior of the WPC sheet piling, and the 1D Findlay's power law model was used to predict the creep behavior of the WPC sheet piling that has shown good agreement with the experimental data. Dura (Dura 2005) conducted one, seven, and 15-day creep experiments on WPC dumbbell shaped tensile specimens in at 15, 30, and 45% of the average tensile strength, to evaluate the time-dependent behavior of the WPCs. In addition to the creep in tension, Dura (Dura 2005) also conducted creep tests in compression at the same stress levels used for tensile creep experiments, but with respect to the average maximum compression stress and to the same creep duration. Many researchers (Alvarez-Valencia et al. 2010, Dura 2005, Hamel 2011) have studied the large-scale flexural creep behavior (i.e. the WPC specimens had length to span ratios (L/h) exceeding the value recommended by ASTM International, (2013) for WPC specimens. Dura (2005) conducted a 90-day flexural creep experiments (edgewise) on WPC specimens with a span length of 2515 mm with and without a layer of fiber reinforced polymer layer (FRP) and their creep behaviors were reported. (Dura 2005). Dura (Dura 2005) used the experimental response to verify a nonlinear 1D long-term viscoelastic model. Alvarez-Valencia (Alvarez-Valencia 2010)

conducted a flexural creep rupture experiment on Z-shape WPC sheet pile with a span length of 4700 mm subjected to 55% of the flexural load at failure (11.7 kN). Hamel (Hamel et al. 2014) performed a three-year tensile creep test experiment on WPC dumbbell shaped specimens subjected to two different level of stresses, 20% and 50% of the average maximum stress at failure, to predict the creep behavior of 2.13m WPC boards in flexure. Hamel (Hamel et al. 2014) developed a 2D finite element (FE) model that predicted the flexural creep behavior (edgewise) based on the uniaxial quasi-static testing using Abaqus ("Abaqus/CAE "2017) software. However, Hamel (Hamel et al. 2014) and other researchers (Alvarez-Valencia et al. 2010, Dura 2005, Slaughter 2006) have not implemented a finite element analysis to model the long-term creep behavior of WPC (Hamel et al. 2014).

The two objectives of the research presented here were: (1) to experimentally characterize the long-term (180 days) flexural creep behavior (flatwise) of WPC lumber made from thermally modified wood and compare it with the flexural creep behavior of HDPE lumber currently used in the construction of aquaculture fish cages (Aquapod Net Pen cages), and (2) to implement a power law model to describe the long-term viscoelastic creep behavior of WPC and HDPE lumber in flexure (flatwise) for a duration of 180 days, respectively. Furthermore, the model was implemented to predict the occurrence failure at the outer layer of the WPC and HDPE lumber for a duration longer than the 180 days.

In this study, thirty 4-point bending creep frames (flat wise) located in a climate controlled creep room in the Advanced Structures and Composite Center (ASCC) at the University of Maine, Orono, Maine, USA were utilized to conduct 180-day creep experiments in 4-point bending (flatwise) of the WPC and HDPE lumber subjected to three different levels of

stresses and each level of stress was applied to five specimens (i.e., the total number of WPC and HDPE specimens is 30).

4.3 Experimental

4.3.1 Material

The WPC lumber with cross section dimensions [width (w), thickness (h)], (139 mm, 33.5 mm) was produced using a twin-screw Davis-Standard Woodtruder^{TM} in the ASCC at the University of Maine, Orono, Maine [20]. The WPC lumber cross section has two grooves along the longitudinal direction (extrusion direction) of the lumber at the top layer with 3 mm width and 1.8 mm depth, and these grooves are located at 21.9 mm from the short edges of the WPC lumber, as shown in the cross section A-A in Figure 4.2(A). The WPC examined here is based on a patent-pending formulation combining thermally modified wood flour that has been produced at Uimaharju sawmill in Finland and a high strength styrenic copolymer system in an equivalent weight ratio to each of the two constituents. Section A-A in Figure 4.2 (A) shows the cross section of WPC and HDPE lumber. However, a simplifying assumption was made to consider the WPC cross-section is a rectangular cross-section and eliminate the grooved areas at the top layer in the computations. The commercially available HDPE lumber has a rectangular cross section with the width of 140 mm and the thickness of 38 mm is used in the construction of the Aquapod Net Pen cages and was provided by InnovaSea [11], to conduct this study.

4.3.2 WPC And HDPE Sample Preparation

WPC and HDPE lumber specimens with cross section dimensions (width, thickness), (139 mm, 33.5 mm) and (140 mm, 38 mm), respectively, were cut in an adequate length to fit the span of the creep test rig, 853 mm with an adequate length for the overhang at each support of the test rig [51 mm at each overhang (a) in Figure 4.2 (A)], as shown in Figure 4.2 (B). To

achieve the magnetic mounting of the string potentiometer that measures the creep deflection to the mid-span of the specimens, 3- minute flame treatment to each specimen and followed by a 5-minute epoxy to adhere a square metal piece (19 × 19 mm) to the mid-span of each specimen (flatwise) at the compression outer fibers. Thereafter, a magnetic hook was mounted on the square metal and the string potentiometer was attached to the hook during the creep loading, and hence, the creep mid-span deflection was acquired, accordingly.

4.3.3 180-Day Creep Experimental Setup

Prior to the creep loading and in accordance with ASTM D618, WPC and HDPE specimens were preconditioned in the climate control creep room at the ASCC for one week. Thereafter, and according to ASTM D6109 and ASTM D6815 (ASTM), the long-term WPC and HDPE specimens were loaded in 4-point bending (flat wise) with values of L/h of 25 and 22, respectively. The relative humidity (RH) and temperature were controlled during the 180 days of the creep experiment to be 50±5% and 21±2℃. The crosshead speed used to load the WPC and HDPE specimens for creep was the same crosshead speed used in the quasi-static testing to obtain the mean ultimate flexural stress (i.e. to ensure the initial applied loading will be applied to the specimens not less than one minute and not greater than 10 minutes). The measurements and the recording of the; applied flexural level, creep displacements, and the relative humidity and the temperature of the climate control creep room, were managed by a data acquisition system (DAQ) located at the climate control room at the ASCC at the University of Maine, Orono, ME, USA. Based on the applied flexural stress level relative to the flexural strength (Fb), the WPC and HDPE specimens have been divided into three groups: 7.5% of Fb, 15% of Fb, and 30% of Fb, respectively.

4.4 Quasi-Static Tests

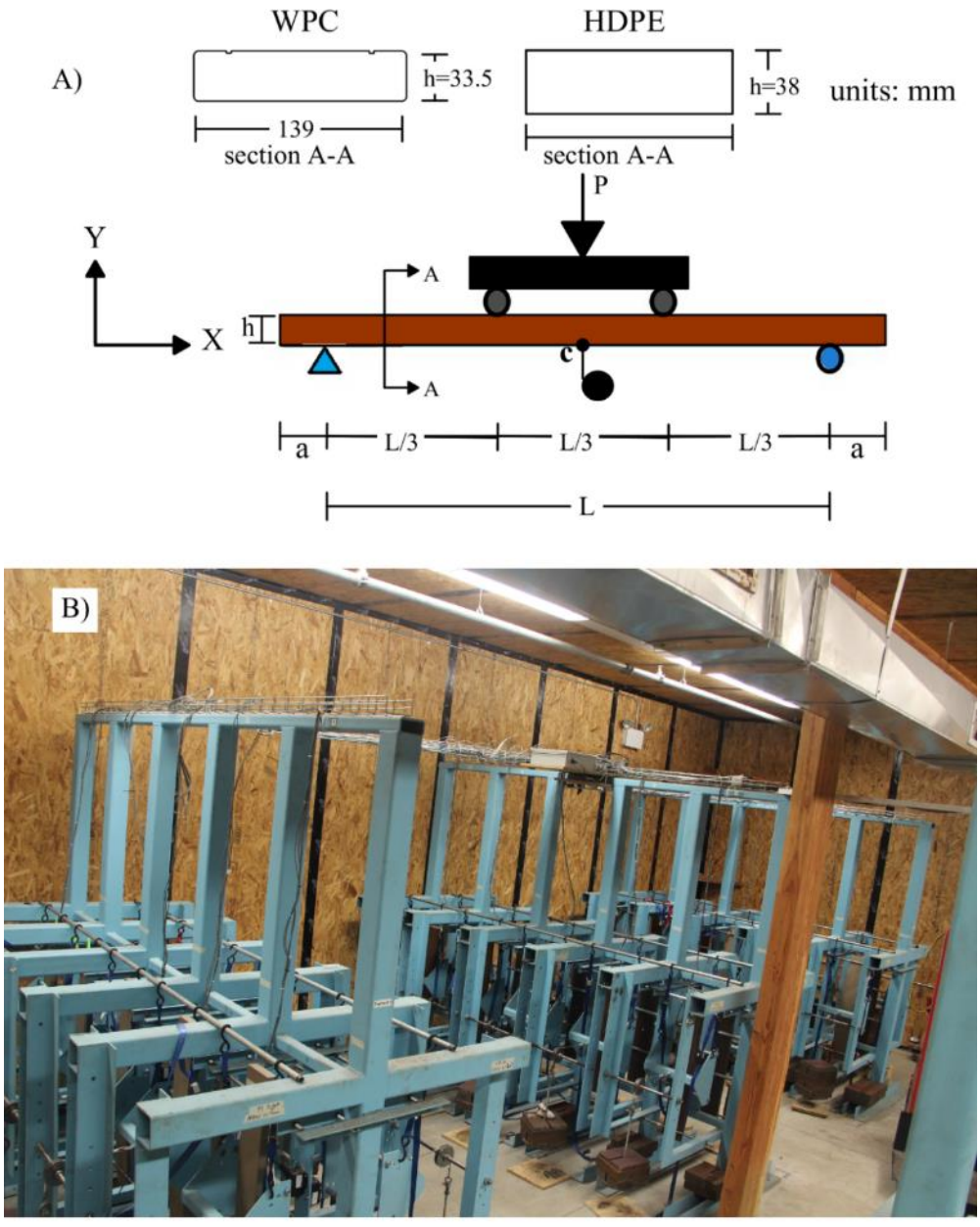

Figure 4.2. A) Four-point bending test configuration used for both quasi-static tests and creep tests, B) Creep frames experimental setup.

To obtain the apparent elastic modulus (E) and the mean of the flexural strength, five specimens of each of the WPC and HDPE lumber were cut with a span to depth ratio 16:1 with an adequate overhang length over the supports of the fixture, and were tested in 4-point bending in accordance with ASTM D6109, as shown in Figure 4.2 (A). The support spans of the WPC and HDPE specimens were L=545 mm and L=620 mm, respectively. The crosshead rate used on the WPC and the HDPE specimens during the 4-point bending test were selected in accordance with ASTM D6109 (ASTM), to be 15.9 and 18 mm/min, respectively. For the 180-day creep experiments, three levels of flexural creep stress were applied to the WPC and HDPE specimens (five specimens in each level). These three levels were: 7.5%, 15%, and 30% of the mean of the flexural strength obtained from the quasi-static tests. These three levels were; 7.5%, 15%, and 30% of the mean of the flexural strength obtained from the quasi-static testing, as shown in Figure 4.3. The selection of the stress levels was made based on; (1) the use of the WPC and HDPE lumber in submerged Aquapod net pen cage is expected to be under low stresses (the structural members of the cage does not carry the weight of the cage, except to withstand the mooring and the buoyancy system (InnovaSea Systems 2015, Page 2013, Vandenbroucke & Metzlaff 2013), (2) researchers in previous studies (Chassagne et al. 2005, Dura 2005, Hamel 2011, Hamel et al. 2013, King & Hamel 2013, Tamrakar et al. 2011) have studied the creep behavior of WPCs under stress levels that were greater than or equal to 30% and recommended further studies using low stress levels (Chang et al. 2011, Hamel et al.2011), thus, it is important to investigate the creep behavior of WPCs under low stress levels. Table 4.1 shows the values of the apparent elastic modulus of the WPC specimens and the HDPE with their coefficient of variation (COV) and the selected levels of the creep flexural stress. The determination of the apparent elastic modulus of WPC and HDPE specimens was performed in accordance with

ASTM D6109 (ASTM), by computing the slope of the line obtained from the linear regression to the linear portion in the load-midspan deflection curve. Since the span to depth ratio (L/h) of the tested WPC and HDPE specimens was 16 which met the recommended L/h in the ASTM standards, the shear deformation was ignored in the computation of the apparent elastic modulus (further discussion on shear deformation in the computation of the elastic modulus of the WPCs with similar formulation was described elsewhere (Alrubaie et al. 2019, Alrubaie et al. 2019)). Then, the flexural strength (Fb) was determined: (1) for WPC, as the ultimate flexural stress at midspan at failure, (2) for HDPE, as the flexural stress at midspan corresponding to 3% of outer fiber strain. The results are reported in Table 1. The mechanical properties of the HDPE lumber tested in this study agreed with the mechanical properties reported in the data sheet of the manufacturer (Tangent Technologies, 2015). In accordance with ASTM D6109, the flexural strength is determined as the maximum stress in the outer fibers at failure or when the strain in the outer fibers equals 3%, whichever occurs first.

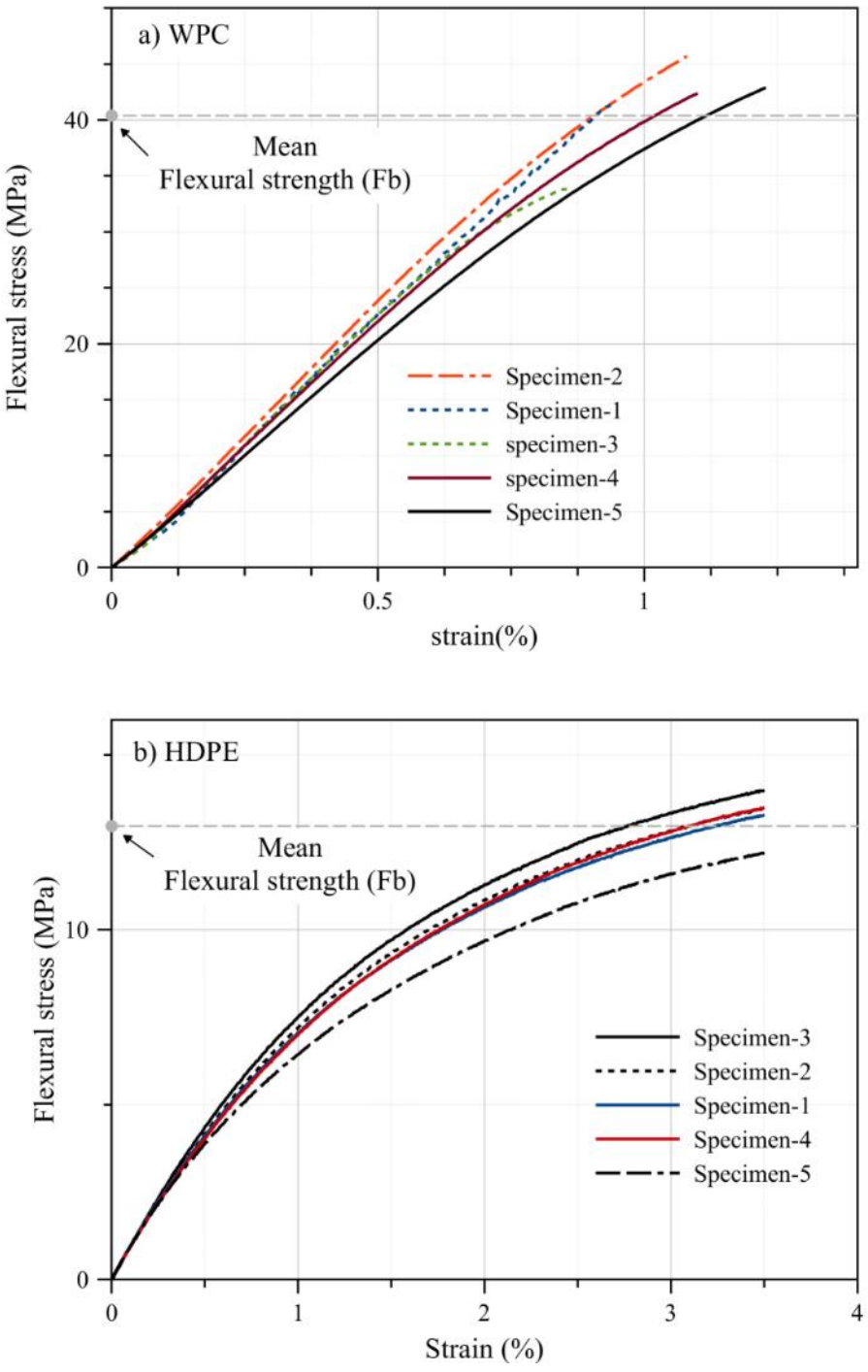

Figure 4.3. Stress-strain relationship curves of the a) WPC and b) HDPE lumber, respectively, in 4-point flexural test.

Table 4.1. Values of elastic modulus (E), flexural strength, and the applied creep stress level of WPC and HDPE lumber obtained from 4-point quasi-static testing.

Material	**Applied stress level**	**E (GPa)**	**Mean Fb (MPa)**	**Applied Flexural Creep Stress Level (MPa)**
WPC	7.5% Fb	4.34±0.26	41.2±4.53	2.98±0.08
	15% Fb			5.88±0.04
	30% Fb			11.84±0.09
HDPE	7.5% Fb	0.93±0.03	14.1±0.70	1.14±0.05
	15% Fb			2.22±0.04
	30% Fb			4.4±0.09

4.5 Discussion of Results

4.5.1 Determination of the Creep Stress Levels

The applied flexural stress levels for WPC and HDPE lumber were selected to be as percentages of the mean of the flexural strength obtained from the quasi-static tests, Fb=41.2 MPa, and Fb=14.1 MPa, respectively. Thus, the flexural creep stress levels applied on the three groups of each of WPC and HDPE lumber were approximately 7.5%, 15%, and 30% of the ultimate flexural strength, as shown in Table 4.1.

4.5.2 Experimental Comparison Between the Long-Term Creep of WPC and HDPE Lumber

Three levels of stress were applied on each group of five specimens of WPC and HDPE lumber. The mean of the mid-span creep deflection of each group of WPC and HDPE lumber was reported, as shown in the log-log space axes Figure 4.4.

In accordance with ASTM D6815 (ASTM), the acceptance criteria of the creep behavior of the specimen is evaluated via: (1) the decrement in the creep rate (all the subsequent creep rate data should be decreasing during the duration of the creep test), (2) the fractional deflection (FD) should not exceed 2, which is obtained from dividing the mid-span creep deflection at the end of the creep experiment by the initial mid-span deflection (D_0)(ASTM). The values of initial midspan displacement measured during the first four minutes of the creep test and were reported in Table 4.2. The creep rate in this study was measured at each 30 days as reported in Table 3. Table 4.3 shows the 30-day creep rate of the three groups of each of WPC and HDPE specimens during the 180-day creep experiment. It can be seen that the values of the WPC fractional

deflection under the three different flexural stress levels were within the acceptable limit recommended by ASTM D6815, whereas, the values of the HDPE fractional deflection failed to meet the recommended fractional deflection limit. However, all the WPC and HDPE groups exhibited a decreasing creep rate during the 180-day creep experiment as reported in Table 4.3, except a noticeable increase in the creep rate of the HDPE group-15% Fb for the time between the 150 and 180 days. This increase can be attributable to the assumption that the creep of HDPE specimens entered the steady-state of creep in the secondary region (ASTM).

For further comparison between the creep behavior of WPC and HDPE specimens, a statistical analysis of variance study (ANOVA) of the mid-span creep deflection of each specimen at each group of the WPC and HDPE was conducted and the results shown in Figure 4.5. At the applied flexural stress level of 7.5% of the flexural strength, HDPE specimens showed a mid-span creep deflection exceeding two times the mid-span creep deflection of the WPC specimens. As the levels of applied flexural stress increased from 7.5% to 15% and 30%, the HDPE specimens showed mid-span creep deflections exceeding five times and seven times the mid-span creep deflection of the WPC at the same applied flexural levels of stress, respectively. The rate of increase in the mid-span creep deflection between the HDPE specimens subjected to 7.5 and 15% (i.e., HDPE specimens for-7.5% Fb, and15% Fb) of the flexural strength was below 150%, whereas it was below 35% for the WPC specimens (WPC specimens in group-7.5% and 15% of Fb). When the applied flexural stress levels increased from 15% to 30% of the flexural strength, the creep rate between groups-15% and 30% of Fb was below 215% for the HDPE specimens, and below 110% for WPC specimens. This low time-dependent mid-span deflection creep behavior of the WPC specimens compared with the behavior of HDPE specimens can be anticipated based on their initial compliances (the reciprocal of the elastic

modulus); 0.232 GPa^{-1} and 1.11 GPa^{-1}, respectively. In regards to the comparison of the time-dependent viscoelastic behavior of the WPC with the WPC in previous studies; a short-term time-dependent behavior comparison of the WPC with the same formulation of WPC in this study was presented elsewhere (Alrubaie et al. 2019), and Alrubaie et al. (Alrubaie et al., 2019) have presented a comparison between the creep behavior of the group-30% of Fb of WPC presented in this study and the creep behavior of WPC from previous studies. Thus, a comparison to the creep behavior of the WPC used in this study with WPC material from previous studies is not discussed here.

Table 4.2. Initial midspan deflection (D_0) of WPC and HDPE lumber at three different stress levels.

Material % of Fb	**D_0 (mm)**
WPC-7.5%	2.96
WPC-15%	5.8
WPC-30%	11.3
HDPE-7.5%	5.5
HDPE-15%	8.74
HDPE-30%	18.71

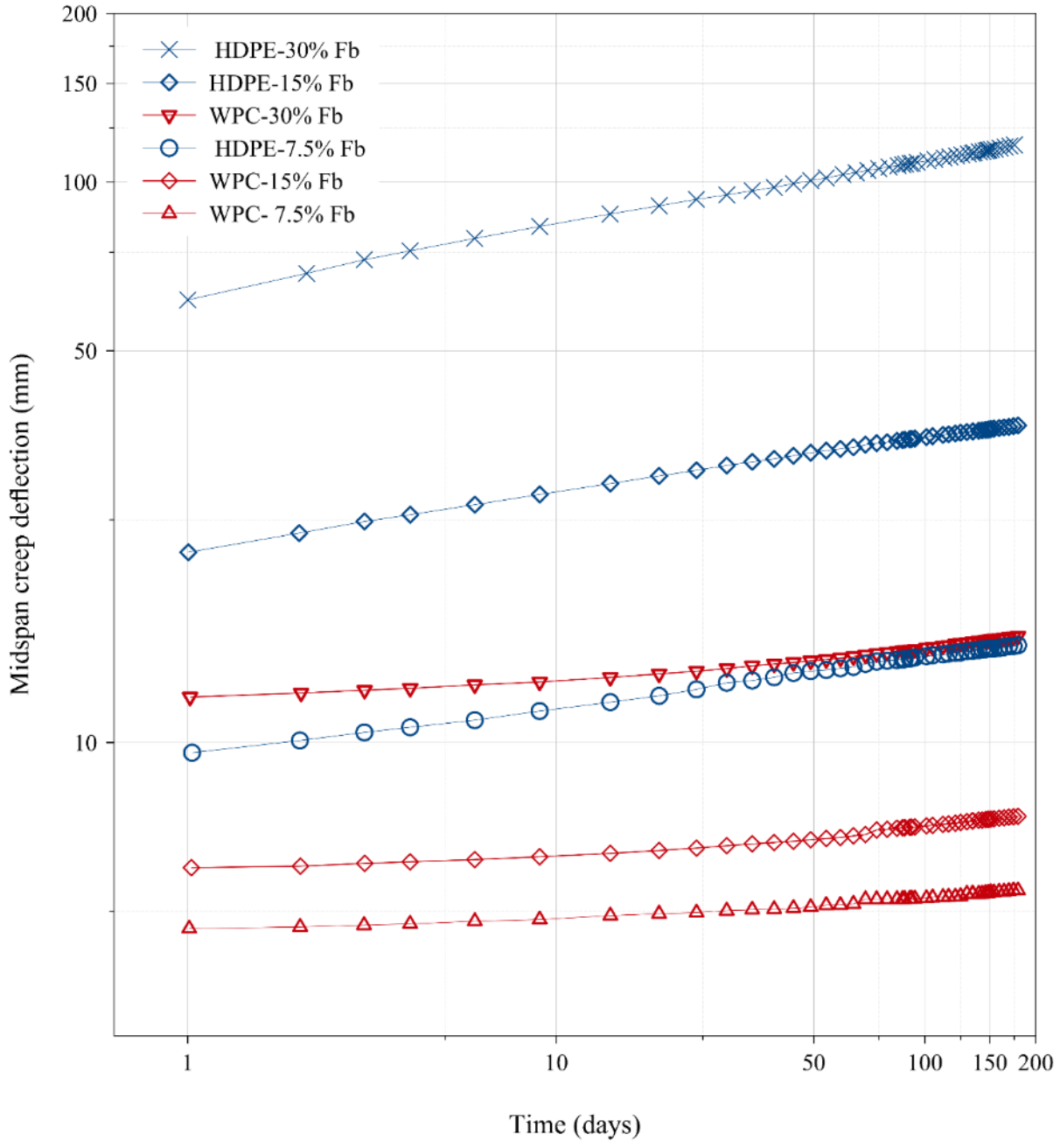

Figure 4.4. Time-dependent mid-span creep displacement for WPC and HDPE specimens at different stress levels.

Table 4.3. Values of creep rate deflection (D) (mm) of all the groups of WPC and HDPE specimens at 30th, 60th, 90th, 120th, 150 and 180th day respectively and the fractional deflection (FD) at the 180th day with respect to initial deflection D_0.

Creep rate and FD	**Material -% of Fb**					
	WPC-7.5%	**WPC-15%**	**WPC-30%**	**HDPE-7.5%**	**HDPE-15%**	**HDPE-30%**
D_{30}-D_0	0.54	0.99	2.35	7.31	15.57	72.54
D_{60}-D_{30}	0.13	0.21	0.57	0.77	1.72	7.80
D_{90}-D_{60}	0.12	0.28	0.45	0.51	1.04	4.62
D_{120}-D_{90}	0.05	0.12	0.35	0.36	0.65	3.45
D_{150}-D_{120}	0.08	0.12	0.29	0.25	0.5	2.87
D_{180}-D_{150}	0.06	0.09	0.23	0.22	0.62	2.47
FD_{180}	1.22	1.33	1.28	2.71	3.88	5.11

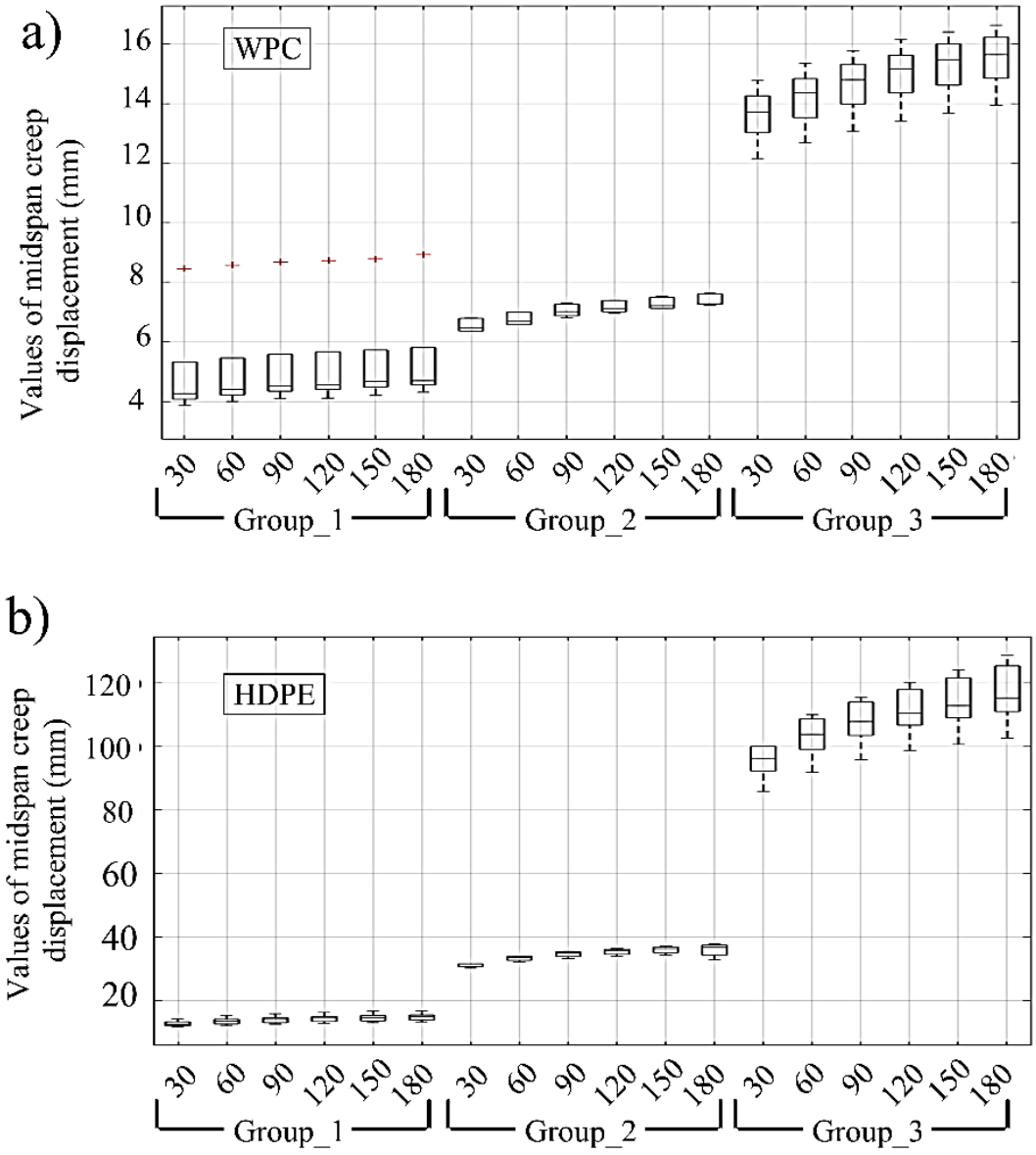

Figure 4.5. a) Statistical analysis of variance (ANOVA) that investigates the reduction in creep rate of the WPC specimens subjected to three applied flexural creep stress levels. b) ANOVA that investigates the reduction in creep rate of the HDPE specimens subjected to three applied flexural creep stress levels.

4.5.3 Time-Dependent Creep Modeling

An empirical power law model was used to describe the 180-day mid-span flexural creep displacement. The model showed a good degree of agreement with the experimental data of the WPC and HDPE lumber in 4-point bending creep test (flatwise). Based on the assumption that the WPC should fail at a flexural strain in outer fiber of 1%, and the HDPE lumber should fail at a flexural strain in outer fiber of 3% (similar to the failure strain value mentioned in ASTM D6109), the computed mid-span creep the predicted failure occurrence for WPC and HDPE in flexure and under a flexural stress of 30% of Fb will occur after 150 years and 1.5 years, respectively, as shown in Figure 6. To investigate the stress-independency behavior (viscoelastic behavior) of the WPC and HDPE lumber with regards the three applied stress levels (7.5%, 15%, and 30% of Fb), a power law model was implemented to describe the normalized mid-span creep displacement behavior (d(t)). Equation (4.1) describes the normalized midspan creep displacement behavior.

$$d(t) = \frac{D(t)}{D_0} \tag{4.1}$$

Where d(t) is the time dependent midspan deflection. For a 4-point bending test configuration, the initial mid-span creep displacement (D_0) is related to the applied flexural stress, as shown in Equation 4.2.

$$D_0 = \frac{23}{108}\frac{\sigma_b}{E}\frac{L^2}{h} \tag{4.2}$$

Where σ_b and E are the flexural stress and elastic modulus, respectively, L is the support span, and h is the depth of the WPC and HDPE specimen. The normalized mid-span creep displacement is predicted, as shown in Equation 4.3.

$$d(t) = 1 + d_1 t^m \quad (4.3)$$

where d_1 and m are the stress-independent power law parameters. These parameters (d_1 and m) were computed from the experimental least square error data fitting using a Matlab code. The creep behavior of HDPE lumber and WPC lumber has been predicted for ten years using the power law model, as was reported in Table 4.4. According to InnovaSea systems Inc., the estimated service life of aquaculture cages is ten years. The prediction showed the failure occurrence (maximum strain at outer fiber layer) will not occur for both WPC and HDPE specimens for the stress levels 7.5% and 15% of Fb. Whereas, the failure occurrence was predicted in 1.5 years for the HDPE lumbers subjected to 30% of Fb. For this reason WPCs are considered in the construction of aquaculture cage structures subjected to stress levels 30% below Fb.

Table 4.4. 10 year prediction of the creep displacement of the WPC and HDPE lumber (in accordance with ASTM D6109).

Material name -% of Fb	**Outer fiber strain at failure %**	**Mid-span displacement at failure (mm)**	**Predicted mid-span creep displacement in 10 years (mm)**
WPC-7.5%	1.040	46	6
WPC-15%			11
WPC-30%			22
HDPE-7.5%	3.004	120	21
HDPE-15%			50
HDPE-30%			165

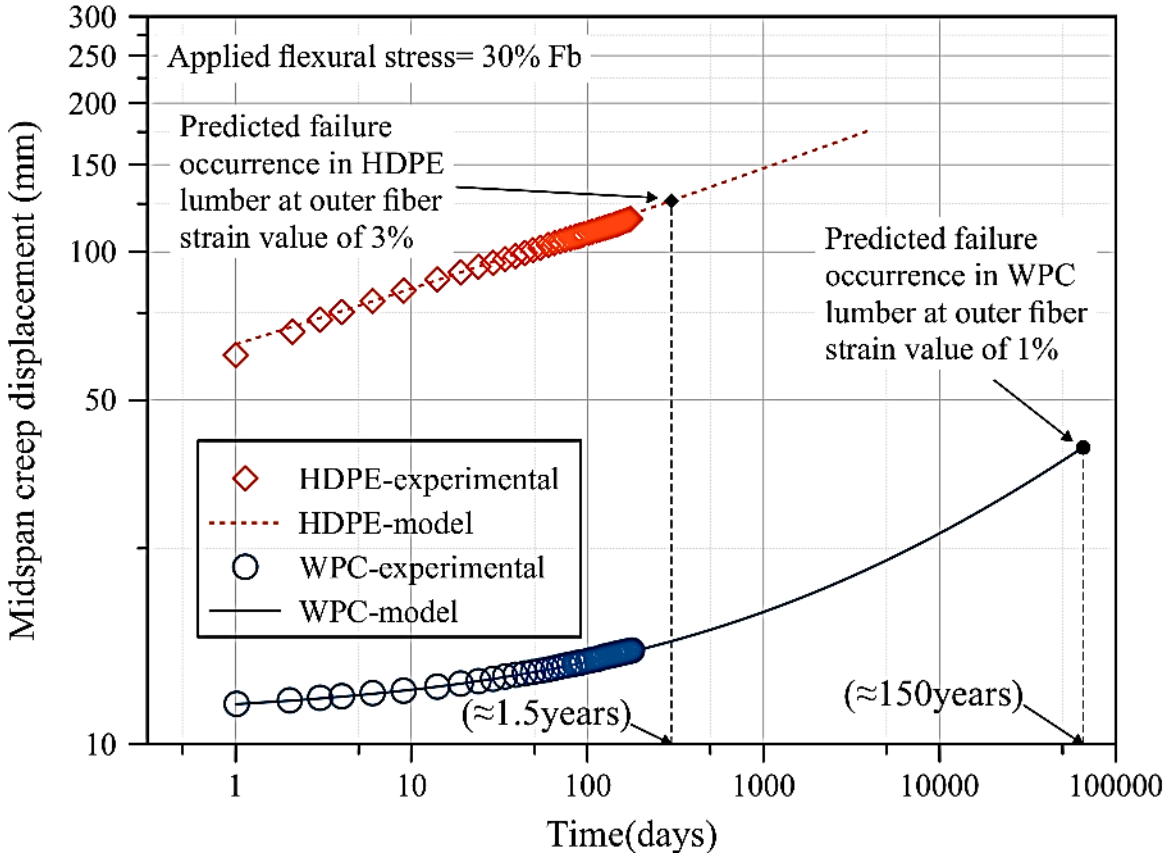

Figure 4.6. Predicted failure occurrence in the outer fiber strain of WPC and HDPE lumber for the specimens subjected to 30% Fb flexural stress using the power law model.

Values of the normalized mid-span creep displacement were reported in Table 4.5. The normalized power law model showed the stress-independency [18] of the WPC and HDPE lumber by having similar values of the normalized power law model (d_1 and m) at different flexural stress levels, respectively. Figures 4.7 and 4.88 illustrate the stress-independency behavior of each group of the WPC and HDPE lumber via describing the normalized mid-span creep displacement by the normalized creep behavior.

Table 4.5. Power law model parameters.

Material type	model parameters	
	d_1	m
WPC	0.011	0.596
HDPE	0.018	0.494

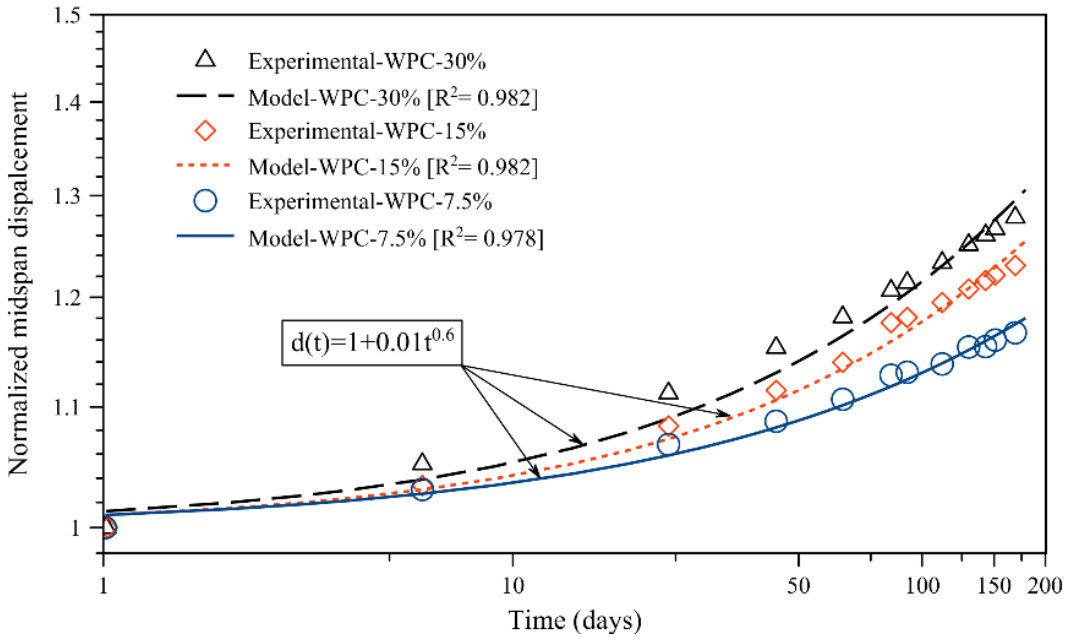

Figure 4.7. Comparison of power law model and experimental creep result for WPC lumber.

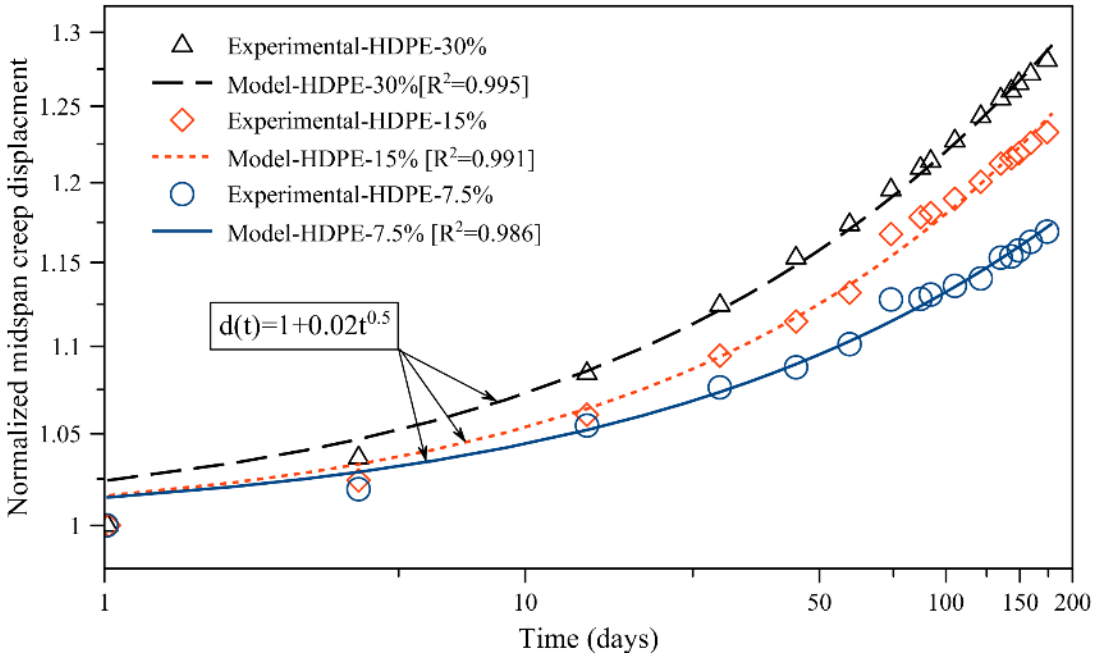

Figure 4.8. Comparison of power law model and experimental creep results for HDPE lumber.

Conclusions

1. The WPC in this study showed an enhanced time-dependent creep behavior compared to HDPE. WPCs show potential to replace HDPE lumber in the construction of aquaculture cage structure.

2. While previous studies have studied the creep behavior of WPC at relatively high level of stresses, this study conducted the creep experiments using levels of stresses that were below 30% of the ultimate flexural strength, which are typical for the intended design application. During the comparison between the creep behavior of WPC and HDPE specimens at the low stress levels (7.5% and 15% of Fb), the fractional deflections (FD) of HDPE were 122% and 192% higher than the FD of the WPC specimens, respectively. Whereas, the FD of HDPE specimens at 30%

stress level was 300% higher than the FD of the WPC specimens. This can be advantageous for using WPC lumber as a replacement of the HDPE lumber in the construction of aquaculture cages.

3. The power law model was a useful tool to describe and predict the creep behavior of both WPC and HDPE lumber for all the stress levels (7.5%, 15%, and 30% of Fb). This model predicted that both HDPE lumber and WPC lumber show low creep rate during ten years at stress levels below 15% of Fb. Whereas, at stress level 30% of Fb, failure occurrence at outer fiber is predicted to happen at 1.5 years for HDPE lumber and at 150 years for WPC lumber.

CHAPTER 5

EXPERIMENTAL STRUCTURAL PERFORMANCE OF HDPE AND WPC LUMBER OF AQUACULTURAL GEODESIC SPHERICAL CAGE COMPONENTS

5.1 Abstract

The buckling load of Aquapod connected triangular panel components of an aquacultural geodesic cage structure 1:4 size of the full-scale spherical cage (volume =4700 m^3 with an approximate diameter of 21 m) made from HDPE and WPC struts with and without the steel plastic coated mesh was experimentally measured and characterized. The metallic mesh of the panels contributed to increasing the buckling capacity of the connected triangular panels by approximately two times the buckling capacity of the connected panels without steel mesh made from WPC and HDPE struts, respectively. The typical failure mode of the HDPE panels made from HDPE struts with and without metallic mesh was buckling failure in the struts and the metallic mesh, whereas the failure of the WPC panels with and without metallic mesh was buckling failure (bending) at the weak section of the bolted struts.

5.2 Introduction

Aquaculture cages for fish farming are made in different ways. Unlike other types of aquaculture fish cage structures, the Aquapod Net Pen cage is a rigid-frame geodesic spherical cage structure. The cage structure is comprised of individual triangular panels made from high density polyethylene (HDPE) lumber (strut) and these panels are fastened to each other to form the geodesic spherical shape of the cage (Vandenbroucke & Metzlaff 2013). These triangular panels contain wire mesh netting, and is affixed to the struts of the panels by mechanical fastening (stapling). Five panels (P1, P2, P3, P4, and P5) are the main structural components to construct the spherical shape of the Aquapod cage, as shown in Figure 5.1. These triangular

panel components are designed to contribute to facile construction by reducing the time and manpower required to construct the cage structure (Page 2013). The cage structure is utilized in a fully submerged situation; except for cleaning, where it will be partially (30%) exposed to the air (Vandenbroucke & Metzlaff 2013).

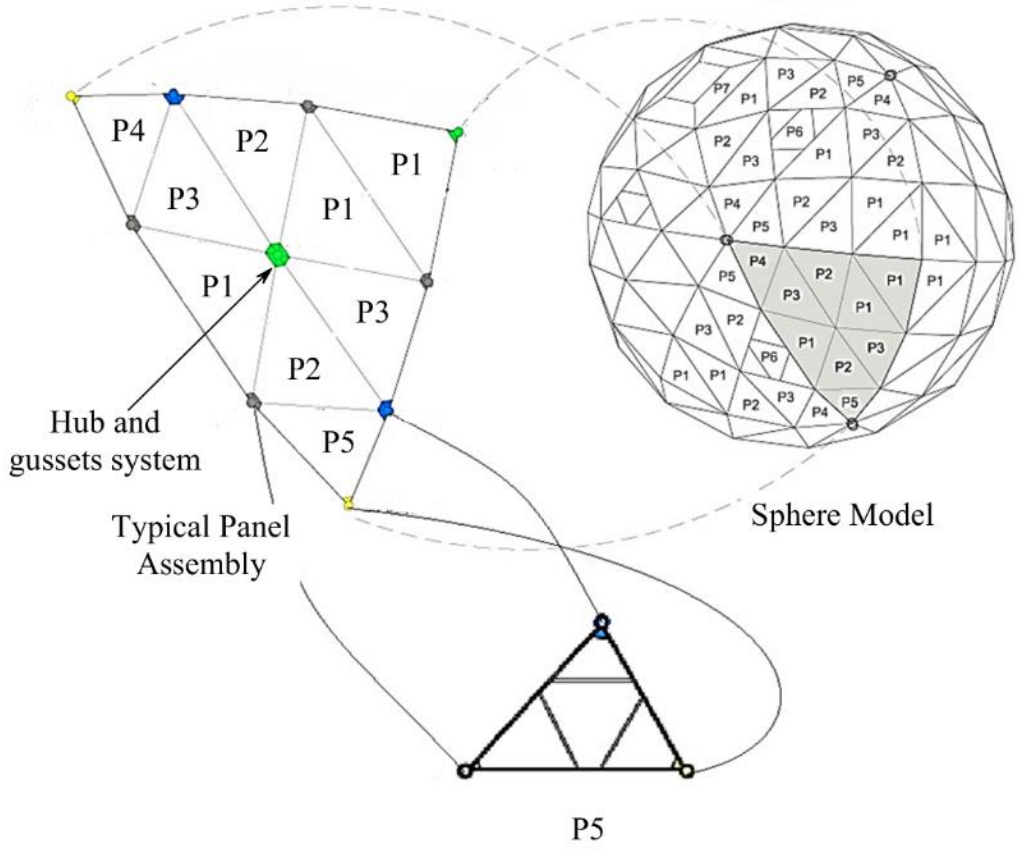

Figure 5.1. Details of; connected struts in the panels and the connected panels to form the cage faces, types of hubs, and the types of the panels of the aquacultural geodesic spherical cage structure with an approximate diameter of 21 m (Page 2013, Vandenbroucke & Metzlaff 2013).

Because of the increased demand for aquaculture structures that have useful features (high volume capacity, rigid frame, and durable structure for up to 10 years) compared with other aquaculture cage structures, the aquacultural geodesic spherical cage structure has been constructed in different volume capacities and diameters since 2006 (InnovaSea Systems 2016) to its most recent product, Aquapod 4700, with a volume capacity of 4700 m^3 (dia. of approximately 21 m)(InnovaSea Systems 2016). The cages function under submersion without any apparent problems from the marine exposure. However, damage to cage structures was reported in the Gulf of Mexico in 2015(InnovaSea Systems 2015) , when the structures were exposed during cleaning to destructive surface waves during a hurricane. InnovaSea systems, Inc. decided to explore a better material option to replace the HDPE lumber (struts). An extruded wood plastic composite (WPC) lumber made from high strength styrenic copolymer and thermally modified wood flour appears to be a promising alternative to replace HDPE, attributable to its features compared with HDPE lumber. For instance, the elastic modulus of WPC lumber is approximately five time the elastic modulus of the HDPE lumber. Although WPCs have been investigated for structural applications (Alvarez-Valencia 2010, Balma 1999, Brandt & Fridley 2003, Brandt & Fridley 2007, Dura 2005, Haiar 2000, Slaughter 2006, Tamrakar 2011) , the performance of WPCs requires evaluation to be utilized for marine applications, where the material will be exposed to the combined effect of temperature and saltwater immersion. Nevertheless, it is very difficult to evaluate the structural performance of the full-scale structure of the cage structure that is made from HDPE or WPC lumber in such combined conditions (temperature and water immersion). WPCs are similar to other thermoplastic materials that exhibit viscoelastic behavior, hence, their time-dependent behavior was investigated. Previous studies have focused on the time-dependent behavior of WPCs

(Alvarez-Valencia et al. 2010, Chang 2011, Hamel et al. 2011, Pooler & Smith 2004, Tamrakar et al. 2011). For the WPC lumber that is considered as alternative to HDPE lumber in the construction of the cage structure, Alrubaie et al. conducted a 180-day creep experiment to compare the time-dependent behavior of HDPE and WPC lumber under similar conditions (temperature 23℃± 2℃ and relative humidity 50%±5%). Furthermore, the short-term time-dependent behavior of the WPCs (that is considered an alternative for the HDPE in the construction of the aquacultural geodesic spherical cage structure) was investigated and modeled under the synergistic effect of elevated temperature and water immersion (Alrubaie et al. 2019, Alrubaie et al. 2019). InnovaSea systems, Inc. conducted mechanical testing at the Advanced Manufacturing Center, University of Maine, Orono in 2006 to evaluate the buckling capacity of full-scale fastened panels (with and without netting) of Aquapod A4700 made from glass bar-reinforced HDPE lumber.

The objective of the research presented here was to experimentally investigate and characterize the buckling capacity of two connected panels made from WPC and HDPE struts with and without metallic mesh, to compare the structural performance of WPC lumber in aquacultural structures.

In this study, 24 triangular panels with struts length; 965 mm, 1003 mm, and 1321 mm were tested in compression along the longest strut. Twelve panels were made from WPC struts and twelve panels were made from HDPE struts. Six of each of these panels were constructed with plastic coated steel wire mesh with 38.1 mm openings and 2.8 mm thickness of the steel wire (Caccese 2006). A set of two panels were connected using three steel galvanized bolts with a diameter of 12.7 mm and two steel galvanized square washers with dimension of 51 mm to each bolt. Four types of panels were experimentally investigated in the buckling experiment:

WPC panels without steel mesh condition (WPC-panel), WPC panels with steel mesh condition (WPC-M-panel), HDPE panels without steel mesh (HDPE-panel), and HDPE panels with steel mesh (HDPE-M-panel). Three sets were tested for each panel type (Tangent Technologies 2015).

5.3 Experimental

5.3.1 Materials

The commercially available HDPE lumber with cross section dimensions (b=140 mm and h= 38.1 mm) was provided by InnovaSea system, Inc. to be used in the manufacture of the HDPE triangular panels with and without steel wire mesh. The struts (made from WPC and HDPE lumber) of the triangular panels were connected to each other to form the panel via a triangular blocks (gussets) made from the same HDPE of the struts. The WPC lumber with cross section dimensions (b= 139 mm and h=33.5 mm was produced using a twin-screw Davis-Standard Woodtruder^{TM} in the Advanced Structures and Composites Center at the University of Maine's Orono campus (Davis-Standard Woodtruder) were used in the manufacture of the WPC triangular panels with and without steel wire mesh . The WPC lumber examined is based on a patent-pending formulation that combines a thermally modified wood flour that was produced at a sawmill in Uimaharju, Finland and a high strength styrenic copolymer system in an equivalent weight ratio to each of the two constituents. The elastic modulus and the flexural strength of the WPC and HDPE lumber were reported elsewhere (Alrubaie et al. 2019). Figure 5.2 shows representative specimens of WPC and HDPE lumber tested in accordance with ASTM D6109 to obtain the elastic modulus and the flexural strength (F_b). Table 5.1 shows the mechanical properties of The WPC and HDPE lumber used in this study.

Table 5.1. Mechanical properties of WPC and HDPE lumber used as struts of the aquacultural geodesic components of Aquapod net pen geodesic spherical cage structure.

Material	**Flexural modulus (E) GPa (COV%)**	**Flexural strength (Fb) MPa (COV%)**
WPC	4.34 (6)	41.2 (11)
HDPE	0.93 (3)	14.1 (5)

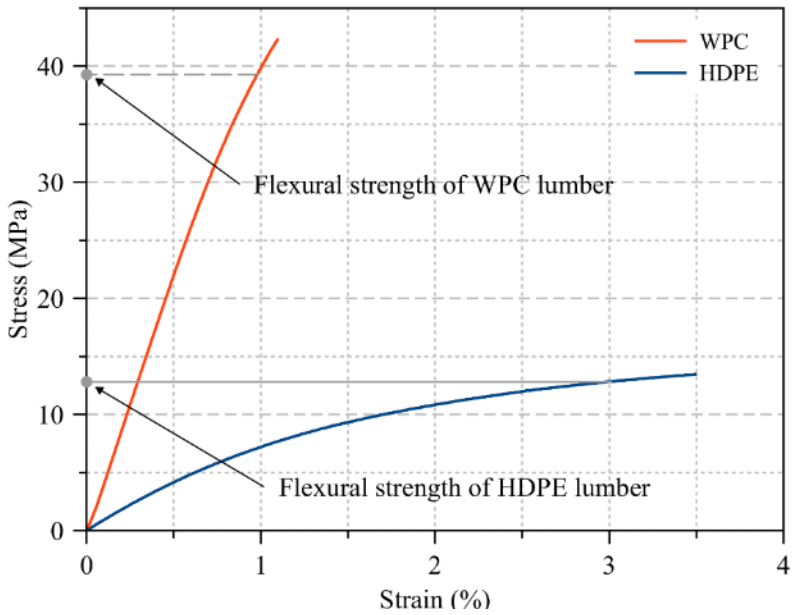

Figure 5.2. Typical stress versus strain relationship to obtain the elastic modulus and the flexural strength of WPC and HDPE lumber in accordance with ASTM D6109.

5.3.2 Equipment and Test Setup

The panel manufacture was conducted by InnovaSea system, Inc. The fixture to test the connected panels in compression was manufactured at the Advanced Structures and Composite Center, University of Maine, Orono, Maine. Figure 5.3 shows the connected triangular panels and the test fixture. An Instron test frame with a load cell capacity of 1334 kN was used. The data acquisition system (DAQ) with a written labview software was used to collect: the applied axial load (negative Y-direction in Figure 5.4), the axial displacement (of the actuator, the in-plane displacement of the struts), the in-plane displacement (negative and positive direction of X-axis as shown in Figure 5.4), and the out of plane displacement (negative and positive direction of Z-axis as shown in Figure 5.4). The tests were conducted in displacement control with a crosshead speed of 1 mm/min.

Figure 5.3. (Left) the test frame and the buckling test setup, (right) the WPC and HDPE connected triangular panels with and without metallic mesh.

5.3.3 Degrees of Freedom of the Supports System of the Triangular Panels

Table 5.2 and Figure 5.4 summarize the degree of freedom of each support of the triangular panels during the buckling test.

Table 5.2.Two dimensional degrees of freedom of the triangular panels during the buckling experiment.

Supports boundary conditions (free=0, fixed=1)	**Supports**			
	a	**b**	**c**	**d**
Ux	1	1	1	1
Uy	0	1	1	1
θz	0	0	0	0

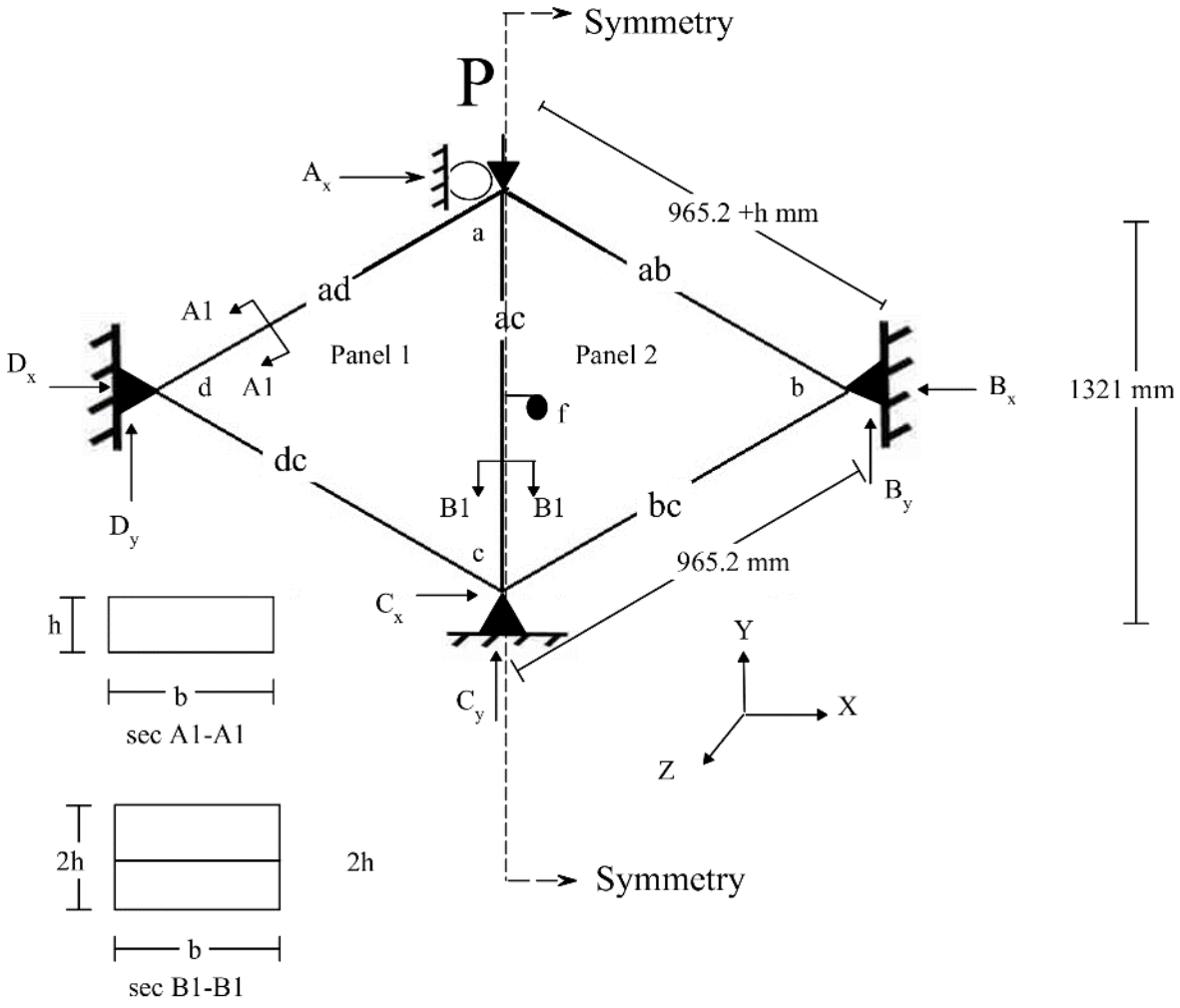

Figure 5.4. Schematic of the 2D free body diagram of the tested connected (bolted) of WPC and HDPE triangular panels with and without mesh.

5.4 Discussion of Results

The relationship between the applied buckling load and lateral deflection of the middle vertical strut ac at point f (Figure 5.4) for the connected components (panels) made from WPC and HDPE struts are reported in Figures 5.5, 5.6, 5.8, and 5.9. The buckling capacity of the panels made from WPC struts was three times the buckling capacity of the panels made from HDPE struts. The steel wire mesh contributed to the increased buckling capacity of the panels. A 2D FE analysis model provided a useful assessment of the multiplier factor (α) that can be used in the

computation of the reactions and the member of forces under different values of applied loads. Table 5.3 reports the values of α.Table 5.4 reports the average maximum buckling load of the HDPE and WPC struts connected panels at each condition (with and without metallic mesh) and their corresponding type of failure.

The buckling failure of the cage components (panels) made from WPC struts was the dominant type of failure at one of the regions of the galvanized bolts that connect the two panels causing a net section failure at the region where the bolts were located, whereas, no such net section failure was noticed at the buckling failure occurred for the panels made from HDPE lumber. This is attributable to the brittle behavior of the high wood flour content WPC lumber compared with the HDPE plastic lumber. Table 5.4 summarizes the type of failure of the structural components of the cage structure with and without metallic mesh. Table 5.5 summarizes the implementation of the multiplier load factor (α) to compute the allowable member force of strut ac based on the buckling load values obtained from Southwell's method (Barbero & Tomblin 1993).

Regarding the connected components (panels) made from WPC lumber (strut) without metallic mesh, the buckling failure tended to be abrupt after reaching the maximum applied load, as shown in Figure 5.5. A similar pattern of the failure propagation was observed in the panels made from HDPE lumber without metallic mesh, the panels showed propagated deformation after reaching the maximum applied load without an abrupt failure, as shown in Figure 5.6. However, panel number three (HDPE-panel-3), as shown in Figure 5.6, exhibited a different load-lateral deflection curve. The panels (the middle strut ac) started deforming with the propagation of the applied load. This can be attributed to the geometry of the panels or to an eccentricity has been developed while the load was imposed to the panel.

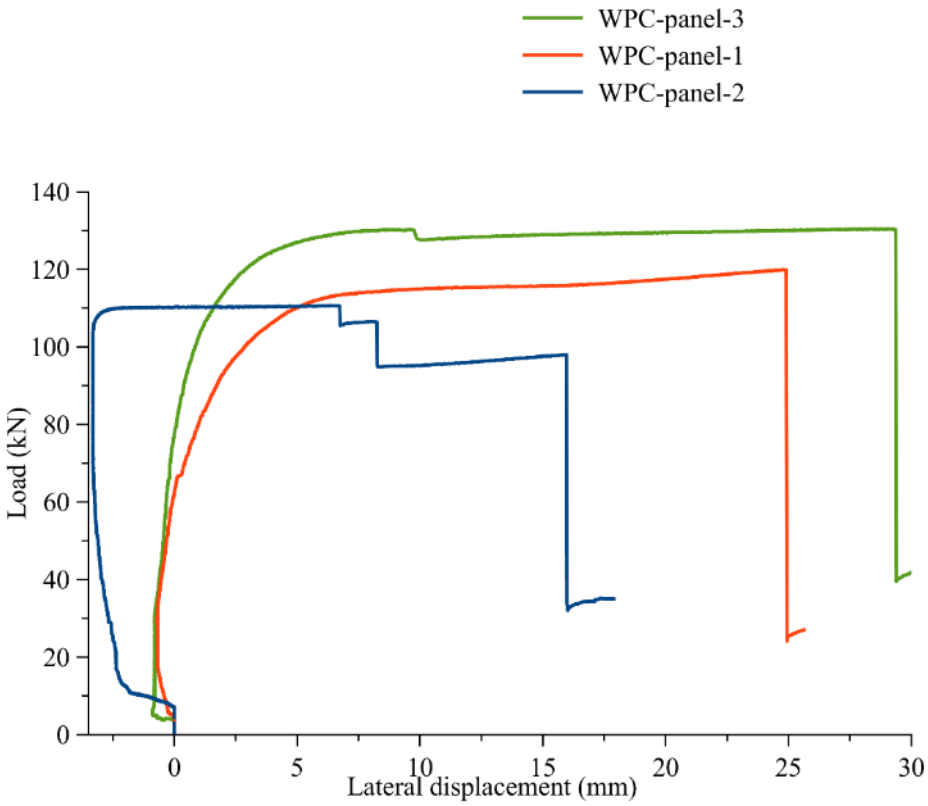

Figure 5.5. The relationship between the applied buckling load and lateral mid-span deflection (point f in Figure 5.4) of the vertical strut ac in the panels made from WPC struts and without metallic mesh.

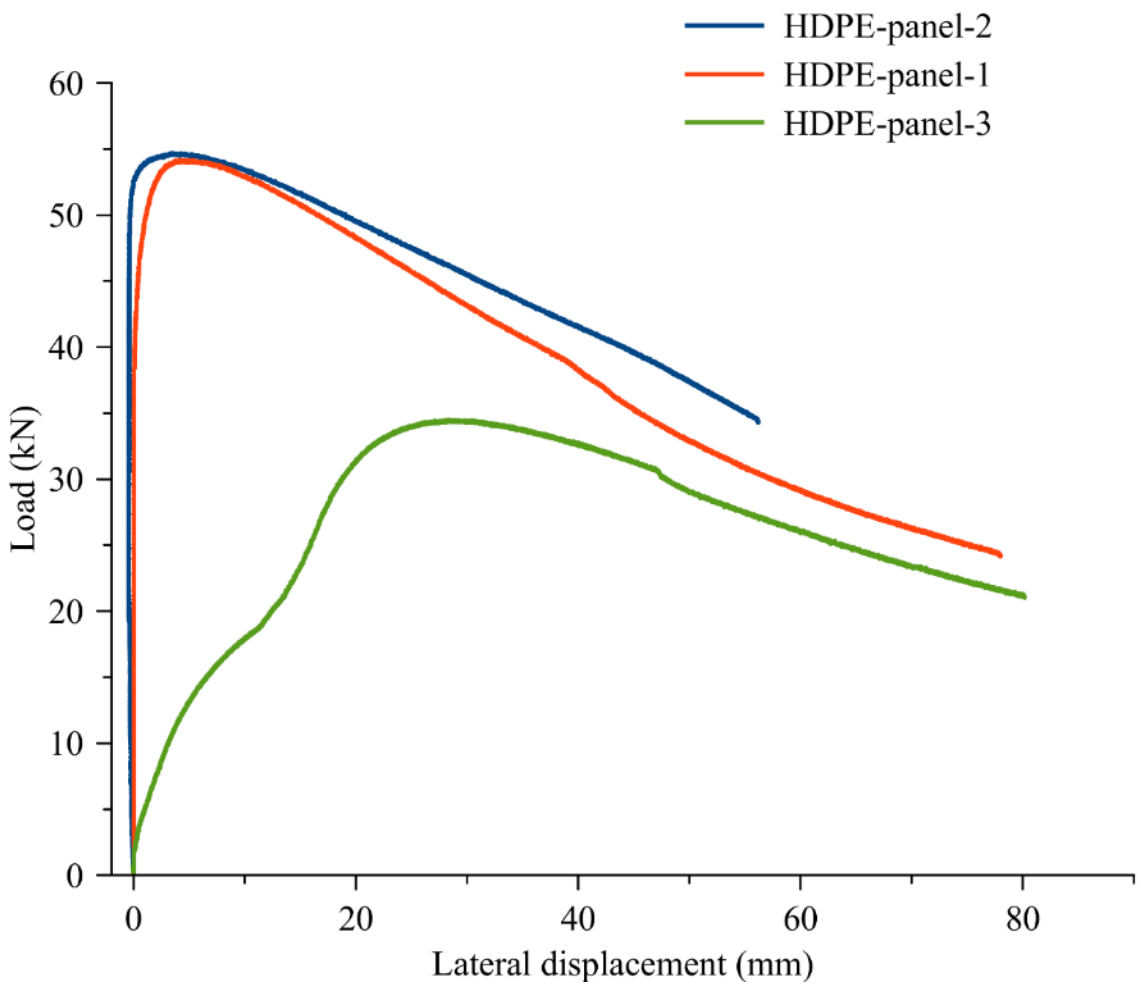

Figure 5.6. The relationship between the applied buckling load and lateral mid-span deflection of the vertical strut ac in the panels made from HDPE struts and without metallic mesh.

Regarding the failure behavior of the panels made from WPC with metallic mesh, the metallic mesh contributed into an increase in the buckling capacity (maximum applied load) approximately three times of the buckling capacity (maximum applied load) of the panels made without the metallic mesh. However, as regards to improving the ductility of the panels, the metallic mesh did not contribute into improved ductility of the panels made from WPC struts. The

panels showed a lateral deformation smaller than 2 mm before reaching the maximum applied load and then experiencing abrupt failure. Moreover, the failure mode (of the panels made from WPC struts with mesh) in the struts did not change from the failure mode of the panels without the metallic mesh, which is the net section failure at the connected struts attributable to the buckling in X-axis at the strut ac (Figure 5.3). Figure 5.7 shows the failure mode of the panels made from HDPE and WPC lumber for the four different cases.

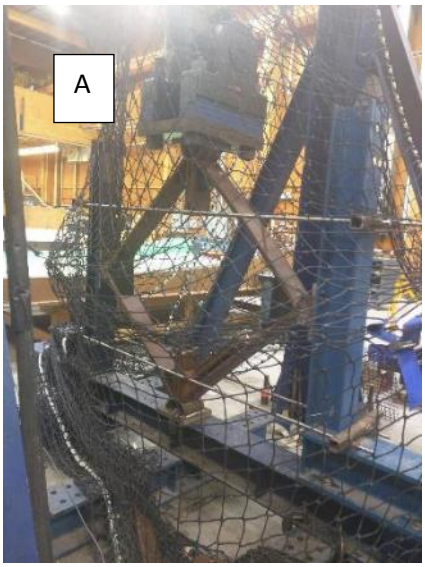

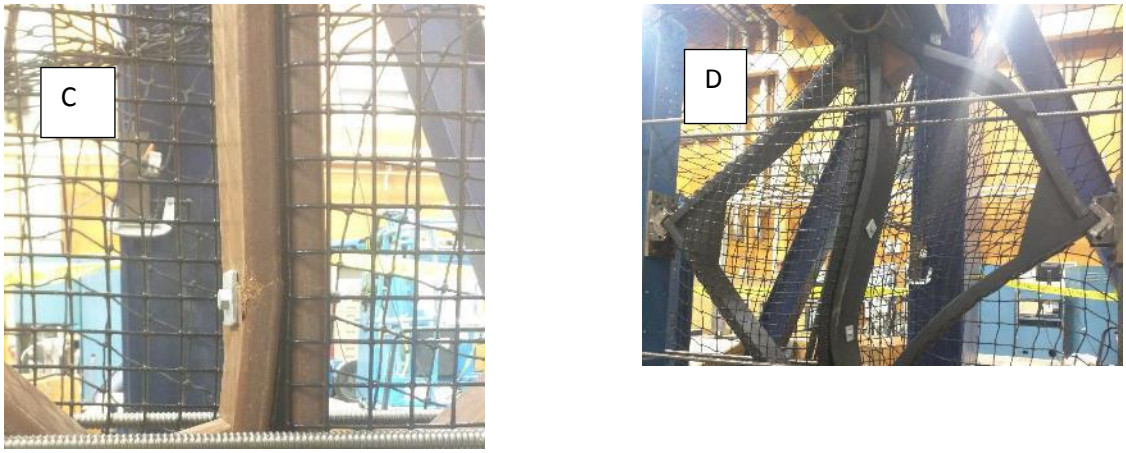

Figure 5.7. Failure modes of the panels made from HDPE and WPC lumber for the four different cases; A) net section failure at the middle strut ac at the location of the bolt connection of the panels made from WPC without metallic mesh, B) buckling mode failure of the strut ac of the panels made from HDPE without metallic mesh, C) net section failure mode of panels made from WPC struts with metallic mesh, and D) buckling failure mode of the panels made from HDPE struts with metallic mesh.

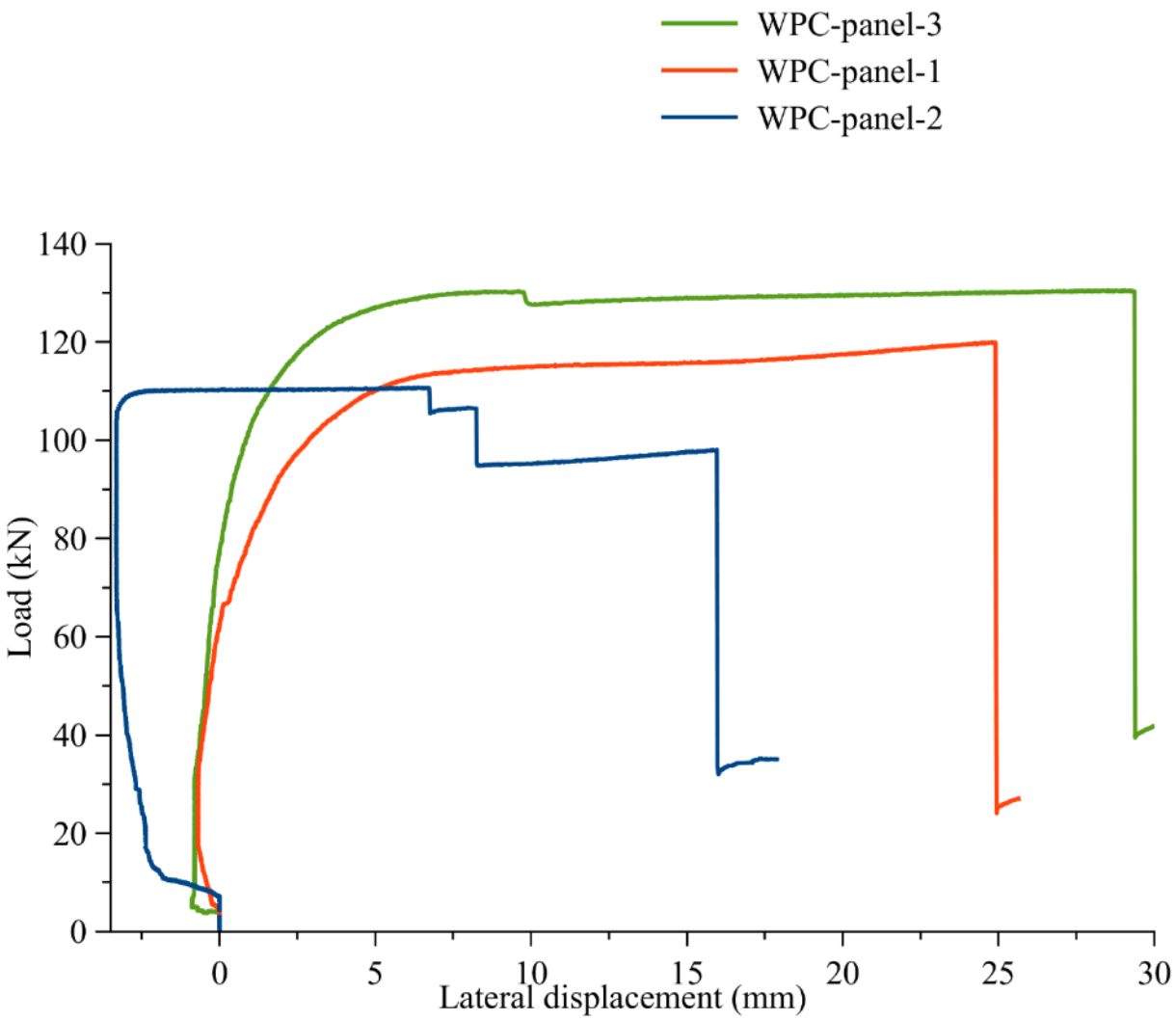

Figure 5.8. The relationship between the applied buckling load and lateral mid-span deflection of the vertical strut ac in the panels made from WPC struts and with metallic mesh.

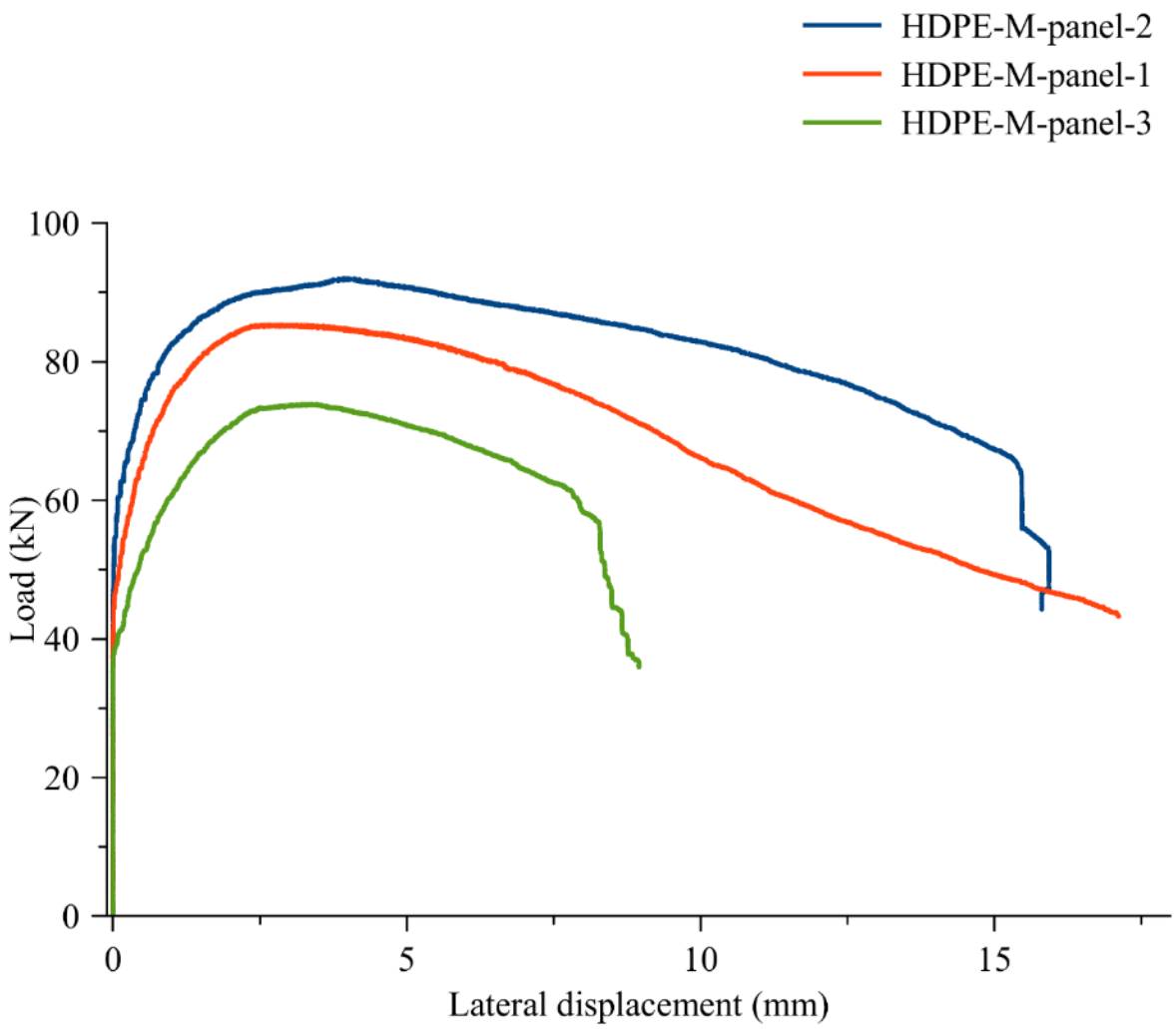

Figure 5.9. The relationship between the applied buckling load and lateral mid-span deflection of the vertical strut ac in the panels made from HDPE struts and with metallic mesh.

The metallic mesh is affixed to the WPC and HDPE struts by staples on the perimeter of the struts (on the width b of the cross section of the struts (sec A1-A1 and B1-B1) in Figure 5.4). The staples have shown good resistance to the applied load and in developing buckling capacity of the panels with the metallic mesh. This can be observed with the small lateral displacement of the panels (with metallic mesh) made from WPC and HDPE struts 1.5 mm and 3.4 mm , corresponding to the maximum buckling capacity, respectively. Whereas, the lateral displacements for the same

type of panels without metallic mesh were; 20.1 mm and 12.5 mm, respectively.

5.4.1 Structural Analysis of the Tested Structural Components (Panels) of the Aquacultural Geodesic Spherical Cage Structure

To compute the reaction and the section forces at the supports and the struts of the connected, respectively, 2D (two dimensional) finite element (FE) linear elastic analyses models were conducted to the four types of the test panels (WPC-M-panel, WPC-panel, HDPE-M-panel, and HDPE-panel) using commercially available software Abaqus/CAE("Abaqus/CAE 2017," 2017) with the following assumptions:

1. Based on the symmetry of the connected panels, panel 1 in Figure 5.4 was used on the 2D FE model to compute the member forces and the support reactions.

2. The supports at points b,c, and d were assumed to be as pin supports (vertical (Y-axis) and horizontal (X-axis) movement restriction), whereas, point a was assumed to be as s roller support (horizontal (X-axis) movement restriction). This assumption was made based on the design of the fixture used in the experiment and the ability of the structure to have rotation at the points a,b,c, and d.

3. A slender beam element B23 (cubic beam in plane) was chosen from the available types of beam elements available in the used commercial software Abaqus and was used in the 2D linear finite element (FE) analysis of the structural components of the aquacultural geodesic spherical cage structure. The selection was made based on the assumption that both the struts of the components and the metallic mesh are slender even some of the beams have a slender ratio (span (l)/ radius of gyration (r)) less than 200. This assumption eliminated the need to have the values of Poisson's ratio of the materials of the components (steel of the metallic mesh, WPC struts, and HDPE

struts), i.e. the elastic moduli were the required input for the mechanical properties of the materials in the 2D FE linear analysis model.

4. Regarding the connected panels with metallic mesh, the metallic mesh was modeled as vertical and horizontal beam elements [type B23(Abaqus Analysis User's Guide)] (each wire mesh modeled as a beam) spaced 38.1 mm from each other and has a circular cross-section with a diameter of 3 mm to each beam. The geometry and the space of the wire mesh was implemented based on the specification of the metallic wire mesh, Aquamesh®(RIVERDALE, 2019) used in the manufacture of the structural panels of the aquacultural geodesic spherical cage structure.

5. The elastic moduli of the WPC and HDPE lumber used in the structural analysis were obtained from the 4-point bending test conducted on specimens with a span to depth ratio of 16 to be 4430 MPa and 930 MPa as reported in Table 5.1, respectively. The elastic modulus of the wire mesh was assumed to be the elastic modulus of steel, E_{steel}=200000MPa.

6. The 2D FE model was conducted to investigate the response of the structure in the linear region. Thus, the values of the applied load were assumed to be a unit load (1 N) to be applied to the structure. The computed member forces and reactions at the supports represented a multiplier coefficient that can be used to compute the reactions and member forces at any value of the applied load.

The reaction values at the supports were computed from the 2D FE model. Furthermore, the member forces were computed for the tested panels in the four cases, to provide an understanding to the distribution of the applied load through the struts of the panels. However, the strut cd for the

panels made from HDPE or WPC lumber without metallic mesh had no member force. Whereas, the metallic mesh contributed into distributing the applied load among the struts; ac, cd, and ad. Furthermore, the value of the member force varied along the length of the strut attributable to the presence of the metallic mesh. The maximum values of member forces of the struts of the panels made from HDPE and WPC struts with metallic mesh are shown and reported in Table 5.3 and Figure 5.10, respectively.

Table 5.3. Reactions and member forces computed from the 2D FE linear analyses obtained from applying unit load on panel 1 (Figure 5.4 at point a) of the aquacultural geodesic spherical cage structure for four sample types: WPC-M-panel, WPC-panel, HDPE-M-panel, and HDPE-panel.

Reactions and member	**Condition of the panels made from WPC struts**	**Condition of the panels made from HDPE struts**

forces (N)	M-panel	panel	M-panel	panel
A_x	-0.4	-0.414	-0.37	-0.414
C_x	-0.004	0.001	0.01	0.001
C_y	0.66	0.64	0.7	0.64
D_x	0.404	0.413	0.38	0.413
D_y	0.34	0.36	0.32	0.36
F_{ad}	-0.54	-0.55	-0.54	-0.55
F_{ac}	-0.60	-0.64	-0.54	-0.64
F_{cd}	-0.04	0	-0.1	0

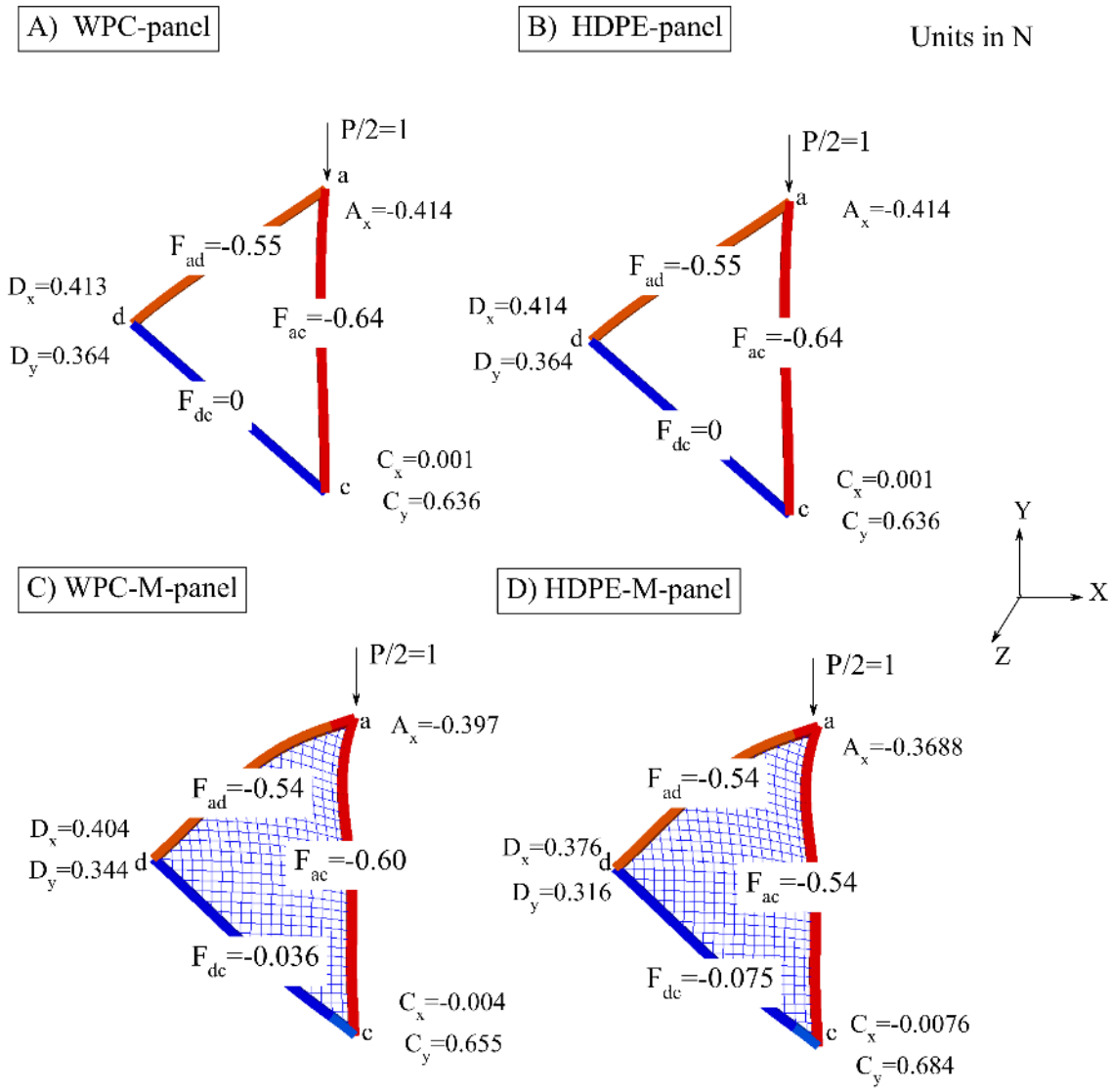

Figure 5.10. Reactions and member forces in N units of panel 1 of the aquacultural geodesic spherical cage structure obtained from 2D FE linear analyses; A)WPC-Panel, B)HDPE-panel, C)WPC-M-panel, and C) HDPE-M-panel.

5.4.2 Southwell's Method to Determine the Critical Load

To investigate the critical load mode for the four cases of the panels made from WPC and HDPE struts in the cases of metallic wire mesh and without wire mesh, Southwell's method(E. Barbero & Tomblin, 1993) was implemented. The method can be summarized by creating a plot based on the relationship between; the ratio of the lateral displacement (deflection) (Δ) over the applied buckling load (P), and the lateral displacement (Δ). If this relationship can be described by a linear relationship, then, the inverse of the slope of this line represents the critical buckling load (P_{cr}) and the buckling mode is global. This critical load does not account for imperfections or mode of interactions. Southwell's method was implemented on the relationships reported in Figures 5.11-5.14 after modifying the relationship to include the load vs later deflection only at the limit of the maximum applied load (i.e., the data points after the maximum applied load has not been considered in the application of Southwell's method). By using linear regression to obtain the slope of the equation of the line, hence, the inverse of the slope of the line represents the value of $P_{cr.}$ Figures 5.11=5.14 show the implication of Southwell's method on the four sample panels (WPC-panel, WPC-M-panel, HDPE-panel, and HDPE-M-panel) and the obtained slope of each tested set of panels. Based on the linear relationship between Δ/P versus Δ, the critical load can be determined.

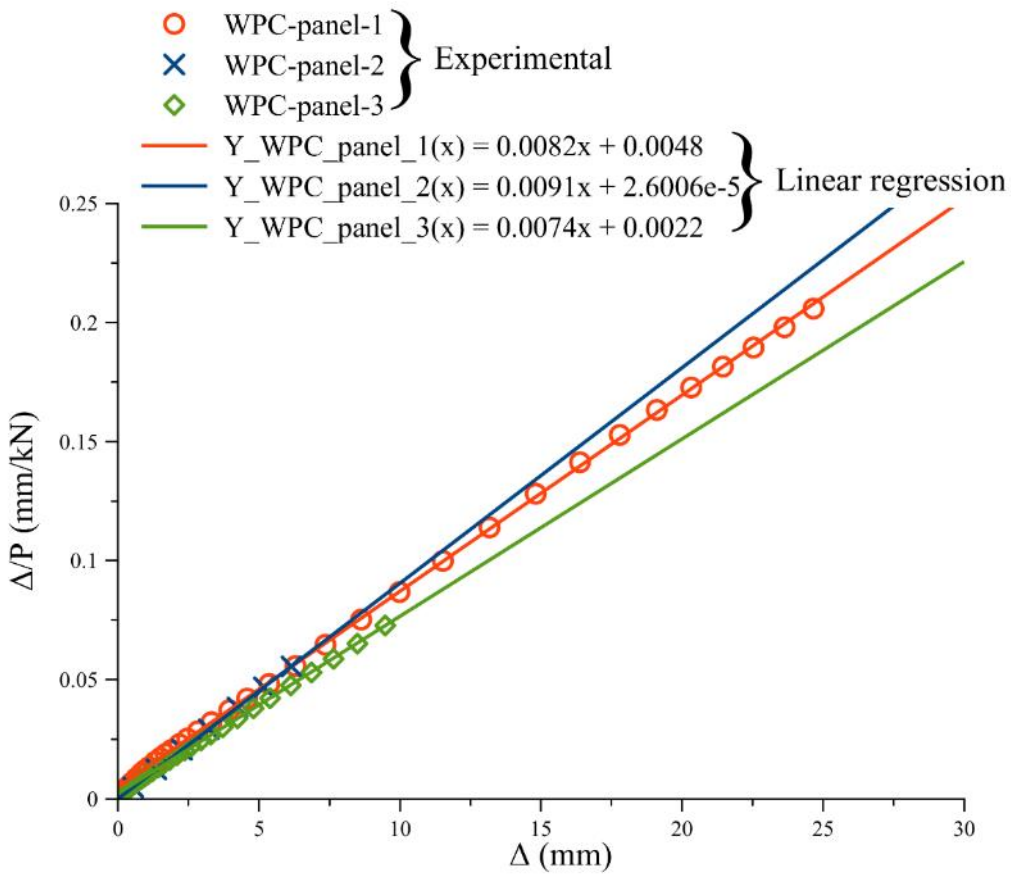

Figure 5.11. Application of Southwell's method to obtain the critical buckling load of the structural panels of the cage structure made from WPC struts without metallic mesh.

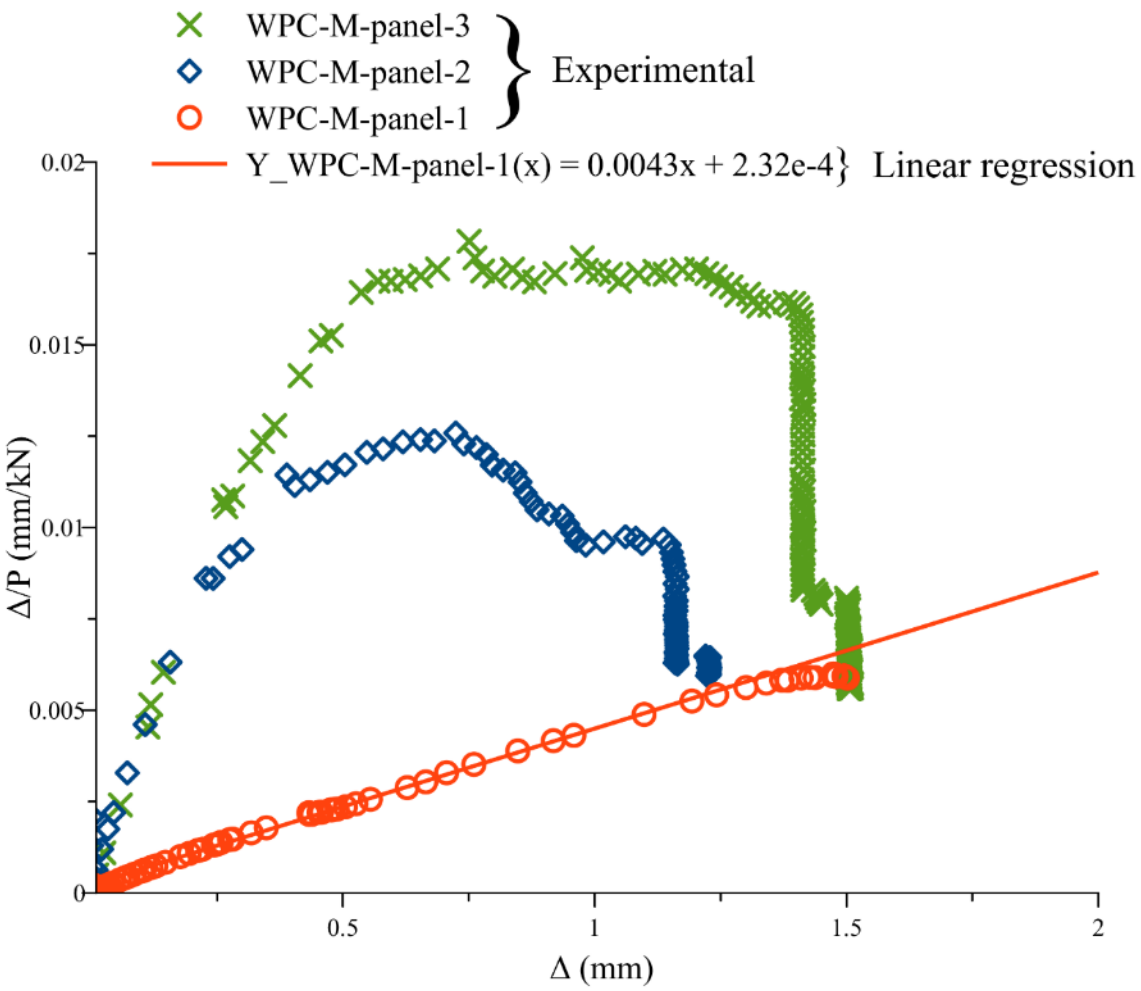

Figure 5.12. Application of Southwell's method to obtain the critical buckling load of the structural panels of the cage structure made from WPC struts with metallic mesh with the shaded region of the linear relationship between Δ/P versus Δ.

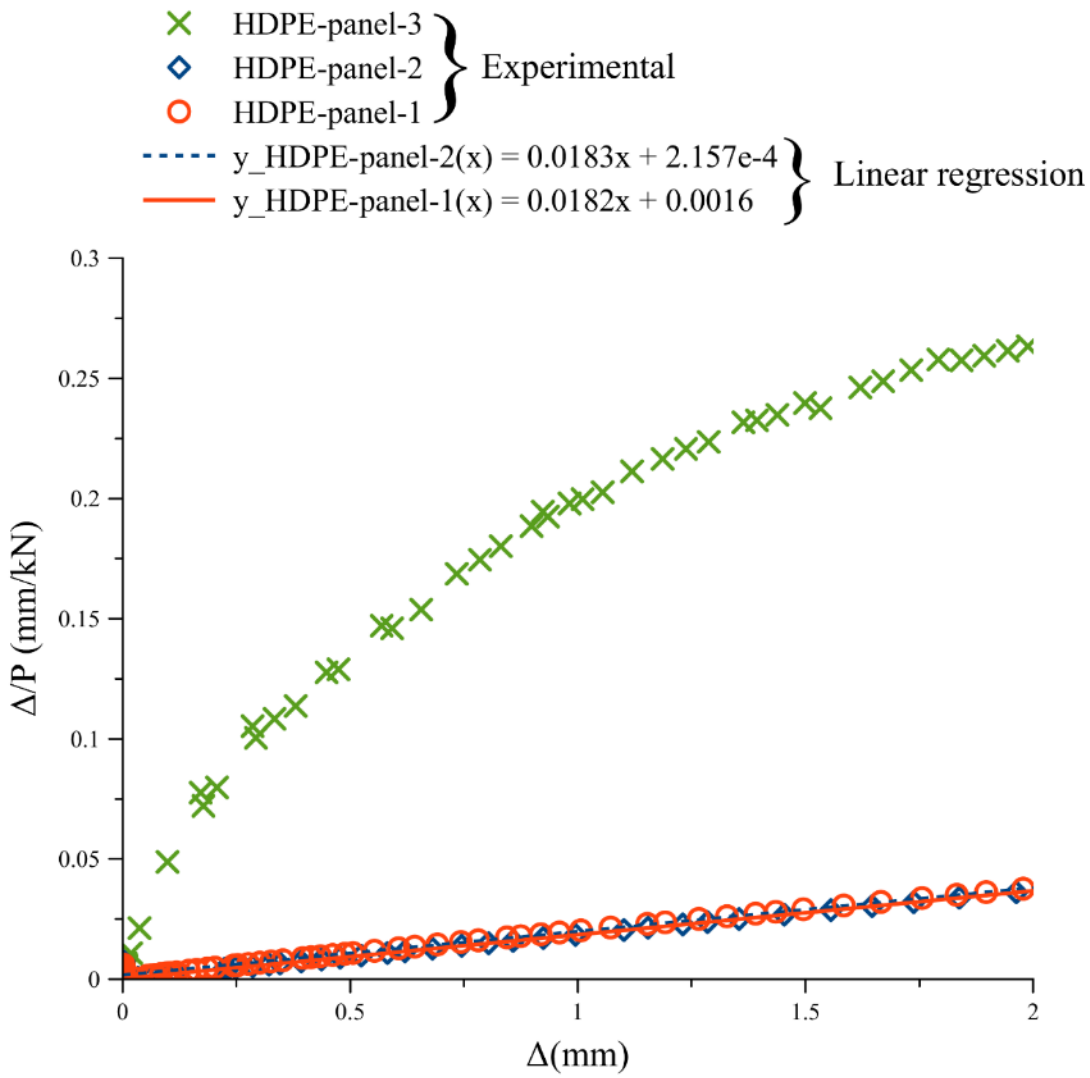

Figure 5.13. Application of Southwell's method to obtain the critical buckling load of the structural panels of the cage structure made from HDPE struts without metallic mesh.

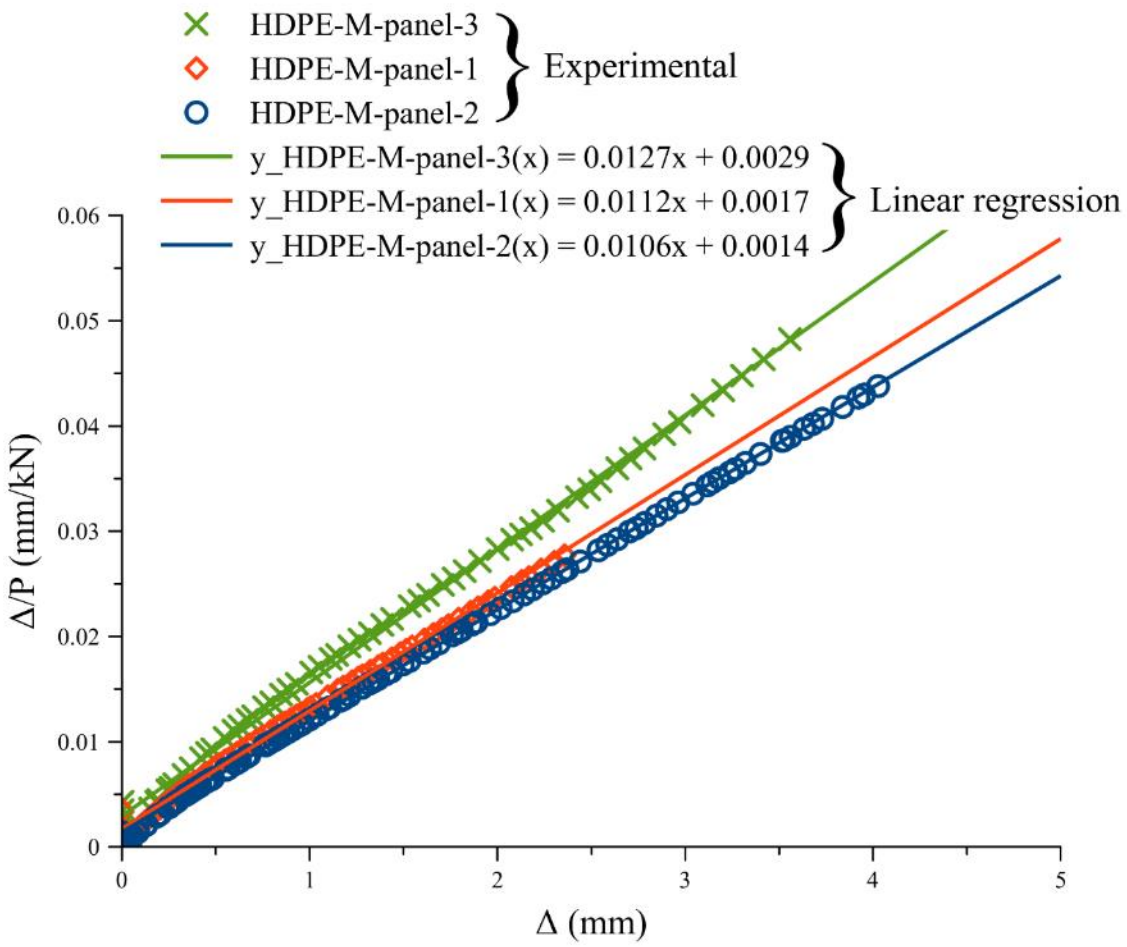

Figure 5.14. Application of Southwell's method to obtain the critical buckling load of the structural panels of the cage structure made from HDPE struts with metallic mesh.

Table 5.4. The experimental maximum buckling load and the failure type and occurrence sequence

in the structural components of the aquacultural geodesic spherical cage structure.

Connected triangular panels		Experimental buckling load for each panel (kN)			Failure type and location of occurrence in the component	
Struts Material	**Mesh condition M-panel=with mesh panel=without mesh**	**P1**	**P2**	**P3**	**M-panel**	**panel**
WPC	M-panel	294	207	270	Struts Buckling failure (X-axis) and metallic mesh buckling (Z-axis)	Buckling failure (X-axis)
WPC	Panel	120	111	131		
HDPE	M-panel	85	92	74	Metallic mesh buckling (Z-axis) followed by struts buckling (X-axis)	Buckling failure (X-axis) in the struts
HDPE	panel	54	55	35		

Table 5.5. The buckling load of the member ac based on multiplying the multiplier value α obtained from the 2D FE linear analyses by the value of critical load obtained from Southwell's

method.

Connected panels	Experimental	Southwell's method	Euler's method	Allowable buckling load
	Max. average load (kN)		$\frac{4\pi^2 EI}{l^2}$	
Material and mesh condition	F_{ac}	$F_{ac\text{-}Southwell\ critical}$ (kN)	$F_{ac\text{-}Euler\text{-}critical}$ (kN)	$F_{ac\ (kN)}$
WPC-M-panel	129	116	NA	70
WPC-panel	60	61	43	39
HDPE-M-panel	42	44	NA	24
HDPE-panel	24	27	14	17

5.5 Conclusions

1. The buckling behavior of the structural components of the aquacultural geodesic spherical cage structure made from HDPE and WPC lumber was experimentally investigated and characterized. The buckling capacity (load) of the triangular panels made from WPC struts and with mesh was 256.81 kN, whereas, the buckling capacity of the same type of panels made from HDPE struts was 83.80 kN. Furthermore, the buckling capacity of the panels made from WPC struts and without steel mesh was 120.42 kN which was 2.5 times the buckling capacity of the same condition of panels but made from HDPE struts.

2. The metallic mesh contributed into distributing the member forces through the struts: ac, ca

and da of the component (panel). Whereas, the panels without metallic mesh experienced strut (cd) without member force.

3. Attributable to the brittleness behavior of WPC lumber (50 wt.% wood flour) compared with the ductile behavior of HDPE lumber (100 wt.% plastic), an abrupt failure to panels made from WPC was observed in the experiments.

4. According to the linear structural analysis, the short struts in the connected panels (struts bc and strut cd) did not carry load values and this contributed to the buckling occurrence to be initiated in the longest strut (ac) and then at the shorter struts (ab and ad) for the panels made from WPC and HDPE lumber and without metallic mesh.

5. As a containment aquaculture structure system in open ocean environments, it is preferable to have a structural material (strut) that shows an indication prior to failure or to defect without breakage, than an abrupt failure, so that the member can be replaced properly.

6. Attributable to the viscoelastic behavior and the brittleness behavior of the WPC in this study, it is preferable to consider using the WPC lumber in structural application where the applied load should be at a low level compared with strength of the WPC, to avoid the abrupt failure of the structural member during the service life of the structure.

CHAPTER 6

CONCLUSIONS AND FUTURE WORK

6.1 Conclusions

Marine structures require an investigation of the viscoelastic behavior under the combined effect of temperature and water immersion. The short-term (30-minute) creep and creep-recovery in this study provided an understanding to the viscoelastic behavior of WPC lumber under the combined effect of temperature and water immersion. Evaluating the short-term time-dependent behavior of the WPC lumber in this study and comparing it with the time-dependent behavior of the WPCs from previous studies under different conditions have emphasized on the potential capabilities of the WPCs in this study to be used in structural application attributable to the lower creep strain rate. Moreover, the WPCs in this study and attributable to its property of maintaining the modulus of elasticity at values of temperature below the glass transition temperature has the ability to be used in application that are exposed merely to the effect of elevated temperature.

Attributable to the viscoelastic and the brittle behavior (attributed to high content of wood flour in the formulation of the WPCs of this study), the use of WPC members in structural application under different environmental conditions can be accomplished by taking in consideration: (1) the applied levels of stress have to be low below 30% of the maximum strength of the WPCs, and (2) avoid the environments where the temperature level is higher than the glass transition zone of the WPCs of this study.

In addition to the elastic modulus of the WPC lumber in this study is approximately five times the elastic modulus of HDPE lumber and attributable to the short-term and long-term time dependent behavior of the WPCs of this study compared with the long-term time-dependent behavior of the HDPE material, the WPC lumber in this study is considered a competing alternative to replace the HDPE lumber in the manufacturing of the Aquapod structures.

However, limitations have to be taken into consideration as regards the size of the aquaculture structure manufactured using the WPCs, attributable to the developed weight of the structure (the density of the WPC lumber is higher than the density of the HDPE lumber) and the accompanied developed stresses (should not exceed the level of 30% of the maximum strength) on the structural members made from WPCs.

6.2 Future Work

1- Further studies to evaluate the structural performance of the WPC lumber as structural members are required to provide a sufficient understanding to the use of WPC lumber in the construction of Aquapod cage structures. For instance, the evaluating of the bolt connections where each strut is connected to the adjacent strut by bolts. Furthermore, the evaluating of bolt connections of each strut in the triangular panel to the hub system that holds six panels.

2- Long-term (more than three years) creep experiments are essential to study the creep behavior of the WPC used in this study in high temperature environments and under the field temperature (ambient temperature). For instance, Southern Iraq region where the temperature during summer season (from April till October) can reach 50℃.

3- Field Conditioning (ambient temperature and moisture) to the WPC in marine environments and evaluate the reduction in the mechanical properties by series of mechanical testing on a regular basis duration. For instance, having WPC lumber immersed at the Gulf of Maine, Maine, USA and have the lumber conditioned at the ambient temperature and saltwater immersion. Followed by series of mechanical testing and water uptake to evaluate the reduction in the mechanical properties and to evaluate the water uptake wt%.

BIBLIOGRAPHY

Abaqus/CAE (2017). Rohde Island: SIMULIA Inc.

AbaqusAnalysisUser'sGuide. Euler-Bernoulli (slender) beams. *Abaqus 6.14.* Retrieved from https://www.sharcnet.ca/Software/Abaqus/6.14.2/v6.14/books/usb/default.htm?startat=pt06ch29s03alm08.html.

Alrubaie, M. A. A., Lopez-Anido, R., Gardner, D., Tajvidi, M., & Han, Y. (2019). Experimental Investigation of the Hygrothermal Creep Strain of Wood Plastic Composite (WPC) Lumber Made from Thermally Modified Wood. *Journal of Thermoplastic Composite Materials*, 21. doi:https://doi.org/10.1177/0892705718820398

Alrubaie, M. A. A., Lopez-Anido, R., Gardner, D., Tajvidi, M., & Han, Y. (2019). Modeling the Hygrothermal Creep behavior of Wood Plastic Composite (WPC) Lumber Made from Thermally Modified Wood. *Journal of Thermoplastic Composite Materials*, 16. doi:https://doi.org/10.1177/0892705718820404

Alrubaie, M. A. A., Lopez-Anido, R., Gardner, D.. (2019). Flexural Creep Behavior of HDPE Lumber and WPC Lumber made from Thermally Modified Wood. *Journal of Construction and Building Materials*. Under review.

Alvarez-Valencia, D., Dagher, H. J., Davids, W. G., Lopez-Anido, R. A., & Gardner, D. J. (2010). Structural performance of wood plastic composite sheet piling. *Journal of Materials in Civil Engineering*, *22*(12), 1235-1243.

ASTM International, (2010). Standard Practice for Sampling and Data-Analysis for Structural Wood and Wood-Based Products *D2915-10*. West Conshohocken, PA.

ASTM International, (2010). Standard Test Method for Water Absorption of Plastics *D570-98(Reapproved 2010)*. West Conshohocken, PA.

ASTM International,(2011). Standard Guide for Evaluating Mechanical and Physical Properties of Wood- Plastic Composite Products *D7031-11*. West Conshohocken, PA.

ASTM International, (2013). Standard Test Methods for Compressive and Flexural Creep and Creep-Rupture of Plastic Lumber and Shapes *D6112-13*. West Conshohocken, PA.

ASTM International, (2013). Standard Test Methods for Flexural Properties of Unreinforced and Reinforced Plastic Lumber and Related Products *D6109-13*. West Conshohocken, PA.

ASTM International, & (2015). Standard Specification for Evaluation of Duration of Load and Creep Effects of Wood and Wood-Based Products *D6815-09 (Reapproved 2015)*. West Conshohocken, PA.

ASTM International, (2015). Standard Test Method for Glass Transition Temperature (DMA Tg) of Polymer Matrix Composites by Dynamic Mechanical Analysis (DMA) *D7028-07 (Reapproved 2015)*. West Conshohocken, PA.

ASTM International,(2017). standard Test Methods for Flexural Properties of Unreinforced and Reinforced Plastics and Electrical Insulating Materials *D790-17*. West Conshohocken, PA.

Balma, D. A. (1999). Evaluation of bolted connections in wood plastic composites. *Washington State University.*

Barbero, E., & Tomblin, J. (1993). Euler buckling of thin-walled composite columns. *Thin-walled structures, 17*(4), 237-258.

Barbero, E. J. (2013). Finite element analysis of composite materials using AbaqusTM: *CRC press.*

Berube, K., Lopez-Anido, R., & Goupee, A. (2016). Determining the flexural and shear moduli of fiber-reinforced polymer composites using three-dimensional digital image correlation. *Experimental Techniques*, *40*(4), 1263-1273.

Brandt, C. W., & Fridley, K. J. (2003). Load-duration behavior of wood-plastic composites. *Journal of Materials in Civil Engineering, 15*(6), 524-536.

Brandt, C. W., & Fridley, K. J. (2007). Effect of load rate on flexural properties of wood-plastic composites. *Wood and fiber science, 35*(1), 135-147.

Bright, K. D., & Smith, P. M. (2007). Perceptions of new and established waterfront materials by US marine decision makers. *Wood and fiber science, 34*(2), 186-204.

Carlsson, L. A., Adams, D. F., & Pipes, R. B. (2002). *Experimental characterization of advanced composite materials*: CRC press.

Chakraverty, A., Mohanty, U., Mishra, S., & Satapathy, A. (2015). *Sea water ageing of GFRP composites and the dissolved salts.* Paper presented at the IOP conference series: materials science and engineering.

Chang, F.-C. (2011). Creep behaviour of wood-plastic composites. *University of British Columbia.*

Chang, F.-C., Lam, F., & Kadla, J. F. (2013). Application of time–temperature–stress superposition on creep of wood–plastic composites. *Mechanics of Time-Dependent Materials, 17*(3), 427-437.

Chang, F.-C., Lam, F., & Kadla, J. F. (2014). The effect of temperature on creep behavior of wood-plastic composites. *Journal of Reinforced Plastics and Composites, 33*(9), 883-892. doi:10.1177/0731684414523691.

Chang, W.-P., Kim, K.-J., & Gupta, R. K. (2009). Moisture absorption behavior of wood/plastic composites made with ultrasound-assisted alkali-treated wood particulates. *Composite Interfaces, 16*(7-9), 937-951.

Chassagne, P., Saïd, E. B., Jullien, J.-F., & Galimard, P. (2005). Three dimensional creep model for wood under variable humidity-numerical analyses at different material scales. *Mechanics of Time-Dependent Materials, 9*(4), 1-21.

Cheng, Q. (2005). Microstuctural Changes in Wood-Plastic Composites (WPC) Due to Extended Moisture Cycling and its Relationship to Mechanical Performance Changes.

Commerce, D. o. (2018, 11-Jun-2018). Water Temperature Table of All Coastal Regions. Retrieved from https://www.nodc.noaa.gov/dsdt/cwtg/all.html

Danawade, B., Malagi, R., Kalamkar, R., & Sarode, A. (2014). Effect of span-to-depth ratio on flexural properties of wood filled steel tubes. *Procedia Materials Science, 5*, 96-105.

Davids, W. G., Willey, N., Lopez-Anido, R., Shaler, S., Gardner, D., Edgar, R., & Tajvidi, M. (2017). Structural performance of hybrid SPFs-LSL cross-laminated timber panels. *Construction and Building Materials, 149*, 156-163.

Davis-Standard Woodtruder. (2018). Retrieved from https://composites.umaine.edu/equipment-and-facilities/thermoplastic-composite-extrusion-lab/.

Decew, J. (2011). Development of engineering tools to analyze and design flexible structures in open ocean environments: *University of New Hampshire.*

Dura, Matthew Jonathan, "Behavior of Hybrid Wood Plastic Composite-Fiber Reinforced Polymer Structural Members for Use in Sustained Loading Applications" (2005). *Electronic Theses and Dissertations*. 853. https://digitalcommons.library.umaine.edu/etd/853

Esteves, B., & Pereira, H. (2008). Wood modification by heat treatment: A review. *BioResources, 4*(1), 370-404.

Ferdous, W., Manalo, A., & Aravinthan, T. (2016). Behaviour of composite sandwich beams with different shear span-to-depth ratios. Paper presented at the Mechanics of Structures and Materials XXIV: *Proceedings of the 24th Australian Conference on the Mechanics of Structures and Materials (ACMSM24, Perth, Australia, 6-9 December 2016).*

Fortini, A., & Mazzanti, V. (2018). Combined effect of water uptake and temperature on wood polymer composites. *Journal of applied polymer science*, 46674.

Fredriksson, D. W., DeCew, J. C., & Tsukrov, I. (2007). Development of structural modeling techniques for evaluating HDPE plastic net pens used in marine aquaculture. *Ocean Engineering, 34*(16), 2124-2137.

Gardner, D., & Han, Y. (2010). Towards structural wood-plastic composites: technical innovations. *Paper presented at the Proceedings of the 6th Meeting of the Nordic-Baltic Network in Wood Material Science and Engineering (WSE), Tallinn, Estonia.*

Gardner, D. J. (2015). Development of structural wood plastic composite timber for innovative marine application. *Retrieved from The University of Maine, Orono, Maine, ME 04469.*

Garoushi, S., Lassila, L. V., & Vallittu, P. K. (2012). The effect of span length of flexural testing on properties of short fiber reinforced composite. *Journal of Materials Science: Materials in Medicine, 23*(2), 325-328.

Gibson, R. F. (2016). Principles of composite material mechanics: CRC press.

Hadid, M., Rechak, S., & Tati, A. (2004). Long-term bending creep behavior prediction of injection molded composite using stress–time correspondence principle. *Materials Science and Engineering: A, 385*(1), 54-58.

Haghighi-Yazdi, M., & Lee-Sullivan, P. (2013). Stress relaxation of a polycarbonate blend after hygrothermal aging. *Mechanics of Time-Dependent Materials, 17*(2), 171-193.

Haiar, K. J. (2000). Performance and design of prototype wood-plastic composite sections. *Washington State University*.

Hamel, S. E. (2011). Modeling the time-dependent flexural response of wood-plastic composite materials.

Hamel, S. E., Hermanson, J. C., & Cramer, S. M. (2013). Mechanical and time-dependent behavior of wood–plastic composites subjected to tension and compression. *Journal of Thermoplastic Composite Materials, 26*(7), 968-987.

Hamel, S. E., Hermanson, J. C., & Cramer, S. M. (2014). Predicting the flexure response of wood-plastic composites from uni-axial and shear data using a finite-element model. *Journal of Materials in Civil Engineering, 26*(12), 04014098.

Herzog, B., Gardner, D. J., Lopez-Anido, R., & Goodell, B. (2005). Glass-transition temperature based on dynamic mechanical thermal analysis techniques as an indicator of the adhesive performance of vinyl ester resin. *Journal of applied polymer science, 97*(6), 2221-2229.

Hosseinaei, O., Wang, S., Enayati, A. A., & Rials, T. G. (2012). Effects of hemicellulose extraction on properties of wood flour and wood–plastic composites. *Composites Part A: Applied Science and Manufacturing, 43*(4), 686-694.

InnovaSea Systems, I. (2015). *Report on Structural Damage to A4800 AquaPod*. Retrieved from 52 South Main Streeet Morrill, Maine 04952, USA:

InnovaSea Systems, I. (2016). A4700 BRIDLE SYSTEM IN GRID MOORING CELL. Retrieved from www.innovasea.com

Instruments, T. (2018). Dynamic Mechanical Analysis: Basic Theory & applications Training. Retrieved from http://people.clarkson.edu/~skrishna/DMA_Basic_Theory_Applications.pdf

Kahl, Melissa, "Structural Design of Hollow Extruded WPC Sheet Piling" (2006). *Electronic Theses and Dissertations*. 117. https://digitalcommons.library.umaine.edu/etd/117.

King, D., & Hamel, S. (2013). The Tensile Creep Response of a Wood-Plastic Composite in Cold Regions *ISCORD 2013: Planning for Sustainable Cold Regions* (pp. 771-778).

Klyosov, A. A. (2007). Wood-plastic composites: *John Wiley & Sons.*

Král, P., Klímek, P., Mishra, P. K., Wimmer, R., & Děcký, D. (2015). Specific modulus and density profile as characterization criteria of prefabricated wood composite materials. *Acta Universitatis Agriculturae et Silviculturae Mendelianae Brunensis*, *63*(2), 433-438.

Lenth, C. A., & Kamke, F. A. (2007). Moisture dependent softening behavior of wood. *Wood and fiber science*, *33*(3), 492-507.

Mark, J. E. (2007). Physical properties of polymers handbook (Vol. 1076): *Springer.*

. MATLAB. (1994-2018). The MathWorks, Inc: MathWorks®. Retrieved from https://www.mathworks.com/products.html?s_tid=gn_ps

Matuana, L. M., Jin, S., & Stark, N. M. (2011). Ultraviolet weathering of HDPE/wood-flour composites coextruded with a clear HDPE cap layer. *Polymer degradation and stability*, *96*(1), 97-106.

Mehndiratta, A., Bandyopadhyaya, S., Kumar, V., & Kumar, D. (2018). Experimental investigation of span length for flexural test of fiber reinforced polymer composite laminates. *Journal of materials research and technology*, *7*(1), 89-95.

Nair, K. M., Thomas, S., & Groeninckx, G. (2001). Thermal and dynamic mechanical analysis of polystyrene composites reinforced with short sisal fibres. *Composites Science and Technology*, *61*(16), 2519-2529.

Najafi, S. K., & Kordkheili, H. Y. (2011). Effect of sea water on water absorption and flexural properties of wood-polypropylene composites. *European Journal of Wood and Wood Products, 69*(4), 553-556.

Kazemi, S., Sharifnia, H., & Tajvidi, M. (2008). Effects of Water Absorption on Creep Behavior of Wood—Plastic Composites. *Journal of Composite Materials*, *42*(10), 993–1002. https://doi.org/10.1177/0021998307088608

Nuñez, A. J., Marcovich, N. E., & Aranguren, M. I. (2004). Analysis of the creep behavior of polypropylene-woodflour composites. *Polymer Engineering & Science, 44*(8), 1594-1603.

Ocean®, I. (2018). Instant Ocean® Sea Salt. Retrieved from http://www.instantocean.com/Products/Sea-Salt-Mixes/sea-salt-mixture.aspx

Page, S. H. (2013). Aquapod Systems aquaculture Aquapod systems for Sustainable Ocean Aquaculture Aquaculture *Sustainable Food Production* (pp. 223-235): Springer.

Pedrazzoli, D., & Pegoretti, A. (2014). Long-term creep behavior of polypropylene/fumed silica nanocomposites estimated by time–temperature and time–strain superposition approaches. *Polymer bulletin, 71*(9), 2247-2268.

Pooler, D. J. (2001). The temperature dependent non-linear response of a wood plastic composite. *Washington State University.*

Pooler, D. J., & Smith, L. V. (2016). Nonlinear Viscoelastic Response of a Wood–Plastic Composite Including Temperature Effects. *Journal of Thermoplastic Composite Materials, 17*(5), 427-445. doi:10.1177/0892705704038220

RIVERDALE. (2019). Aquamesh Specifications. Retrieved from https://riverdale.com/wp-content/sellsheets/Aquamesh.pdf

Shao, Y. (2006). Characterization of a pultruded FRP sheet pile for waterfront retaining structures. *Journal of Materials in Civil Engineering, 18*(5), 626-633.

Slaughter, A. E. (2006). Design and fatigue of a structural wood-plastic composite.

Stark, N. (2008). Outdoor durability of wood-polymer composites: *Woodhead Publishing, Philadelphia.*

Storage, T. M., Brockman, R. A., & Tienda, K. M. (2013). *Analysis of Data Reduction Strategy used in TA Instruments Q800 DMA Test System*.

Struik, L. (1989). Mechanical behaviour and physical ageing of semi-crystalline polymers: 3. Prediction of long term creep from short time tests. *Polymer, 30*(5), 799-814.

Sullivan, J. (1990). Creep and physical aging of composites. *Composites Science and Technology, 39*(3), 207-232.

TAinstruments.com. (2010). TAinstruments Thermal Analysis. Retrieved from http://www.tainstruments.com/pdf/brochure/dma.pdf

Tajvidi, M., Falk, R. H., & Hermanson, J. C. (2005). Time–temperature superposition principle applied to a kenaf-fiber/high-density polyethylene composite. *Journal of applied polymer science, 97*(5), 1995-2004.

Tajvidi, M., & Simon, L. C. (2015). High-temperature creep behavior of wheat straw isotactic/impact-modified polypropylene composites. *Journal of Thermoplastic Composite Materials, 28*(10), 1406-1422.

Tamrakar, Sandeep, "Effect of Strain Rate and Hygrothermal Environment in Wood Plastic Composite Sheet Piles" (2011). *Electronic Theses and Dissertations*. 1576. https://digitalcommons.library.umaine.edu/etd/1576

Tamrakar, S., & Lopez-Anido, R. A. (2011). Water absorption of wood polypropylene composite sheet piles and its influence on mechanical properties. *Construction and Building Materials, 25*(10), 3977-3988.

Tamrakar Sandeep, R. A. L.-A., Alper Kiziltas, Douglas J Gardner (2011). Time and temperature dependent response of a wood–polypropylene composite. *Composites Part A: Applied Science and Manufacturing, 42*(7), 834-842.

Tangent Technologies, L. (2015). Polyforce sturctural recycled plastic lumber. Retrieved from http://tangentusa.com/wp-content/uploads/2016/01/PolyForce_DataSheet_01_20_16.pdf

Thomas Snape, S. E. (2015). Fish Cage Plastic Lumber Testing: Compression Properties (15-39-1263). Retrieved from UMaine Advanced Structures and Composite Center, 35 Flagstaff Rd, University of Maine, Orono, ME 04469:

Timoshenko, S., & Goodier, J. Theory of elasticity. 1951. *New York, 412*, 108.

Vandenbroucke, K., & Metzlaff, M. (2013). Abiotic stress tolerant crops: genes, pathways and bottlenecks *Sustainable Food Production* (pp. 1-17): Springer.

Vincent Caccese, P. D., P.E. (2006). Structural Testing of Various Configurations for the AquaPod Net Pen (C2004-018-01).

Xu, B., Simonsen, J., & Rochefort, W. s. (2001). Creep resistance of wood-filled polystyrene/high-density polyethylene blends. *Journal of applied polymer science, 79*(3), 418-425.

BIOGRAPHY OF THE AUTHOR

Murtada Abass A Alrubaie was born in Amara City, Maysan Province, Iraq, on February 12, 1983. He was raised in Amara, Maysan and graduated from Althawra High School in 2001. He attended the University of Basra, Iraq, and graduated in 2005 with a Bachelor's of Science degree (B.Sc.) in Civil Engineering. He spent two years working international company (Mott MacDonald) as a site and supervisor engineer. He then travelled to New Delhi, India, to attend a six-month course for academic writing in Inlingua® from Dec 2007 to June 2008. Murtada attended the Universiti Putra Malaysia, Serdang, Selangor Darul Ehsan, Malaysia, and graduated in 2010 with a Master of Science degree (M.Sc.) Structural Engineering and Constructions. Before Murtada Joins the University of Maysan, Amara, Mayan, Iraq, as associate lecturer in 2014, he worked as a site construction manager with two International petroleum companies (Weatherford Oil Tool Middle East Limited, PetroChina International Iraq FZE Iraq Branch) from 2010 to 2013. Murtada joined the University of Maine in Fall 2014 as a Doctor of Philosophy student in the department of Civil and Environmental Engineering as a sponsored student from the High Committee for Education Development in Iraq (HCED-Iraq). Murtada is a candidate for the Doctor of Philosophy degree in Civil Engineering from the University of Maine in May of 2019.